



Wireless colorimetric readout to enable resource-limited point-of-care

Zur Erlangung des akademischen Grades eines

DOKTORS DER INGENIEURWISSENSCHAFTEN (Dr.-Ing.)

von der KIT-Fakultät für Maschinenbau des
Karlsruher Instituts für Technologie (KIT)
angenommene

DISSERTATION

von

Suzanne Smith

Tag der mündlichen Prüfung: 26 June 2019

Hauptreferent:
Korreferentin:

Prof. Dr. Jan G. Korvink
Prof. Dr. Uli Lemmer

Karlsruher Institut für Technologie
Institut für Mikrostrukturtechnik
Hermann-von-Helmholtz-Platz 1
76344 Eggenstein-Leopoldshafen

Betreuer: Dr. Dario Mager
Dr. Kevin Land

*For my dearest Stu, and my family.
Thank you for your love and support, always.*

Contents

Abstract	1
Zusammenfassung	3
List of abbreviations	5
1 Introduction	7
1.1 Motivation	7
1.2 Objectives	8
1.3 Hypothesis	10
1.4 Impact	10
1.5 Dissertation outline	11
2 Scientific background	13
2.1 POC diagnostics for resource-limited settings	13
2.1.1 Paper-based solutions	13
2.1.2 External instrumentation	15
2.1.3 Resource-limited clinic perspective	17
2.2 REASSURED solution	18
2.3 Printed functionality	19
2.3.1 Printing techniques and materials	20
2.3.2 Printed circuits and components	22
2.3.3 Connectivity	25
2.4 Integrated and scalable paper-based solutions	29
3 Technical background	33
3.1 Clinical aspects	33
3.2 Proposed solution	34
3.3 Colour detection	36
3.4 Sensing RFID	40
3.5 Tag design	40
3.6 Printing and assembly	42

3.7	Wireless readout	45
3.8	Packaging	46
4	Substrates	49
4.1	Overview	49
4.2	Methods	50
4.2.1	Substrates	50
4.2.2	Characterisation of printed features	53
4.3	Results	55
4.4	Discussion	63
5	Detection	65
5.1	Overview	65
5.2	Methods	66
5.2.1	Model lateral flow test devices	66
5.2.2	Colour sensing	67
5.2.3	Colour detector tags	68
5.2.4	Experimental set-up	69
5.3	Results	71
5.3.1	Colour readout	71
5.3.2	Colour detector tag performance	72
5.4	Discussion	77
6	Communication	79
6.1	Overview	79
6.2	Methods	80
6.2.1	Printed RFID tags	80
6.2.2	Antenna characterisation	81
6.2.3	Read range measurements	82
6.3	Results	86
6.3.1	Printed RFID tags	86
6.3.2	Antenna characterisation	87
6.3.3	Read range measurements	88
6.4	Discussion	94
7	Packaging and integration	97
7.1	Overview	97
7.2	Methods	98
7.2.1	Packaging designs	98

7.2.2	Integrated device testing	102
7.3	Results	103
7.3.1	Packaging designs	103
7.3.2	Integrated device testing	103
7.4	Discussion	108
8	Real-world tests and usability	109
8.1	Overview	109
8.2	Methods	110
8.2.1	Real-world tests	110
8.2.2	Usability	112
8.3	Results	115
8.3.1	Real-world tests	115
8.3.2	Usability	117
8.4	Discussion	122
9	Scalability	125
9.1	Overview	125
9.2	Automation and scale up	126
9.2.1	Printing	126
9.2.2	Assembly	127
9.2.3	Device testing	131
9.2.4	Packaging	133
9.2.5	Wireless communication and deployment	134
9.3	Cost analysis	134
9.4	Optimisation of printed components and functionality	136
9.5	Discussion	137
10	Conclusion and outlook	141
	Bibliography	145
A	Own publications	165
B	Usability questionnaire	171
	Acknowledgements	177

Abstract

The work presented in this dissertation details a scalable, generic wireless colour detector for point-of-care diagnostics in resource-limited settings. The challenges faced in these settings have limited the effectiveness of point-of-care diagnostics. By combining the growing fields of paper-based diagnostics and printed electronics with Southern African clinic perspectives, a mass-producible, low-cost, paper-based solution for result readout and communication was developed.

Printed radio frequency identification devices with sensing capabilities were manufactured onto different low-cost and paper-based substrates to assess the practical functionality of these devices. The resulting print quality and wireless readout ranges were found to be adequate for clinical requirements (> 75 mm read ranges obtained in passive mode), and illustrated that various low-cost substrates can be utilised as different packaging and adhesive label options for paper-based diagnostic tests. Substrates tested included paper and cardboard substrates typically used for printing and packaging.

The devices were further developed to target colour detection from lateral flow test strip devices and other typical paper-based rapid test formats. The results were compared to those obtained from manual readout using colour charts, a commercial lateral flow test strip reader and image analysis using ImageJ, and demonstrate suitability for delivering automated readout and communication of results. The wireless colour detector is compatible with different test strip form factors, including lateral flow test strips with and without plastic housing, and pH test strips. This provides a modular solution, which would ease training requirements for each test type, reducing the skills and time needed to perform the tests.

The solution is low-cost and maintenance-free, and thus fitting for resource-limited settings. A scalable version of the solution has been developed, making use of standard manufacturing processes for printing and packaging industries, initially using sheet-to-sheet formats, but with the goal of being scalable to roll-to-roll processes. This would enable the possibility of local manufacture, as well as mass distribution of the devices to those resource-limited areas where they are most needed, and where they will have the greatest impact on point-of-care testing.

Zusammenfassung

Patientennahe Diagnostik in Entwicklungsländer birgt spezielle Herausforderungen, die ihren Erfolg bisher begrenzen. Diese Arbeit widmet sich daher der Entwicklung eines in seiner Herstellung skalierbaren und vielseitig einsetzbaren funkbasierten Auslesegerätes für Laborteststreifen. Durch die Kombination einer wachsenden Auswahl an papierbasierten Teststreifendiagnostiken mit gedruckter Elektronik und unter Berücksichtigung des diagnostischen Alltags im südlichen Afrika wurde ein Gerät entwickelt, das Teststreifen zuverlässig ausliest und die Daten per Funk an eine Datenbank übertragen kann.

Die Technik basiert auf RFID-Tags (radio frequency identification devices), welche auf verschiedene flexible Substrate gedruckt wurden, um die technische Umsetzbarkeit und Funktionalität zu evaluieren. Um den Preis für die geplante Anwendung niedrig zu halten, wurden unter anderem Papier und Karton als Substrate genutzt. Das Ergebnis dieser Studie sind passive RFID-Tags auf unterschiedlichen, meist günstigen Substraten, die über eine Distanz von über 75 mm betrieben und ausgelesen werden können.

Basierend auf der über RFID bereitgestellten Energie und Datenübertragung wurde eine Ausleseeinheit für Standardpapierstreifentests entwickelt und integriert. Durch das Auslesen verschiedener Teststreifen wurde das Gerät evaluiert und in seiner Aussagekraft mit einer scanner-basierten Aufnahme und anschließender Bildanalyse (ImageJ), einem kommerziellen Auslesegerät sowie einer manuellen Auslesung mit Hilfe von Farbtabelle verglichen. Das Gerät kann die Streifen zuverlässig auslesen und die Daten über die RFID-Schnittstelle übertragen. Die funkbasierte Ausleseeinheit ist mit verschiedenen kommerziellen Teststreifen sowohl im biodiagnostischen (lateral flow tests) wie auch im chemischen Bereich (pH-Wert) kompatibel. Die modulare Lösung erlaubt ein breites Einsatzgebiet und führt dadurch zu reduzierten Trainingszeiten der Anwender und einer zuverlässigen Handhabung.

Die vorgestellte Lösung ist äußerst kostengünstig und bedarf keiner Wartung, wodurch sie sich sehr gut für den Einsatz in abgelegenen Feldkrankenhäusern eignet. Es wurde ein skalierbarer Prototyp entwickelt, der auf konventionellen Herstellungsverfahren der Verpackungsindustrie aufbaut. Aktuell handelt es sich noch um einen bogenbasierten Prozess, der sich aber prinzipiell auch auf Rolle-zu-Rolle Maschinen

übertragen lässt. Bei der Entwicklung des Geräts spielte die Möglichkeit der lokalen Herstellung in den Einsatzländern eine große Rolle. Diese hätte neben der Generierung von Arbeitsplätzen auch den Vorteil einer einfacheren Verteilung der Geräte in ländliche Regionen, in denen sie den größten Nutzen für die Diagnostik erzielen würden.

List of abbreviations

Abbreviation	Definition
2D	two-dimensional
3D	three-dimensional
μ PAD	micro paper-based analytical device
ADC	analogue-to-digital converter
AFE	analogue front-end
ASQ	after scenario questionnaire
ASSURED	affordable, sensitive, specific, user-friendly, rapid and robust, equipment free, deliverable to end-users
CIE	International Commission on Illumination
CMOS	complementary metal-oxide semiconductor
EEPROM	electrically erasable programmable read-only memory
EIRP	effective isotropic radiated power
ELISA	enzyme-linked immunosorbent assay
EPC	electronic product code
GUI	graphical user interface
HF	high frequency
HIV	human immunodeficiency virus
HL7	Health Level Seven
HSL	hue, saturation, lightness
HSV	hue, saturation, value
IC	integrated circuit
IOT	internet of things
IR	infrared
ITO	indium tin oxide
LED	light-emitting diode
LF	low frequency
LFT	lateral flow test
LSM	laser scanning microscopy
NFC	near-field communication

Abbreviation	Definition
OLED	organic light-emitting diode
PC	personal computer
PCB	printed circuit board
PEN	polyethylene naphthalate
PMMA	poly(methyl methacrylate)
POC	point-of-care
POE	power over ethernet
PEDOT:PSS	poly(3,4-ethylenedioxythiophene) polystyrene sulfonate
QFN	quad flat no-leads
QR	quick response
REASSURED	real-time connectivity, ease of specimen collection, affordable, sensitive, specific, user-friendly, rapid and robust, equipment free and environmentally friendly, deliverable to end-users
RF	radio frequency
RFID	radio frequency identification
RGB	red, green, blue
ROI	region of interest
RSSI	received signal strength indicator
RTC	real-time clock
SMD	surface mount device
SOLT	short-open-load-through
SPI	serial peripheral interface
SPR	surface plasmon resonance
SUS	system usability scale
TIA	transimpedance amplifier
UHF	ultra-high frequency
USB	universal serial bus
UV	ultra-violet
WHO	World Health Organization

1 Introduction

1.1 Motivation

Point-of-care (POC) diagnostic testing in resource-limited settings – including many of the clinics found across Southern Africa (Figure 1.1a) – remains a challenge. Currently insurmountable constraints, such as cost, infrastructure and trained staff have limited the effective implementation of diagnostics at the POC [1]. The primary technical challenges lie in the accurate readout and communication of results among clinics, hospitals and laboratories [1–3], and the maintenance of equipment [4].

In response to the formulation of the ASSURED criteria (Affordable, Sensitive, Specific, User friendly, Rapid and Robust, Equipment free and Deliverable to end-users) by the World Health Organization (WHO) [5], and more recently, the modified REASSURED criteria to include newer technologies [6], paper-based diagnostic solutions for POC in resource-limited settings have undergone tremendous growth [7, 8] (Figure 1.1b). Paper is well suited to meeting many of the REASSURED aspects, as it is low-cost, disposable and provides automated fluidic handling and visual readout (e.g. typical lateral flow test (LFT) formats, such as pregnancy tests).

Human immunodeficiency virus (HIV) and malaria rapid tests are currently some of the most widely utilised POC tests, with more than 150 million performed each year in Africa [9]. Rapid HIV tests are typically interpreted visually (by eye), often by untrained staff, resulting in errors in running the test and readout of the result, and leading to incorrect diagnosis in approximately 5% of cases [10]. In addition, data capturing is a manual process, making traceability and patient follow up difficult.

In an attempt to address these challenges, external instrumentation solutions have been developed, with colour detection being the most frequently employed for result readout from paper-based tests [11]. Although commercial portable reader devices are available for accurate analysis of rapid tests and other LFT devices, these are typically high in cost, require maintenance and are specific to a single test format; this is problematic for applications in resource-limited settings. It follows that additional cost-effective functionality needs to be incorporated as part of the paper-based

diagnostic solution. Moreover, connectivity of devices and systems, including POC diagnostics, is of increasing importance [12].

The field of printed electronics enables various printed functionalities to be implemented on flexible and paper-based substrates [13–16] (Figure 1.1c). Specialised printable materials, substrate modifications and the integration of various functional blocks have been investigated to realise systems ranging in complexity and automation for POC diagnostic applications [17, 18]. Printed antennas and wireless connectivity solutions such as radio frequency identification (RFID) are increasing in popularity and maturity. Furthermore, paper production, printing and packaging are long-standing, scalable and widely available processes, even in the targeted areas such as Southern Africa and India. The work presented in this dissertation builds on these existing developments to provide unique solutions in POC diagnostics for resource-limited settings that can be manufactured locally and supplied sustainably.

1.2 Objectives

The presented work explores the automation of critical steps in the clinic workflow, including: interpretation of results, data capture, data communication and cost containment. Using printing and paper-based manufacturing techniques, this enables automated result readout using a maintenance-free and modular approach, with the goal of developing scalable, low-cost solutions for effective POC diagnostics in resource-limited settings. Specifically, the objectives of this dissertation are to:

- Confirm current South African clinic workflow restrictions and needs, to enable solutions for readout and capturing of results to be developed accordingly.
- Provide accurate result readout from existing paper-based rapid tests with a low-cost reader unit that does not require maintenance.
- Implement communication of the result from the reader unit to an external agent, which would be a central database in the long term.
- Realise a modular solution where different rapid test formats can be utilised in the reader devices. This adaptable approach removes the need for training for each test type, and reduces the skills and time required.
- Develop a scalable solution making use of standard manufacturing processes for printing and packaging industries to enable mass distribution of the devices to resource-limited areas where they are most needed and could have the most impact on POC testing.

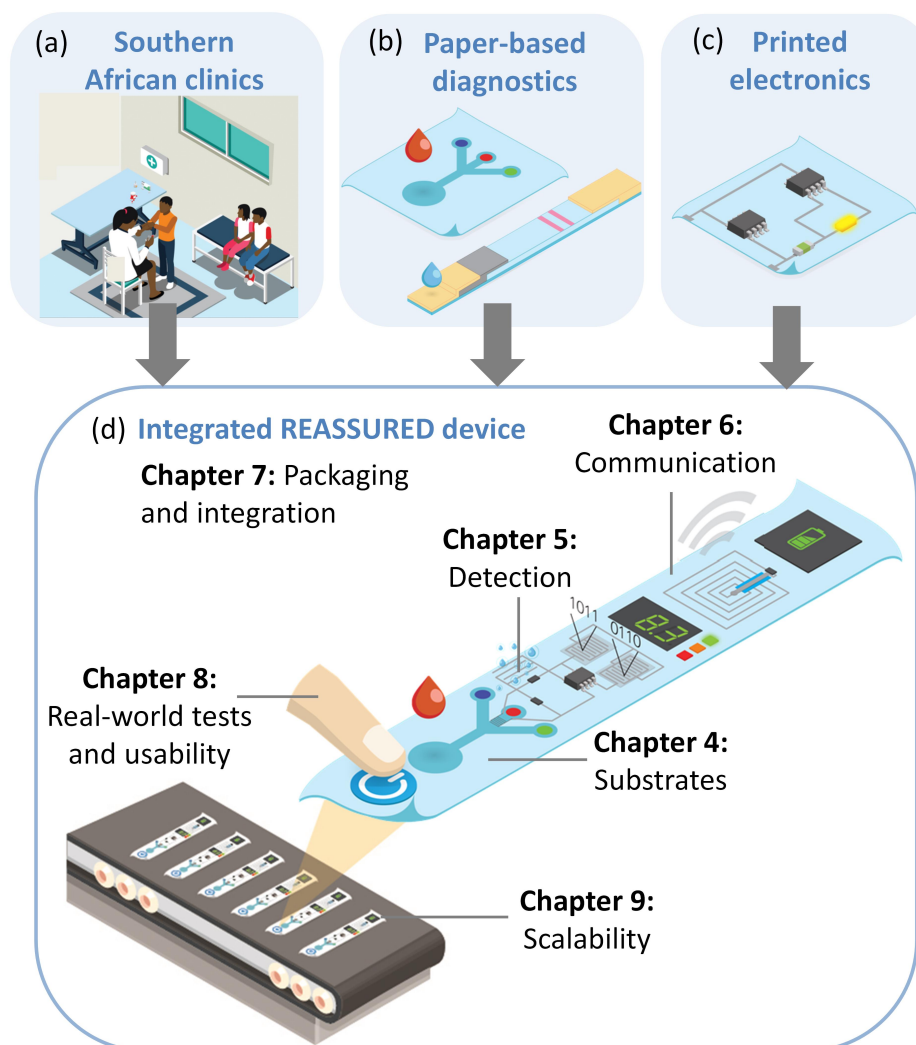


Figure 1.1 Overview of various aspects explored and a breakdown of the chapters of the dissertation. Blocks a) to c) are explored in Chapters 2 and 3 as part of the literature review and approach followed. The remaining chapters are summarised in d) towards the goal of realising effective REASSURED POC diagnostic devices.

1.3 Hypothesis

It is possible to automate result readout and communication from a paper-based diagnostic test to an external agent, and simultaneously conform to the requirements of resource-limited clinics in South Africa.

The main hypothesis can be subdivided into the following sub-hypotheses, each of which have to be proven separately, and once proven, will enable the proof of the main hypothesis:

- It is possible to understand the limitations in resource-limited clinics in South Africa and the effect of these limitations on the implementation of wirelessly connected paper-based diagnostic tests.
- It is possible to implement detection and wireless communication techniques for paper-based diagnostic devices to read out and communicate a diagnostic test result to an external agent.

1.4 Impact

The potential impact of this work will include streamlined POC testing at clinics through providing modules for the automated readout, capturing and transmission of results. Equipment maintenance issues would be alleviated through the semi-disposable printed solutions that are developed, meaning fewer delays and set-backs as a result of equipment repair requirements.

This would enable healthcare workers to have a higher patient throughput, deliver correct results in a timely manner, and have patient records on hand for ease of patient follow-ups for repeat visits. Establishing local manufacturing capabilities within South Africa for paper-based printed devices is a potential long-term goal, which would aid in job creation and boost the economy of South Africa.

This work contributes to the field and long-term goal of all printable paper-based POC diagnostics, as well as meeting the REASSURED criteria. The aim is to further the research on POC diagnostic devices that can be truly effective and make a difference where the need and impact is greatest, such as in resource-limited clinics in South Africa.

1.5 Dissertation outline

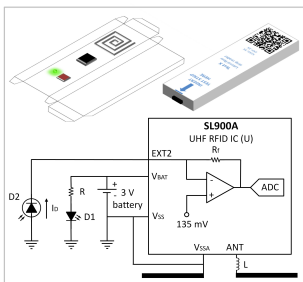
Based on the context provided, it is clear that a number of components need to be investigated for augmented paper-based tests to be successful, and these are divided into different chapters of this dissertation, as listed below and illustrated in Figure 1.1d.

- **Chapter 2 – Scientific background:**



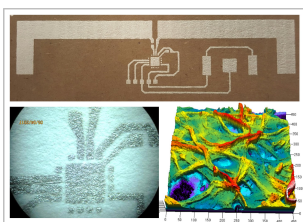
Summarises the literature that forms the basis of the work carried out in this dissertation, and includes the REAS-SURED principles, paper-based diagnostics and printed electronics. The chapter focusses on printed functionality for readout mechanisms, along with communication and connectivity aspects. Integrated and scalable examples are provided, while existing challenges are highlighted.

- **Chapter 3 – Technical background:**



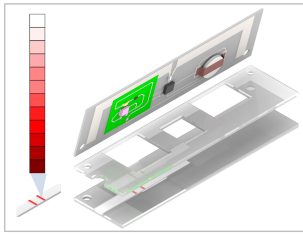
Describes the general methods used in the development process for the work documented in this dissertation, including clinical and technical aspects. The proposed solution is presented and various components of the solution are described, including colour detection, sensing RFID and tag designs. Printing, assembly, packaging and testing methods are summarised.

- **Chapter 4 – Substrates:**



Presents the results of functional tags printed and assembled onto various low-cost and paper-based substrate materials. Microscopy results are used to evaluate the printed features in terms of physical and electrical properties.

- **Chapter 5 – Detection:**



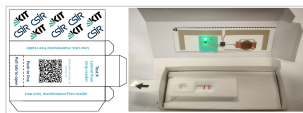
Details the automated colorimetric readout and storage of results for use with paper-based diagnostic tests. Optical readout using an integrated circuit for sensing and wireless communication is showcased, with colour intensity experiments of the model tests presented.

- **Chapter 6 – Communication:**



Summarises the implementation of automated result communication using RFID techniques, including read range measurements in both passive and battery-assisted modes for tags printed onto different substrates and with different sensors connected.

- **Chapter 7 – Packaging and integration:**



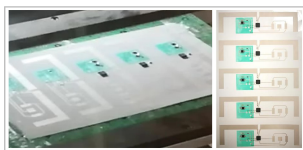
Illustrates the integration of devices into low-cost, robust, and low-maintenance solutions through packaging of components into a feasible, generic and scalable device.

- **Chapter 8 – Real-world tests and usability:**



Presents the results of packaged low-cost reader devices using real-world paper-based rapid tests, including LFT strips. Initial usability studies are also presented to highlight functional and aesthetic improvements to be made in future iterations of the devices.

- **Chapter 9 – Scalability:**



Provides an outlook on mass production and deployment of the devices where they are most needed. Feasibility and costing for production of the devices and the complete solution to be deployed are explored in this chapter.

- **Chapter 10 – Conclusion and outlook:** Presents a summary and analysis of the work carried out, with map of future work.

2 Scientific background

This chapter is based on previously published work [19,20] and parts of the text have been reproduced with permission from the Royal Society of Chemistry and Springer Nature, respectively.

2.1 POC diagnostics for resource-limited settings

In recent years, there has been a drive to develop low-cost, innovative POC diagnostics to reach populations where the burden of disease is greatest and resources are fewest. These developments have been guided by the WHO through formalisation of the ASSURED criteria, to which these diagnostics should conform if they are to be successful in resource-limited settings [5]. More recently, the REASSURED principles [6] have been defined as an update to the ASSURED criteria to incorporate newer technologies and important factors, including Real-time connectivity, Ease of specimen collection, and Environmental friendliness.

2.1.1 Paper-based solutions

Paper-based microfluidics or micro paper-based analytical devices (μ PADs) [7, 21–23] provide a favourable platform on which to develop solutions that address these requirements. pH strips and home-based lateral flow pregnancy tests are examples of the first and most common paper-based microfluidic devices [23] (Figure 2.1a). Enhanced functionality, such as multiplexing and multi-dimensional fluidic handling, can be garnered from advances in paper-based microfluidics through multi-channel designs within a paper substrate (Figure 2.1b), or by stacking and folding of paper into so-called three-dimensional (3D) or “origami” paper-based microfluidics [24] (Figures 2.1c and d).

Wax printing of fluidic channels is often implemented using hydrophobic barriers to contain and guide fluids through a paper device. Inkjet printing, screen printing and flexographic printing have also been utilised [25,26]. Paper exhibits a number of

useful properties that are either inherent or can be achieved through straightforward modifications. This includes the low cost, recyclability and disposability of paper to provide devices that can easily be transported and distributed, and safely incinerated. Paper enables automated fluidic handling through a porous substrate, with simple, visual result readout by the user typically implemented via a colour change. Paper-based solutions also facilitate high-quality mass manufacturing, which is based on a long tradition of paper processing [27].

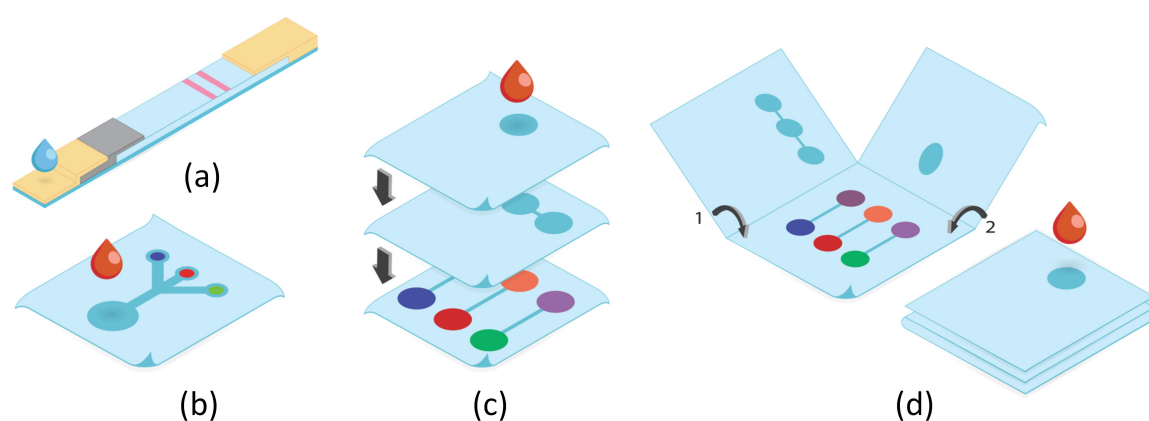


Figure 2.1 Illustration of typical paper-based diagnostic test formats. a) Standard LFT strips with sample pad, conjugate pad, test and control lines and wicking pad, b) two-dimensional (2D) paper-based diagnostics using hydrophobic fluidic barriers (e.g. wax printing), and 3D paper-based diagnostics implemented using c) stacking of multiple layers or d) folding or origami paper devices for enhanced fluidic control and multiplexing. Adapted from [19] with permission from the Royal Society of Chemistry.

Readout mechanisms that are built in to the paper-based test device itself through chemical reactions and biological processes can be utilised (Figure 2.2). Comprehensive reviews of readout and display techniques implemented for paper-based diagnostics summarise recent developments in this field [7, 23]. These techniques have been successfully integrated with paper-based diagnostics towards fully REASSURED solutions, such as a commercial example by Haemokinesis [28] for blood typing using a visual text readout generated from the sample.

These types of paper-based readout solutions are often dependent on the accuracy of the biological and chemical reactions implemented, along with the quality of the paper substrate. Where these aspects may not be optimal, or are implemented sub-optimally to reduce costs, the functionality may be limited. In addition, these readout

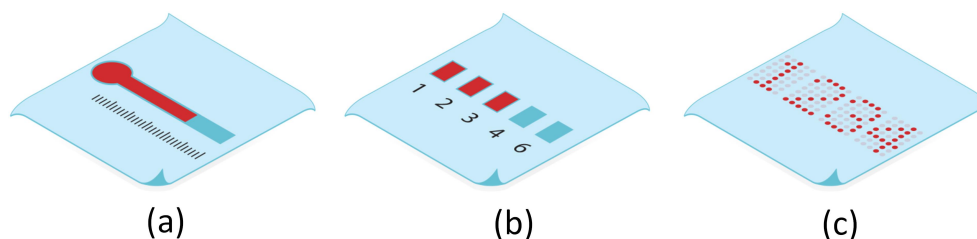


Figure 2.2 Paper-based microfluidic visual indicators, which can be a) time or distance based, b) counting based or c) text based, utilising the sample and resulting flow or reactions to provide user feedback on the test progress and results. Adapted from [19] with permission from the Royal Society of Chemistry.

mechanisms require literacy in many cases, and can result in misinterpretation of the results, given the manual nature of the readout.

Paper-based microfluidics have been implemented for various biological samples, including whole blood, serum, urine and nasal swabs [7], and have successfully been applied to health, environmental and food quality monitoring [29, 30]. Integration with a variety of sensors [23, 24] has enabled automated detection components to be realised.

Examples include optical, electrochemical, electrical and mechanical detection methods [29, 31], many of which have been implemented on paper devices, and with several of these explored as part of this work [32, 33]. Optical detection methods are often used for disease diagnostics as they are robust and sensitive [31]. These include colorimetric, fluorescence, absorbance, chemiluminescence, and surface plasmon resonance (SPR) [31].

Colorimetric result readout is typically implemented in paper-based diagnostics, as many relevant paper-based tests utilise sample processing and reactions that result in a visible colour change [11]. In this manner, the presence and concentration of a specific analyte on the paper-based device can be determined [34].

2.1.2 External instrumentation

Automated readout from paper-based diagnostics with result communication and storage removes user bias and allows for ease of result capture and tracking. Automated result readout generally requires some form of external instrumentation for processing and communication [35] (Figure 2.3). Common methods for the automation of readout from paper-based diagnostics include the use of existing devices such as cam-

eras, scanners, portable glucose meters and smart phones [36, 37], as well as custom-developed systems such as portable potentiostats [33, 38, 39], many of which have been extensively reviewed [7].

Spectrophotometers, which measure reflected or transmitted light at various points on the visual spectrum, are most commonly used for accurate colour measurement. However, for paper-based diagnostics, image analysis of digital images is most widely used as this is simple, easy to use and requires only a digital camera or smartphone to read out colour information using red, green, blue (RGB) or greyscale values from the image [40].

Smartphones in particular have been extensively utilised for quantitative colour and fluorescence readout using the built-in cameras and image processing capabilities [35, 36], and have also been used in the implementation of portable potentiostats [37].

Examples of both commercial [41] and developmental [42, 43] smartphone-based colour detection systems are available. Traditional spectrophotometers can also be used to analyse the colour by measuring the absorbance of the sample at specific wavelengths [34]. Examples of commercial portable readers for automated readout from LFT strips include the ESEQuant LFT strip reader (Qiagen), Deki Reader (Fio Corporation), TSR-100 Test Strip Reader (Allsheng) and ASSURE Rapid Test Reader (MP Biomedicals).

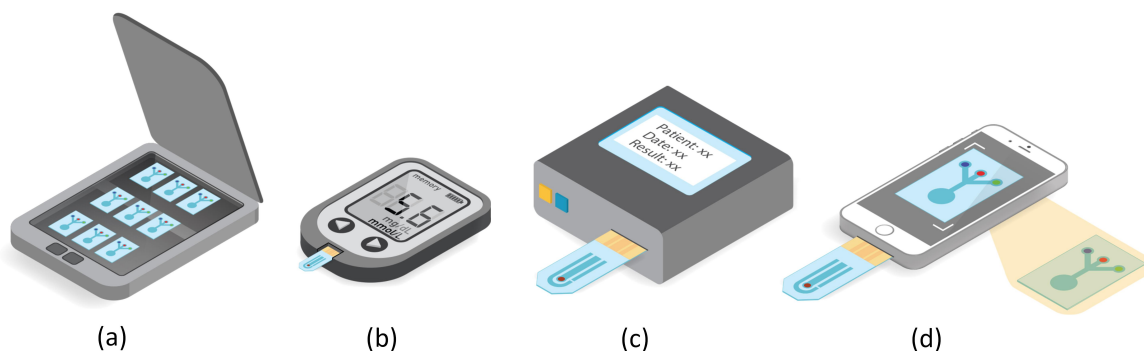


Figure 2.3 Examples of existing external instrumentation solutions that can be used with paper-based diagnostic tests: a) a desktop scanner, b) a portable glucose meter used with custom-made paper-based diagnostic electrochemical sensors, c) a custom-made instrument for the analysis of paper-based diagnostic test devices, and d) a phone camera for image capture and processing of a paper-based device and/or for physical connection and analysis of a paper-based device. Reproduced from [19] with permission from the Royal Society of Chemistry.

Numerous medical diagnostic equipment manufacturers have started to implement connectivity solutions for their instruments. As an example, GeneXpert utilises connectivity software by Cepheid such as GX Dx and Xpertise Software [44]. However, modems and internet connectivity are required, which may be problematic in resource-limited settings.

2.1.3 Resource-limited clinic perspective

Although these instrumentation systems enable quantitative and more accurate results to be obtained, these can introduce a number of challenges in resource-limited settings, including the need for an electricity supply, regular maintenance and user training. Limited network and maintenance infrastructure, intermittent power, and issues with theft in resource-limited settings create challenges in the successful implementation of instrumented solutions. This highlights the need for quantitative detection, readout and connectivity to be integrated into a low-cost, automated and maintenance-free or low-maintenance system.

Visual-based tests such as standard LFT strips are subject to user bias, with incorrect result readout occurring in approximately 5% of cases for rapid HIV tests [10]. This error is for yes/no tests and would be expected to be much higher where quantitative readout is required. Additionally, these manual tests do not allow for effective communication of the result or diagnosis, or for data collection for the assessment of epidemics or therapy strategies. Automated result readout and communication would enable such data to be captured and analysed, contributing to solving various health system needs. To facilitate the effective implementation of readout, displays and communication modules, on-board power may be required to drive these added functionalities, without relying on external power sources.

Of particular relevance to this work, the limitations in Southern African resource-limited settings need to be fully investigated to enable the development of effective solutions. Extensive literature is available for POC testing in South Africa and the associated challenges/shortfalls [9, 45–49]. The main problems highlighted include the increased workload that POC devices introduce to clinics, as user training is required and test times can be lengthy. The maintenance of equipment and supply of consumables are also challenges to contend with [4], along with data connectivity [50] and the storage of results [1]. The Ideal Clinics programme [51] has been formulated by experts in the field as a guideline for future South African clinics to follow if they are to be truly effective.

Although healthcare challenges for resource-limited settings have been clearly highlighted, the application of appropriate technologies to solve these specific challenges

for resource-limited settings in Southern Africa has yet to be implemented effectively. Important aspects addressed by the present work include infrastructure and communication, and would also be applicable to administration and digital health system support.

2.2 REASSURED solution

Taking into account these various challenges and unmet needs, a fully REASSURED device would require the following functional components, each contributing to improvements in different REASSURED aspects found in existing solutions:

- actuation and control modules for the operation of and user interaction with the device, improving usability and providing built-in instrumentation,
- microfluidics for processing and fluidic control of the sample to be tested, contributing to low-cost diagnostics with high specificity,
- electronics to add sensitivity and speed towards automated, integrated testing and instrumentation,
- sensing modules towards built-in, fast and sensitive detection techniques and instrumentation,
- data processing capabilities to analyse the sample accurately and automatically and capture the result digitally, contributing to most aspects of REASSURED,
- readout and display modules to express the result directly to the user, improving result read out times and user-friendliness with built-in instrumentation,
- connectivity for the transmission and storage of results to be accessed remotely or in future as needed, contributing to many REASSURED aspects, and
- energy storage for built-in power to drive the various functional components, assisting with the deployment of devices with on-board instrumentation.

Figure 2.4 summarises the various functional components that could be incorporated into paper-based diagnostic devices towards achieving the required REASSURED criteria.

The envisaged solution utilises a small sample of plasma or blood, processes the sample, reads out the result through sensing and processing steps, and obtains a digitised result that can be transmitted and stored, thereby directly diagnosing a targeted disease. The integration of all components onto a paper substrate strives to meet the environmentally friendly aspects defined by the REASSURED principles.

This dissertation focuses specifically on scalable sensing and connectivity solutions, towards low-cost and automated devices requiring little to no user interaction, all within a maintenance-free approach.

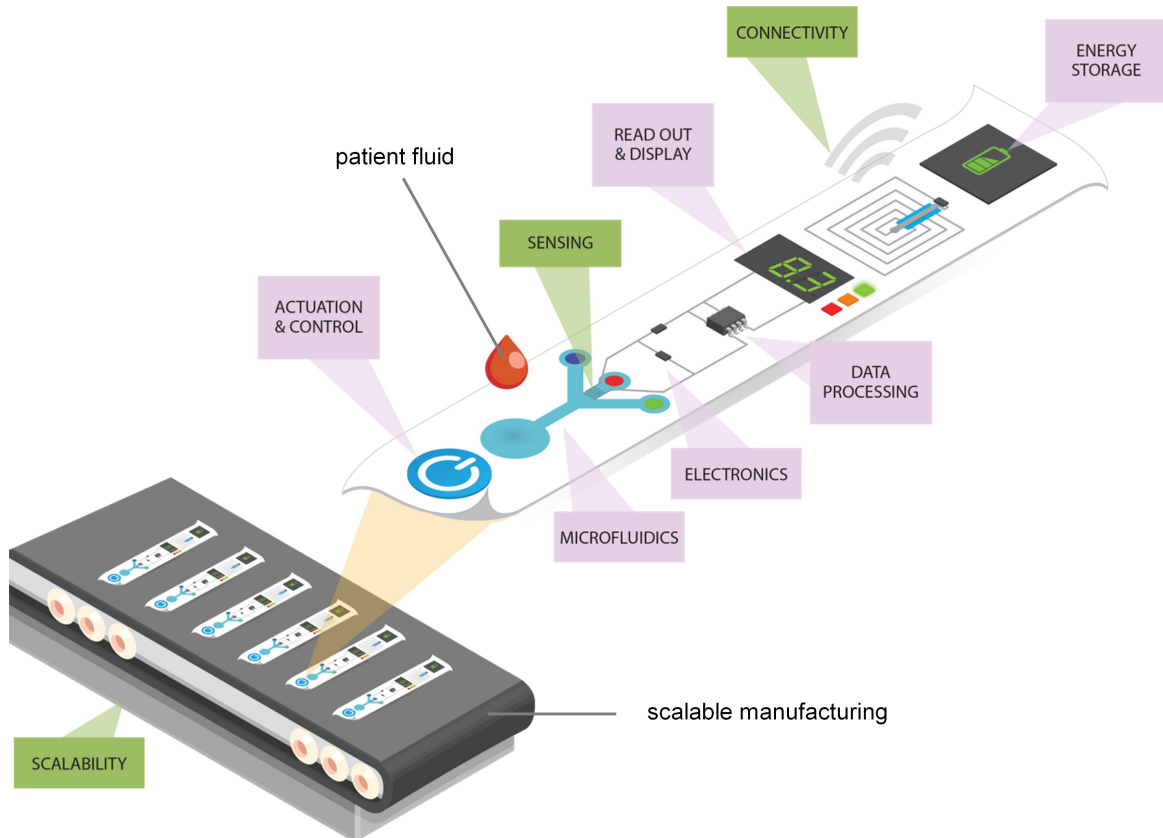


Figure 2.4 Conceptual design of an integrated paper-based REASSURED device showing the various functional requirements and highlighting in green those that form the focus of this dissertation, namely sensing, connectivity and scalability.

2.3 Printed functionality

The envisaged REASSURED solution illustrates that additional functionality needs to be implemented with existing or new paper-based diagnostic devices for usable solutions to be realised for resource-limited settings. Printed functionality, stemming from printed materials development and printed electronics fields [13,16,52,53], offers a

potential solution to realise augmented devices through automated result readout and communication. This also removes the need for training or external instrumentation to perform a test correctly. Building blocks from the field of printed electronics, such as sensors, processors, displays, connectivity and power, can either be integrated as part of or used in conjunction with paper-based devices to extend their functionality [19,54].

Printed devices provide a low-cost and disposable or maintenance-free approach to instrumentation, which could be single-use (if integrated directly with paper-based diagnostics) or re-usable but disposable or maintenance-free (if used as a separate module in conjunction with paper-based devices). Printed solutions can utilise existing printing and packaging technologies, with the potential for locally produced devices in resource-limited countries, enabling solutions to be deployed easily and tests to be more accessible to those who need them most.

The field of printed and flexible electronics has been and continues to be developed, enabling various printed functionalities to be designed and implemented on flexible and paper-based substrates [13–16]. Specialised printable materials, substrate modifications, and integration of various functional blocks have been investigated to realise systems ranging in complexity and automation for POC diagnostic applications [17,18]. An overview of the various aspects of printed functionality are provided in the sections that follow, with additional information available [19].

2.3.1 Printing techniques and materials

Printing technologies are well established and date back to the invention of the printing press in the 15th century. Printing allows for high throughput production by utilizing roll-to-roll processes, making this a desirable platform on which to develop solutions for scale up, including paper-based diagnostics. A variety of printing techniques have been used in paper-based diagnostics, including wax printing of fluidic channels and screen printing of electrochemical sensors. Additional fabrication techniques for microfluidic paper-based devices that utilise printing technologies have been detailed, and include inkjet printing and flexographic printing [25,26].

Printing of electronics can be achieved by using various printing techniques [16], a number of which overlap with those used for paper-based microfluidics. Commonly used methods include screen, inkjet, gravure, flexographic, off-set, slot-die, newer methods of transfer printing, as well as micro-contact and nanoimprinting. Low-cost printing solutions for printing copper tracks using a standard laser printer have also been showcased [55], and examples of printed electronics onto paper substrates using various printing techniques are summarised by [56]. The patterning of paper and alternative flexible substrates for printing of integrated paper-based diagnostics has

also been explored [57–59] with scale up applied for the low-cost production of highly integrated microfluidic devices [60].

Screen printing in both printed electronics and paper-based diagnostics has been a favourable trend as it is an established printing technology that allows for ease of printing onto different substrates and is applicable to both small and large scale manufacturing. Paper-based printed electrodes for biosensing applications are currently extensively implemented using screen printing and many examples have been reviewed [61]. Wax screen printing also allows for fast, simple manufacture of paper-based microfluidic devices [25,26], again highlighting the attractiveness of screen printing for the fabrication of paper-based diagnostics with added functionality. Figure 9.1 illustrates low- and high-volume screen printing processes using manual and semi-automated sheet-to-sheet set-ups as well as large-volume automated equipment for roll-to-roll processing. A number of commercial screen printers are available, including options from THIEME GmbH & Co. KG, Germany, the DEK printing solutions range from ASM Assembly Systems GmbH & Co. KG, Germany, Coruna Printed Electronics GmbH, Switzerland, and many other companies [62].

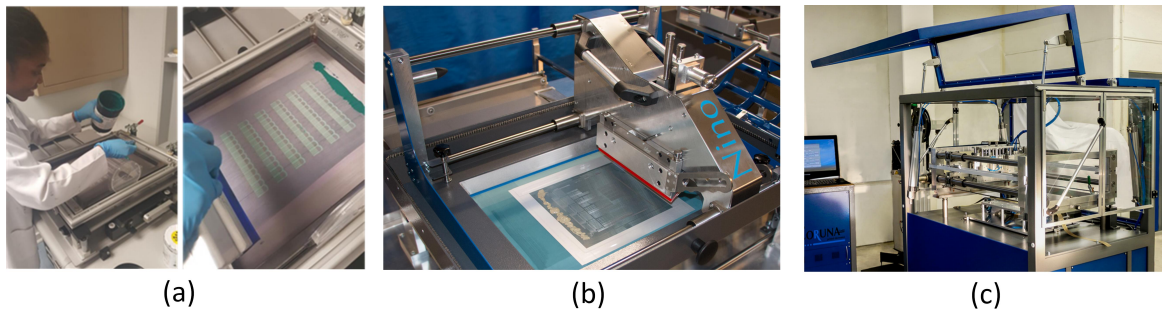


Figure 2.5 a) Manual sheet screen printing process, b) semi-automated sheet by sheet screen printer (Nino – High Precision Screen Printer by Coruna Printed Electronics GmbH, Switzerland), and c) automated screen printer set-up capable of reel-to-reel printing (Risto RtR – High Precision Screen Printer by Coruna Printed Electronics GmbH). Adapted from [20] with permission from Springer Nature.

Printed functionality can be achieved through the paper substrate itself, as well as the printable materials that are applied to the substrate. Modifications in the composition of the paper substrate allow for heightened functionality of paper-based diagnostics [8] and printing of paper substrates themselves are currently being explored, for example, by using printable nanocellulose pulp. The use of nanocellulose for implementing printed electronics has gained attention [52] and along with advances

in paper-based microfluidics and diagnostics [7,26], forms the foundation on which to further develop augmented printed functionality for paper-based diagnostics.

From a printed electronics perspective, conductive inks, which typically consist of metallic particles such as silver, copper, gold, or carbon, are a foundational material. Carbon is generally less conductive than metals but lower in cost and often exhibits favourable chemical properties. Transparent conductors such as indium tin oxide (ITO) and more recently poly(3,4-ethylenedioxythiophene) polystyrene sulfonate (PEDOT:PSS) and graphene are utilised in the printing of components such as solar cells and organic light-emitting diodes (OLEDs) [60]. Functional pressure and temperature sensitive inks are also commercially available [19]. Once printed, ultra-violet (UV) or low-temperature curing is used to remove the solvent and form solid, conductive features that adhere to the substrate.

Functional components often require multilayer printing where a semi-conductor or dielectric printable material is used as an intermediate layer between two conductive layers [16, 56]. This is useful for components such as capacitors or high-frequency antenna designs (Figures 2.6c and 2.8b). Alignment becomes important in these cases and printer technology requirements may be more sophisticated.

Combining functional conductive elements successfully into cellulose substrates such as those used for paper-based diagnostics has been explored, but has proven to be challenging [63]. The substrate choice for printing of functional components is also crucial for control of the printed geometrical dimensions and the successful implementation of the desired functionality [16] and a balance needs to be reached between the achievable printed functionality and the cost of the substrate.

2.3.2 Printed circuits and components

Individual printed passive and active electronic components are required to build up more complex circuitry and enable augmented functionality for paper-based diagnostics. Parallels can be drawn between printed electronics and integrated circuit (IC) manufacturing technologies, with achievable IC lithography line widths in the region of 10 μm in the 1960s. This is similar to the resolution limit currently achievable using printing technologies such as inkjet printing for electronics [60], highlighting the significant progress still required in printed and paper-based electronics. Both hybrid and fully printed approaches can be utilised (Figure 2.6).

Hybrid printed electronics combine printed, flexible electronics with existing IC technologies [64–67] (Figure 2.6a). Successful integration of bare dies with printed electronics is a possibility, improving the flexibility and lowering the cost of the circuit. Advances in resolution limits for printed electronics continue to be made, and

fully printable components realised, including gravure printed transistors with channel widths as small as $5\ \mu\text{m}$ [68].

Low-temperature soldering, conductive epoxies and crimping can be used to secure and connect the components to the printed tracks, and compatibility of these with the paper substrate is an important consideration. The rigidity of the packaged components can also limit the flexibility of the device, but bare die formats or small, thin and flexible packaging can alleviate these challenges to a certain extent. Integration using pick and place equipment for the components is feasible [60], but in smaller quantities, remains a manual process.

Fully printed electronic components such as resistors (Figure 2.6b), capacitors (Figure 2.6c), inductors (Figure 2.6d) and transistors have been realised on various flexible and paper-based substrates [69–71]. Printed functionality can also be implemented for readout and display purposes by using different techniques [19], including printed light sources such as OLEDs.

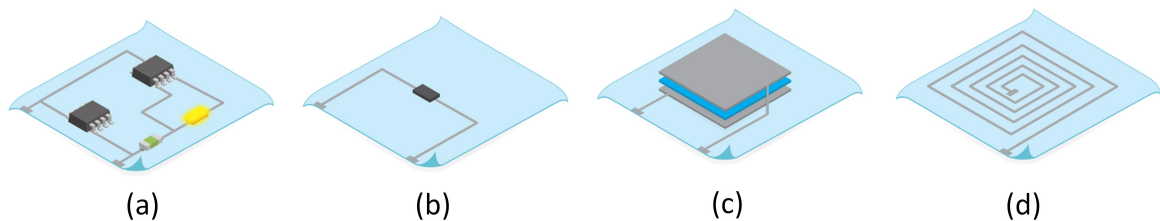


Figure 2.6 Printed circuits and components: a) Hybrid printed electronics with surface mount components such as ICs and light-emitting diodes (LEDs), mounted onto printed circuit tracks on paper. b) Printed resistor with silver tracks and a resistive material to connect the terminals and create a resistive element. c) Printed stacked capacitor structure with a dielectric material printed between two conductive electrodes. d) Printed inductor design with conductive tracks printed in square spiral shape. Adapted from [19] with permission from the Royal Society of Chemistry.

OLEDs enable flexible and printable lighting and display solutions [72]. A layer of organic material is sandwiched between two conductors (an anode and a cathode) (Figure 2.7a). The organic layer of emissive electroluminescent enables bright red, green and blue light to be emitted in response to an electric current [60]. Encapsulation for protection from moisture and oxygen are important design considerations in the printing of OLEDs [60]. Recent developments have enabled OLED components to be screen printed, for ease of integration with scalable manufacturing processes [73].

The development of paper-based OLEDs has been limited as a result of the high sensitivity of OLED active materials requiring exact thicknesses, which can be difficult to

achieve on paper [74], but functional, flexible OLEDs fabricated using standard printing paper [75] and transparent cellulose substrates [76] have been presented. OLEDs manufactured on cellulose have exhibited constant current and power efficiencies in the ranges of 10 to 100 μA and 4 to 8 V. These devices could be integrated as part of low-cost, flexible REASSURED paper-based diagnostics for visual feedback, result readout or as an excitation source, making use of on-board battery power and an environmentally friendly approach.

Printed sensing components have also been developed and include electrochemical, impedance and other biosensors [61], which have been comprehensively reviewed [77]. Printed resistive sensors form a large part of the printed sensing capabilities on paper substrates, where foldable, low-cost designs [78] and multisensory platforms for temperature, humidity, pressure, pH and flow have been implemented [79].

Printable light sensors or photodetectors (Figure 2.7b) have recently been developed [80, 81]. Applications of printed photodetectors include industrial and medical large-area sensing, particularly for colour detection, with potential application to colorimetric detection implemented on paper-based diagnostic devices. In addition, security features for confidential diagnostic testing could potentially be implemented through finger print imaging, which could be integrated as part of future envisaged paper-based diagnostic devices.

Photodetectors printed on to paper have been demonstrated [82] along with inkjet-printed photodiodes [83, 84]. A low-cost paper-based photodetector using ZnS-MoS_2 has recently been presented [85]. The demonstrated sensitivity over a broad spectrum shows promise for the development of devices that could be utilised in integrated REASSURED devices for colorimetric readout of paper-based microfluidic results.

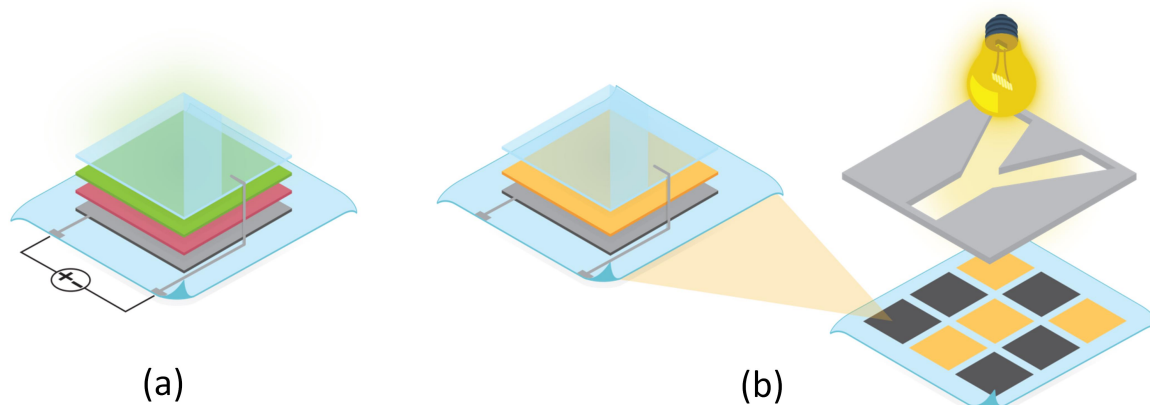


Figure 2.7 a) Printed OLED consisting of two electrodes with a conductive material and an emissive electroluminescent material in between. The latter emits light through the top transparent electrode in response to a current applied at the electrodes. b) Printed light sensor with a conductive electrode (bottom), photosensitive material (middle) and transparent electrode (top). These photodetector elements can also be implemented in a matrix format to realise image sensors. Adapted from [19] with permission from the Royal Society of Chemistry.

2.3.3 Connectivity

Communication of the result from the paper-based diagnostic device will be required for effective result recording and filing of information towards an integrated solution. Connections between paper devices and external instrumentation can be achieved through physical connectors and cables, including disposable universal serial bus (USB) connectors on paper [86] (Figure 2.8a). Wireless communication technologies are particularly advantageous for resource-limited settings, as they eliminate the need for physical connections to instrumentation and prevent contamination. The evolution of the internet of things (IOT) has resulted in a drive to include connectivity between devices and systems [87], including POC diagnostic solutions [12].

Wireless technologies are growing in popularity and maturity, and include RFID, near-field communication (NFC), Bluetooth, WiFi, ZigBee, Infrared, and cellular technologies such as 3G and 4G [88], each making use of different standards, frequency ranges and operational distance ranges. Passive short-range communication technologies such as RFID are better suited from a low-cost, disposable device perspective,

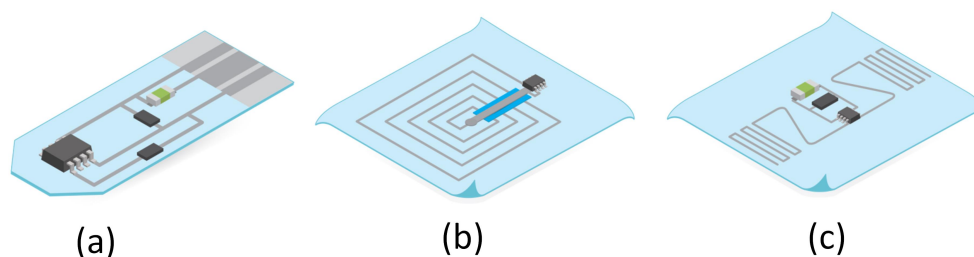


Figure 2.8 a) Physical printed connectors on a paper-based electronic device to connect to standard ports or adapters. Wireless connectivity through printed b) NFC and c) RFID tags. Adapted from [19] with permission from the Royal Society of Chemistry.

where power is not required on the device itself, and have been applied to POC solutions for implantable, wearable and hand-held wireless biosensors [14, 89].

RFID technologies have also been highlighted as beneficial solutions for rural e-health systems [90] and have been used in hospitals for patient monitoring with some success [91]. RFID has emerged as a useful tool for healthcare applications in terms of patient tracking and identification [92], with advances in the field improving the technological capabilities and costs [93]. More recently, design frameworks for sensors and RFID tags with healthcare applications have also been formulated [94], along with privacy preservation in RFID systems for healthcare [95] to enable a secure, confidential method of data communication and storage. RFID offers the potential to address many of the challenges in POC testing performed in South Africa as well as the Ideal Clinic implementation as this can be utilised for device tracking, identification and management.

RFID utilises radio frequency electromagnetic fields to transfer data wirelessly, typically for the purposes of identification and tracking of assets [96]. An RFID system consists of a tag, an antenna and a reader (Figure 2.9). The tag is typically made up of an antenna and an RFID IC on a substrate that may be flexible or rigid, and that can be packaged to take on a variety of form factors [96–98]. The antenna uses power from the reader to generate a field and enable the reader to transmit and receive signals from the tag. Antennas vary in size, cost, polarization (linear, circular) and gain. Readers can be fixed, handheld, or integrated (with a built-in antenna), allowing for portable, mobile systems to be realised. Readers can be powered via batteries, power over ethernet (POE) or USB to interface directly with a personal computer (PC) [96]. Various RFID development kits are readily available, enabling the development of customizable RFID solutions. Several standards of RFID are in

use – ISO, Class 0, Class 1, Gen 2, etc., and each country has its own frequency allocation for RFID [97].

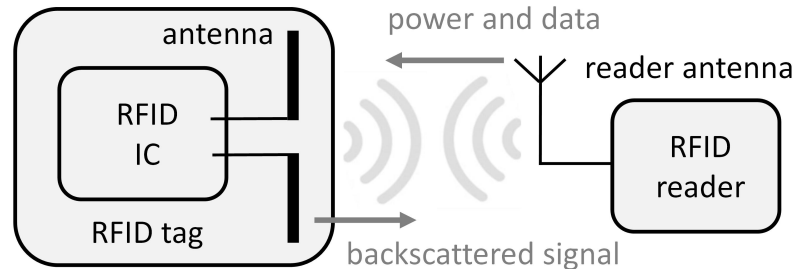


Figure 2.9 RFID system overview showing tag, antenna and reader components. Figure adapted from [97], ©2005 IEEE.

Three primary frequency ranges are used in RFID systems, namely: 125 to 134 kHz for low frequency (LF), 13.56 MHz for high frequency (HF), and 860 to 960 MHz for ultra-high frequency (UHF). UHF systems can be either passive (powered by radio frequency (RF) energy) or active (battery powered), with the latter also operating at 433 MHz and 2.45 GHz. UHF is attractive as it provides much longer read ranges than LF and HF systems. NFC falls within the HF RFID category. In addition, passive UHF RFID tags are low in cost, have a wide range of tag sizes and types, comply with global standards, and have high data transmission rates. A drawback of UHF RFID systems is that infrastructure costs are typically higher, but developments in RFID reader technologies have enabled portable, low-cost solutions to be realised more ubiquitously.

The electromagnetic field surrounding an RFID antenna consists of a near-field and far-field. LF and HF often use near-field antennas and inductive coupling, where a magnetic field is generated by the reader antenna, which activates an electric current in the tag's antenna [99]. Passive UHF typically utilises far-field antennas and backscatter coupling or passive backscatter modulation, where RF energy is generated by the reader to activate the RFID tag. The tag modulates the information and reflects the remaining energy back to the reader antenna. A unique number or electronic product code (EPC) is assigned to each RFID tag and can be read out when the tag is scanned.

This communication is performed according to GS1 EPCglobal UHF Class 1 Gen 2 specifications, which are ratified as an ISO-18000-6C standard. UHF waves are typically in the range of 33 cm in length, and typical passive UHF systems have maximum read ranges up to approximately 30 m. UHF tag antennas are typically

dipole shaped, and include half-dipoles, short dipoles, and modified dipoles, which can be fat, meandering, or tip-loaded [99]. In addition to dipole antennas, slot antennas and patch antennas are also widely utilised [97, 98].

RFID is well-suited to paper-based diagnostics as the tag antennas are printable and paper is suitable for UHF and microwave applications [100]. UHF RFID solutions are attractive from a printing perspective, as the antenna designs typically have simple form factors, such as dipoles, making them easier to print. UHF RFID solutions also have longer read ranges than NFC, for example, where near-contact methods are utilised from a reader such as a mobile communication device.

Printed antennas [101–106] and printed RFID tags [107–112] on low-cost paper and cardboard substrates have been investigated using both inkjet and screen printing techniques [113] (Figures 2.8b and c). Combinations of RF, microfluidics and inkjet printing technologies to implement wireless sensing platforms that are activated by fluids in microfluidic channels have also been studied [114, 115]. Fluids can be used to activate or control the properties of the antennas.

RFID solutions with sensing capabilities have emerged as promising tools for a variety of applications [116–119], and add to the value proposition of RFID technologies for the integrated sensing and connectivity of paper-based diagnostics. RFID sensors may be passive, battery-assisted, or chipless, with battery-assisted being the most mature technology [120].

Some paper-based communication and sensing modules that have been implemented include patch antennas, UHF oscillators, mixers and frequency doublers [121], which make up a variety of communication capabilities. In addition, paper-based microfluidics have been integrated with self-assembling RFID tags to create a self-powered biosensing platform [122]. Examples of cost-effective UHF RFID tags that enable sensing and actuation, computation, data storage and bidirectional communication with the reader have been showcased [123]. ICs such as the SL900A (AMS, Austria) provide attractive UHF RFID sensing solutions, with a variety of on-board sensing capabilities that negate the need for additional complex circuitry.

Commercially available NFC RFID tags embedded into paper substrates are also available [124] for various applications. These technologies can be integrated with paper-based REASSURED devices in their current form to enable effective wireless communication of information and results from the disposable diagnostic devices for processing and storage.

UHF RFID enables a “black box” reader solution to be implemented, providing a favourable implementation for rural clinics [112], and eliminating the risk of theft or tampering with the reader device. This approach also enables the reader to be mounted or enclosed on a wall or surface in the clinic, reducing the risk of dam-

age and maintenance required over long periods as it could be sealed from external environmental factors. The disposable RFID tag can be either passive (without a battery) or semi-passive (with a battery), with the former reducing the cost considerably and increasing the long term reliability. In the case where batteries are required for powering on-board functional components, printed batteries could be utilised [125].

2.4 Integrated and scalable paper-based solutions

The integration of various printed functionality components is required for fully REASSURED paper-based POC diagnostics to be realised. POC diagnostic devices on flexible substrates [14] and integration of printed electronics into the real world [126] have been explored with the potential for future wearable applications. Printed diodes, antennas and electrochromic displays have been combined to form an all-printed electronic tag for IOT applications [127]. Examples of integrated flexible devices include a connected electrochemical sensing platform resulting from a collaboration between Acreo AB and Linköping University [18, 126, 128] (Figure 2.10a), a device to track micronutrient deficiencies [129], and a disposable system to measure hydrogen peroxide and total cholesterol, which is compatible with a mobile application for the readout of results [17] (Figure 2.10b).

Paper-based solutions of co-fabricated microfluidics, electronics and batteries [67] and electrochromic readout for electrochemical sensing with on-board power [130] have been showcased, as well as connected paper-based temperature [119] and gas [131] sensors implemented on RFID wireless platforms. Paper-based piezoresistive pressure sensors combined with visual readout for medical applications, such as measuring bandage compression [132] and infant birth weight [133], have also been presented (Figure 2.10c). Paper-based diagnostics that have been introduced to the market have been summarised [7] and include developments by Diagnostics For All (DfA) [134] for liver function and nucleic acid testing, text-reported blood typing by Haemokinesis [28] and LFT devices for infectious diseases by INSIGHT [135].

Established techniques such as roll-to-roll printing can be utilised for mass production of printed electronics and functional systems. The pilot factory established by PrintoCent [60] has assembly processes in place for the production of hybrid electronic devices. Lateral flow and dipstick tests already use established mass manufacturing techniques, but for newly developed paper-based diagnostics, scalability of microfluidic structure patterning, deposition of assay components, and assembly of multi-layered devices will be crucial for successful mass production [7, 58]. Substrates, inks, manufacturing processes, assembly and integration as well as fabrication time are

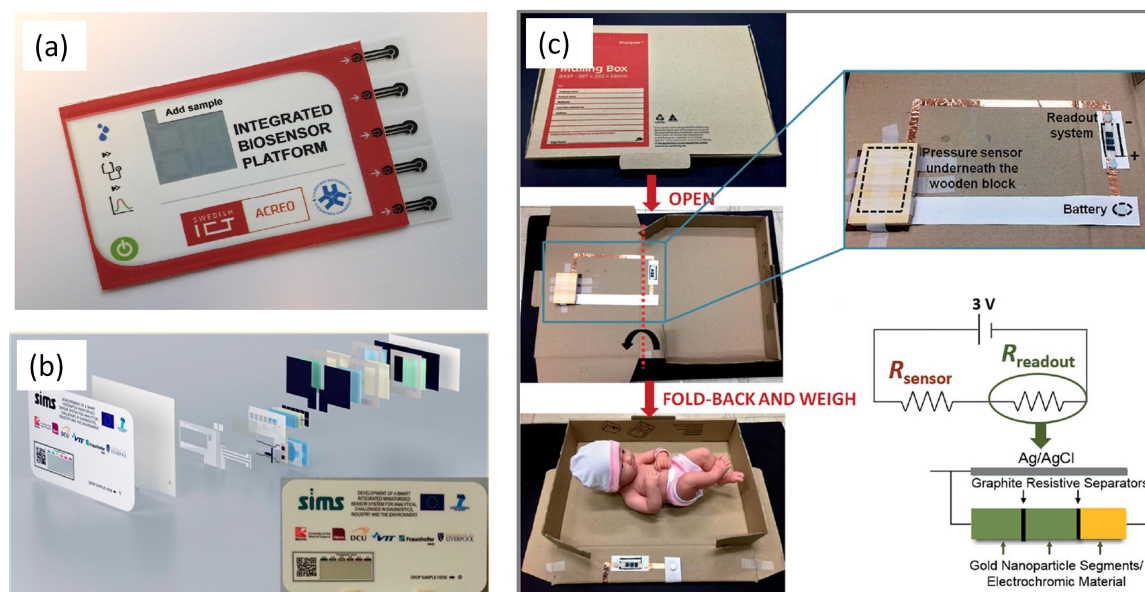


Figure 2.10 Integrated printed solutions towards ASSURED diagnostics. a) Printed electronic components combined to form smart, connected and flexible systems and printegrated biosensors [18], b) integrated printed diagnostic device for measurement of hydrogen peroxide and total cholesterol. Reprinted with permission from [17]. Copyright 2017 American Chemical Society. c) A “balance-in-a-box” birth weight system with paper-based readout and a piezoresistive pressure sensor. Reproduced from [133] with permission from The Royal Society of Chemistry.

important cost factors to consider for the successful commercialization of paper-based diagnostics with enhanced functionality.

RFID, smart packaging and printed electronics technologies are complementary and have seen substantial growth in recent years. An estimation of the total RFID market worth for 2017 was 11.2 billion USD and is projected to reach 14.9 billion USD in 2022 [120]. This includes tags, readers, software and services for various RFID form factors for both passive and active RFID and reflects the growing market for these technologies. The RFID sensor market is estimated to reach 120 million USD in 2022, with a projection of 980 million USD in 2027 [120]. In conjunction, smart packaging has been accelerated in recent years [136] and is poised for pharmaceutical applications, which are likely to extend to more general healthcare applications in future. Smart packaging needs to combine technologies for sensing, communication, computing and storage with packaging for successful solutions to be realised. The

packaging eco-system encompasses packaging companies, transport and logistics, and the consumer or end-user [136]. These trends, combined with the growth and initial commercial success of printed electronics, pave the way for unique solutions to be developed to address global challenges such as healthcare.

Although examples of integrated, augmented printed diagnostic solutions have been presented, many of these systems still require components to be added to provide a complete solution, for example, where communication or automation is required without the use of a mobile communication device, or where lowering of device costs is required. Maintenance, disposability and production feasibility and scalability are also important aspects for consideration as part of the development of these integrated solutions. Paper production, printing and packaging are long-standing and scalable processes, which could not only be utilised to produce these devices, but are also widely available in Africa.

These augmented paper-based devices are to be integrated with clinic requirements and existing infrastructure to realise truly effective solutions. Although initial case studies for the deployment of paper-based diagnostics into clinic settings have been explored [137], investigations into how appropriate and feasible integrated paper-based solutions could be implemented from a Southern African clinic perspective are currently lacking.

This work aims to develop a technology and packaging solution suited to South African rural clinics for readout from paper-based diagnostic devices, which will be described in more detail in the next chapter.

3 Technical background

Parts of this chapter are based on previously published work [138] and have been re-published with permission of IOP Publishing Ltd., with permission conveyed through Copyright Clearance Center, Inc. Sections of this chapter have been submitted to Nature Scientific Reports as part of a manuscript that is awaiting reviewer feedback.

To reach the objectives set out in Chapter 1, a reusable printed RFID-based colour detector and result communication device was realised. The device development was based on findings from interviews conducted at different clinic sites in South Africa, which highlighted the current limitations and requirements in these settings. The low-cost wireless reader device is sufficiently low in cost and can be disposed of after several tens to hundreds of uses, without the need for maintenance. The device provides a modular solution, adaptable to various paper-based test formats. This chapter describes the approach followed in the development of this solution.

3.1 Clinical aspects

Five clinics or community health centres were visited within Tshwane Districts 1, 5, 6 and 7 in Gauteng Province, South Africa. Interviews were conducted with five professional nurses with average work experience of 26 years each. The clinic patient numbers per month range from 4000 to 24000. Interview questionnaires were designed to assess the greatest challenges faced, as well as current workflows for patient and result tracking and documentation. Consent forms were signed by all participants. Ethics approval for the study was obtained from the Council for Scientific and Industrial Research (CSIR), Pretoria, South Africa, once the project was registered with the National Department of Health in South Africa, and permission forms were completed and signed for each district and establishment visited. All research was performed in accordance with the relevant guidelines and regulations. Informed consent was obtained from all participants.

The interviews enabled the current workflows of clinics and their limitations to be summarised (Figure 3.1a). Manual processes for result readout, capture and communication, along with sample and result tracking, make up the current workflow bottlenecks. These findings confirm published work regarding clinic workflows and challenges in South Africa [4, 9, 46, 47, 50], reaffirming the need to find low-cost, automated methods for result readout and communication and storage of results. Other points that emerged from this study included aversity to the use of mobile phones as tools in the clinic settings, with theft being a primary concern. In addition, harsh environmental conditions and lack of skilled technicians result in equipment that is not maintained. Consequently, faulty equipment is used for diagnosis, or equipment is simply unused or discarded. As an example, a module failure rate of more than 40% was reported for early results obtained from Gene Xpert MTB/RIF® systems implemented in nine countries. This figure includes a test failure rate of more than 10%, but the remaining failure rate is attributed to irregular power supplies, dust build up, overheating, and a lack of staff quality control [139, 140].

3.2 Proposed solution

Using the insights gained from the Southern African clinic context along with the context provided in Chapter 2, unique solutions can be developed for POC diagnostics, which can be locally manufactured and sustainably supplied. Important specifications of this solution include:

1. Automated result readout.
2. Automated result capture.
3. Automated sample and result tracking.
4. Automated result communication and connectivity between laboratory and central database.
5. Low cost of diagnostic device.
6. Limited or no maintenance required.
7. Low power requirements and limited dependence on electricity.
8. Scalability of solution for mass production and deployment.
9. Limited user interaction for ease of use (facilitated by 1 – 4, 6 and 7).
10. Limited dependence on network connection – transmission of result when connection is available (facilitated by 2 – 4).

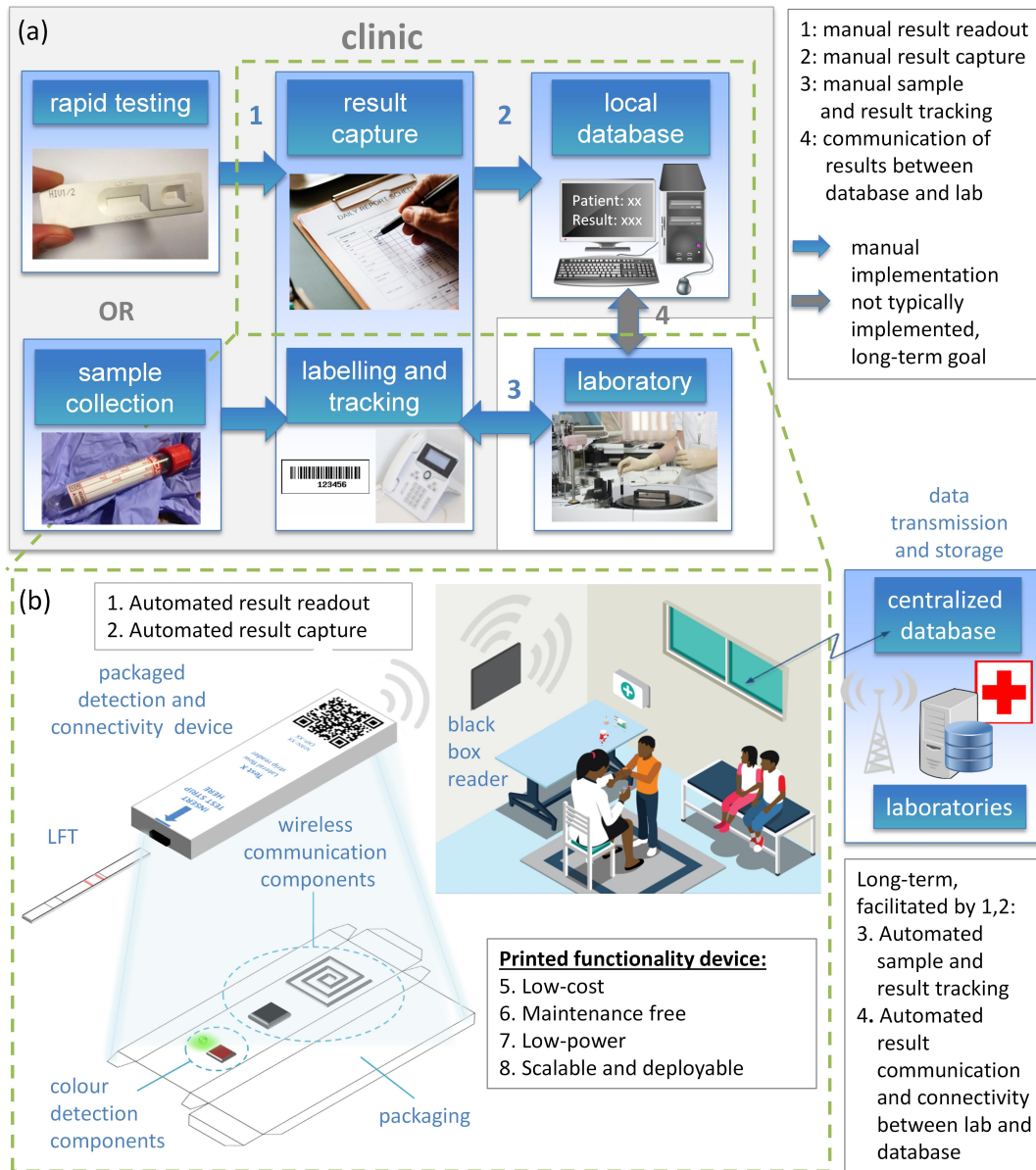


Figure 3.1 a) General workflows applied in South African clinics for HIV and TB testing. Labelling of samples and follow-up of results from the laboratory are performed manually. The presented work falls within the green dotted lines and addresses links 1 and 2 directly, with link 3 strengthened through the implementation of connected devices and systems. Through automated readout and digital labelling, the bottleneck and lack of communication between the clinic and the lab (link 4) can be addressed. b) Conceptual design of the proposed solution for integrated paper-based diagnostics for Southern African resource-limited clinics.

The numbered points correspond to the numbering in Figures 3.1a and b. The work presented proposes a solution that takes into account these specifications, with the goal of developing scalable, low-cost, printed solutions for effective POC diagnostics in resource-limited settings.

To address the highlighted specifications, a re-usable printed RFID-based colour detector and result communication device is proposed (Figure 3.1b). The device is sufficiently low in cost that it can be disposed of after several tens to hundreds of uses without the need for any maintenance. As an initial example, single-use LFTs are used with the device to wirelessly readout a colour result using a “black box” RFID reader, which would be mounted onto a wall or table in the clinic as a permanent fixture to read the printed devices. The RFID reader requires only a small amount of power and can be controlled and inspected remotely, as implemented in retail stores and supply chain management systems [141,142]. The device does not require on-board power and instead can harness power from the RF field when in the range of the reader. Continuous data connectivity would not be required, as the reader system could store data and transmit this when required or when a connection becomes available.

The device consists of components for colour detection and wireless communication, along with printing and packaging to realise a reader solution into which LFTs will be inserted (Figure 3.1b). The development approach for the various components will be described in the sections that follow.

3.3 Colour detection

Colorimetric readout is typically implemented for paper-based diagnostic devices, as discussed in Chapter 2. Many assays use colour as a quantitative or semi-quantitative readout to detect the presence of an analyte of interest [34]. The colour is produced in various manners; in some instances using a conjugated enzyme to generate colour from an added substrate, such as in enzyme-linked immunosorbent assay (ELISA). In other cases, colourful labels are bound to antibodies or analytes of interest and visualised upon their binding by an immobilised capture molecule. These labels include gold nanoparticles, dye filled liposomes, cellulose nanobeads or latex particles, and are available in various colours [143].

As discussed in Chapter 2, image analysis is typically performed for paper-based diagnostics, using images captured by a camera or smartphone that utilise complementary metal-oxide semiconductor (CMOS) sensors. This enables RGB and greyscale values – the latter being most commonly used in image analysis-based colorimetry – to be obtained to relate the colour information to the amount of analyte [40]. However,

for tests that utilise multiple colours (e.g. universal pH test strips), greyscale cannot track these colour changes, and alternative colour systems such as the International Commission on Illumination (CIE) 1931 colour space [144] can be used to measure the colour effectively [40, 145].

The aim of this work is to realise a low-cost solution suited to resource-limited clinics, where external instrumentation such as a camera or the use of mobile phones is undesirable. As such, a simple, low-cost colour sensor will be implemented, consisting of a light source and a sensor to measure the light intensity. Typical commercial colour sensors consist of a white light emitter and an RGB receiver that enables three separate colour components to be measured with peak sensitivities at wavelengths of 580 nm (red), 540 nm (green) and 450 nm (blue). Alternatively, a colour changing light source can be used with a sensor for measure the light intensity to implement a colour sensor. Examples of compact, portable colorimeters are available [146].

Different light source and detector configurations can be utilised depending on the paper test format. Reflectance and transmission measurements are commonly utilised, with the light source and detector either above the paper test, or with the paper test in between the light source and detector, respectively. This work initially explores a LFT device format that utilises gold nanoparticles. A number of commercially available devices (pregnancy tests, etc.), which can readily be purchased over the counter at pharmacies, as well as LFT devices developed in-house for *E. coli* detection in water, make this an accessible approach. A reflectance-based light source and detector configuration is thus developed as part of this dissertation (Figure 3.2a).

Aggregation of gold nanoparticles on the LFT devices occurs as a result of their specific interaction with the analyte (e.g. antigen) and causes a colour to be formed [34]. The greater the aggregation, the greater the intensity of the resulting signal. The LFTs used in this work are described in further detail in Chapters 5 and 8.

Light sources with specific peak wavelengths can be utilised to maximize the absorbance of the gold nanoparticles on the LFTs and to enhance the perceived colour. Matching the peak wavelength of an LED with the peak absorbance of the gold nanoparticles enables optimal detection of the gold nanoparticle concentration. Where various colours need to be detected, LEDs with a broad spectrum can be utilised as a light source, with a resulting broad detection spectrum.

Different photodetectors, including phototransistors and photodiodes, can be used for colour detection by measuring the light intensity. These devices convert light signals into electric current and can be used for different applications, where interface circuitry, wavelength and mechanical alignment need to be optimised accordingly [147].

Photodiodes are commonly used for light sensing applications and produce a current flow when they absorb light, operating either as a photovoltaic diode (solar cell)

or as a photoconductor, which is a reverse-biased photodiode. The resistance of the photodiode to the reverse bias current decreases when light shines on the device, and this current provides a measurement of the intensity of the incident light. Important specifications of photodiodes include the spectral response, sensitivity, gain and response speed, and the performance is largely determined by their material, packaging, and area of the photosensitive material.

Although photodiodes are advantageous as they are typically faster than phototransistors, have a wider frequency response, and are less sensitive to temperature changes, these devices need to be used in conjunction with a transimpedance amplifier (TIA). The TIA converts the low-level current flow into a usable voltage signal (Figure 3.2b).

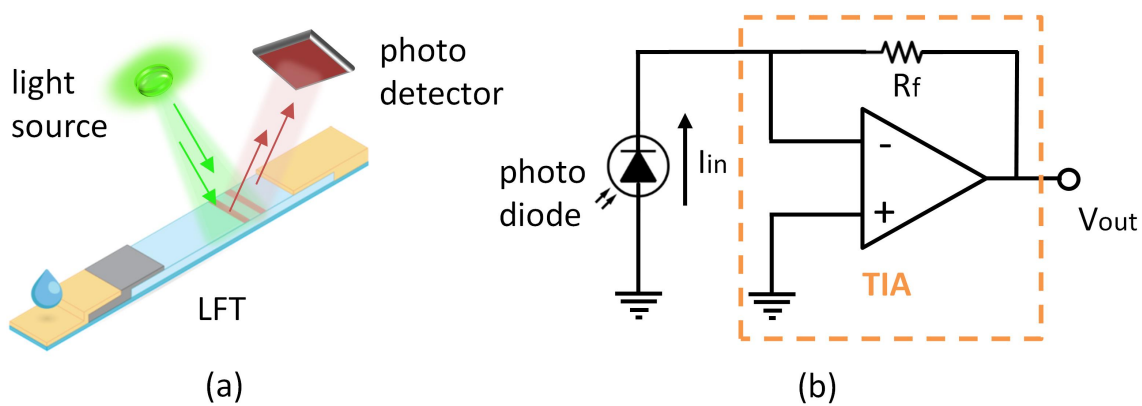


Figure 3.2 a) Example of reflective configuration for colour detection for an LFT and b) schematic of a photodiode for light detection using a TIA to convert low-level current (I_{in}) into a measurable voltage (V_{out}). A feedback resistor R_f is used to set the gain of the amplifier. Adapted from [19] with permission from the Royal Society of Chemistry.

As discussed in the following section, this dissertation focuses on a wireless sensing RFID solution that accommodates external optical sensing capabilities. This enables a photodiode to be connected directly as a colour detector solution with built-in amplification already provided by the sensor front end of the RFID IC.

To assess the performance of the developed colour detector solution, both a commercial portable LFT reader and image processing techniques were used for result comparison. A commercial LFT reader (ESEQuant, Qiagen, Germany) was utilised, which employs LED excitation and photodiode detection for fluorescence and colorimetric detection, with excitation ranges from 365 to 660 nm and emission ranges from 460 to 720 nm.

ImageJ analysis was also performed using a scanned image of the LFTs to quantify the colour information. ImageJ is a widely used open-source image processing program designed for scientific images and is often used for the analysis of LFTs [148]. Images of the LFT strip devices were captured using a scanner (HP Scanjet 2400) and the accompanying HP Solution Centre software. Figure 3.3a shows an example of a scanned image of a model LFT device with dimensions of 55 mm \times 5 mm. The test line width is 1 mm. Details of the model LFT devices used for the initial colour detector tests are provided in Chapter 5. Analysis using ImageJ was performed by first converting the image into greyscale. Next, a region of interest (ROI) was selected on the LFT that falls within the area of the test line (ROI: width = 35 pixels, height = 5 pixels) and analysed to produce a plot profile, which was exported to a .csv file (Figure 3.3b). An average of all the values captured per ROI was then determined to give an average greyscale or intensity value for the test line of interest. For the example shown in Figure 3.3b, small fluctuations in the greyscale values within the ROI on the test line, ranging between 70 and 77, can be seen.

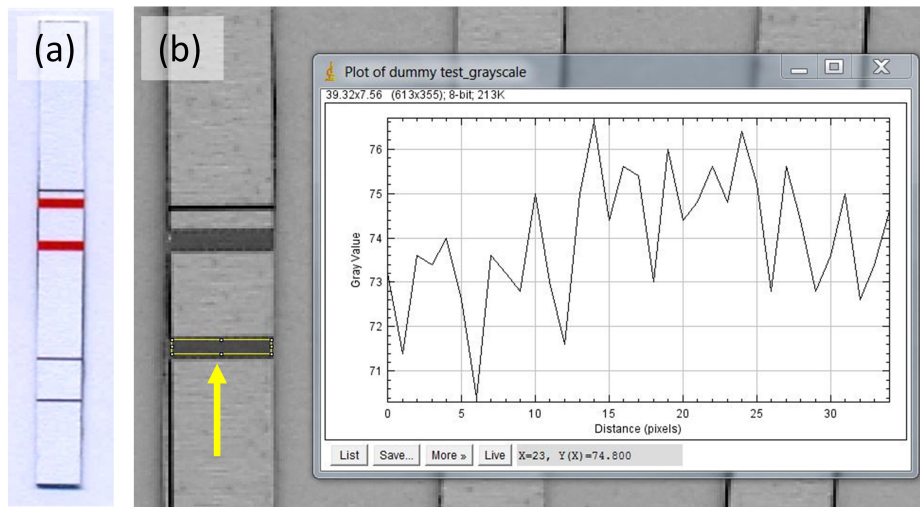


Figure 3.3 a) Example of scanned image of model LFT and b) analysis using ImageJ to obtain intensity measurement. The yellow arrow indicates the ROI selected and corresponding plot profile for this area.

3.4 Sensing RFID

The advantages of UHF RFID were described in Chapter 2, along with sensing RFID solutions to provide integrated solutions for various applications, including medical and environmental monitoring. To expand on this, a sensing UHF RFID IC (SL900A-AQFM, AMS, Austria) was explored with the aim of providing a compact, integrated solution that could enable automated readout and communication of results to an external device in a wireless, contamination-free manner. This approach also aligns strongly with a framework developed for sensing and RFID tag technologies for health-care applications [94], where design decisions between technology, architecture and algorithms are presented.

The SL900A sensing RFID IC is advantageous for both the detection and connectivity of paper-based diagnostics as it is a single chip solution with extensive sensing capabilities, where resistance, capacitance, voltage and current can be measured. The IC complies with the EPC Gen2 1.2 standard, operating in the UHF band (860 to 960 MHz) with a set of custom commands (cool-LogTM). Read distances in the cm to m range are achievable for a wireless solution to be realised using the RFID analogue front-end (AFE) with a straightforward dipole antenna design that can easily be printed. The IC has an on-board temperature sensor (-40°C to 125°C), 9 kbit electrically erasable programmable read-only memory (EEPROM), serial peripheral interface (SPI), sensor front-end and 10 bit analogue-to-digital converter (ADC). The SL900A can operate in fully passive mode (without a battery) or in battery-assisted mode (1.2 to 3.6 V). The IC has low power consumption and energy harvesting through the RF field is possible for powering external components, assisting with the low-power requirements of the proposed solution in section 3.2.

The RFID chip also has a real-time clock (RTC) and enables identification, verification and tracking, as well as data logging, towards fully integrated and connected POC diagnostic solutions. Data security is provided through password protection, which is an important consideration for medical applications. An overview of the functionality of the SL900A is shown in Figure 3.4a.

3.5 Tag design

An RFID tag design utilizing the SL900A IC was realised based on the reference design implemented as part of the SL900A development kit (SL900A-DK-STQFN16, AMS, Austria) and consists of a half wave dipole antenna. The antenna was designed to obtain the same real part of the impedance as the SL900A IC, while matching of

the imaginary part was achieved by placing an SMD inductor on one of the arms of the dipole antenna. The length (l) for a resonant dipole antenna can be calculated from the wavelength (λ) as

$$l = 0.47 \times \lambda = 0.47 \times \frac{c}{f} \quad (3.1)$$

where c is the speed of light (3×10^8 m/s) and f is the frequency in Hz [149–151]. The SL900A is designed to operate in the frequency range of 860 to 960 MHz. In this work, the frequency range is set for frequency ranges in South Africa (see section 3.7), and assuming a central frequency of 915 MHz, l is calculated as 153 mm. In both the development kit and the tag design used for this work, the antenna dimensions are the same, with each dipole arm having a length and width of 73 mm \times 5.5 mm, respectively, with a 3 mm spacing between the two dipole arms. This gives a total length of 149 mm, corresponding closely to the calculated value of l from equation 3.1.

The input impedance of the SL900A quad flat no-leads (QFN) package used in this work is provided by the manufacturer as $31 - j320 \Omega$ [152]. This varies with the frequency, and can be approximated as $31 - j305 \Omega$ for a frequency of 915 MHz as used in this work. Mounting capacitances, typically between 0.6 and 1 pF, also affect the imaginary part of the input impedance [153], resulting in experimental input impedances of $31 - j286 \Omega$ in some cases. The development kit design utilises a 39 nH inductor for effective impedance matching, and the same design is implemented in this work. A 39 nH surface mount device (SMD) inductor (744786139A WE-MK multilayer ceramic, Würth Elektronik, Germany) is connected between one arm of the antenna and the SL900A chip to match the input impedance of the IC.

Dipole antennas have advantageous omni-directional characteristics, allowing for flexibility in the positioning of the tag relative to the reader. A 3 V lithium manganese dioxide coin cell battery (RS CR1220 3V, RS Pro, RS Components, South Africa) can be connected to the SL900A between V_{BAT} and ground (V_{SS}) for operation in battery-assisted mode and to power external electronic components.

Figure 3.4 shows the schematic and printed tag design for the generic SL900A RFID tag utilised in this work (Chapters 4 and 6). A capacitor can optionally be connected between pin V_{POS} and V_{SS} to extend the read range in passive mode. V_{POS} can also be used to power external components, e.g. outputting up to 3.4 V when in the range of the RF field of the RFID reader. The generic tag design was also used to test tag read ranges with loads connected to pins EXT1 and EXT2, which serve as inputs for various external analogue sensors. EXT1 can be used for a variety of resistive and capacitive sensors, while EXT2 can be used for current and voltage source sensors and optical sensors based on reverse biased diode current. The SL900A sensor front end

contains a built-in TIA, enabling direct readout from a photodiode, and is utilised in this dissertation for colour detection.

The colour detector module was made up of SMDs to create a simple reflectance colour detection configuration, consisting of an LED, a 120 Ω resistor (CRG0603F120R, TE Connectivity Ltd., Switzerland) and a photodiode (SFH 2430, Osram Opto Semiconductors GmbH, Germany). Chapter 5 provides further details on the photodiode and colour detection.

Both commercial and in-house LFTs were tested, as well as commercial pH test strips using the colour detector design (Chapter 8). For the LFTs, a 525 nm green LED (LTST-C190TGKT, Lite-On, Taiwan) was used to maximize the absorbance of real-world LFTs that utilise gold nanoparticles. The LFTs developed in house make use of 40 nm colloidal gold with a peak absorbance between 520 and 525 nm, typically around 523 nm (CG-010, DCN Diagnostics, USA), closely aligned with the peak wavelength of the LED. For the pH tests, a white LED (VLMW1300-GS08, Vishay Intertechnologies, USA) was used to provide a broader detection spectrum, and could also be utilised with paper-based tests that implement a variety of colours.

Figure 3.5 shows the schematic and printed tag design for the SL900A based colour detector tag utilised in this work (Chapters 5, 7, 8 and 9). A printed dielectric layer is used in the tag design to enable multilayer printing of electronic circuitry and a single-sided printed solution.

3.6 Printing and assembly

The tag designs shown in Figures 3.4b and 3.5b were printed via manual screen printing using a ZelPrint LT300 stencil printer (LPKF Laser and Electronics, Germany). The printer was modified to house screens manufactured by Chemosol (Pty) Ltd. (Johannesburg, South Africa). The screens consisted of a synthetic mesh with 71 threads/cm (71/180-55 PW, SEFAR PET 1500, Sefar AG, Switzerland). Manual screen printing was carried out using a rubber squeegee (70-75 Blue Apolan, Chemosol). A conductive silver screen printable ink (AG-800, Applied Ink Solutions, USA) was used to print the tag designs, and was cured in an oven at 90°C for 15 min. For the printed dielectric layer of the colour detector tag, a UV-curable dielectric ink (Loctite EDAG 452SS E&C, Henkel, USA) was used and cured at a wavelength of 365 nm using a handheld UV lamp (3UV-38, UVP, UK) for 4 h.

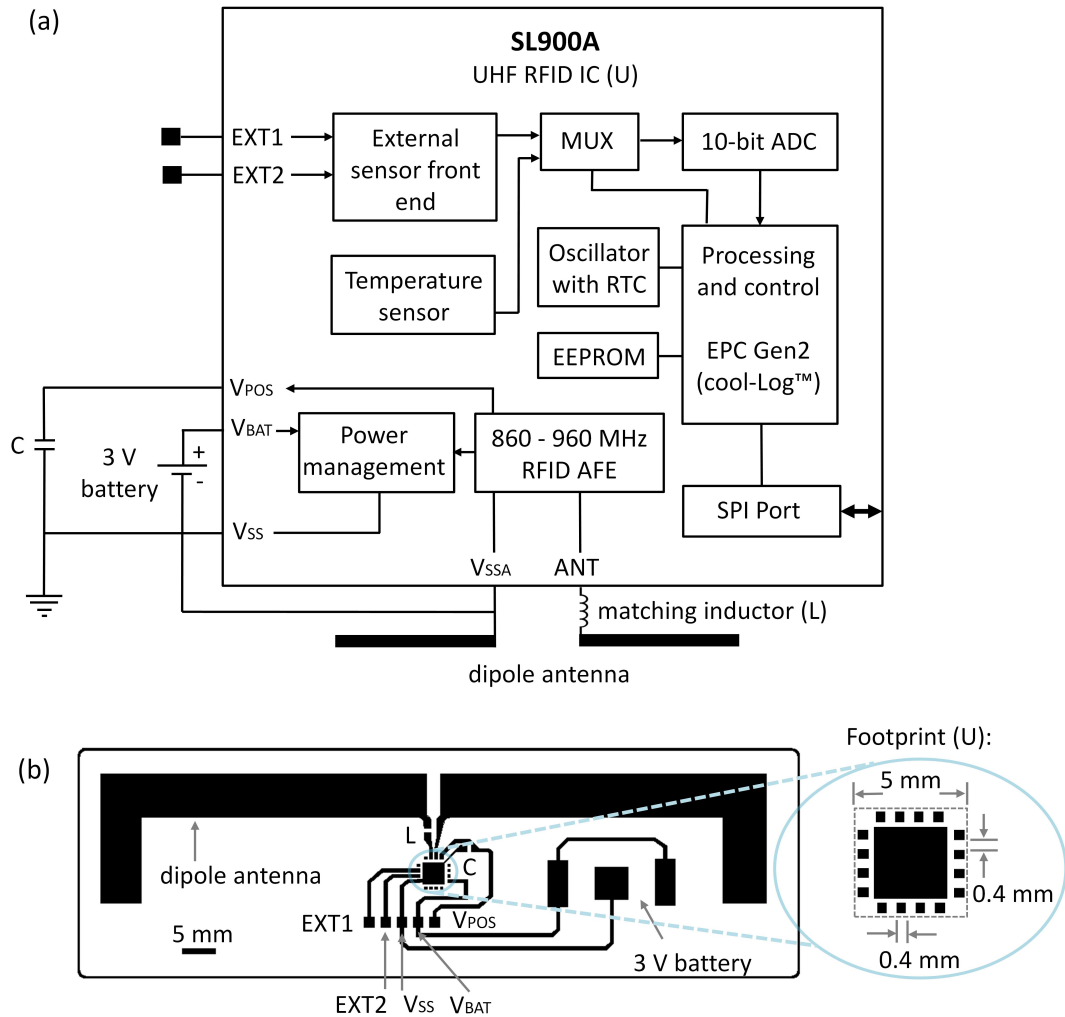


Figure 3.4 Generic SL900A tag design illustrating a) schematic of sensing RFID tag; $L = 39$ nH, C is not utilised. b) Printed design of generic tag, showing the various components, pins and the footprint of the SL900A IC (U). Tag dimensions = 110 mm \times 35 mm. Republished with permission of IOP Publishing Ltd. from [138]; permission conveyed through Copyright Clearance Center, Inc.

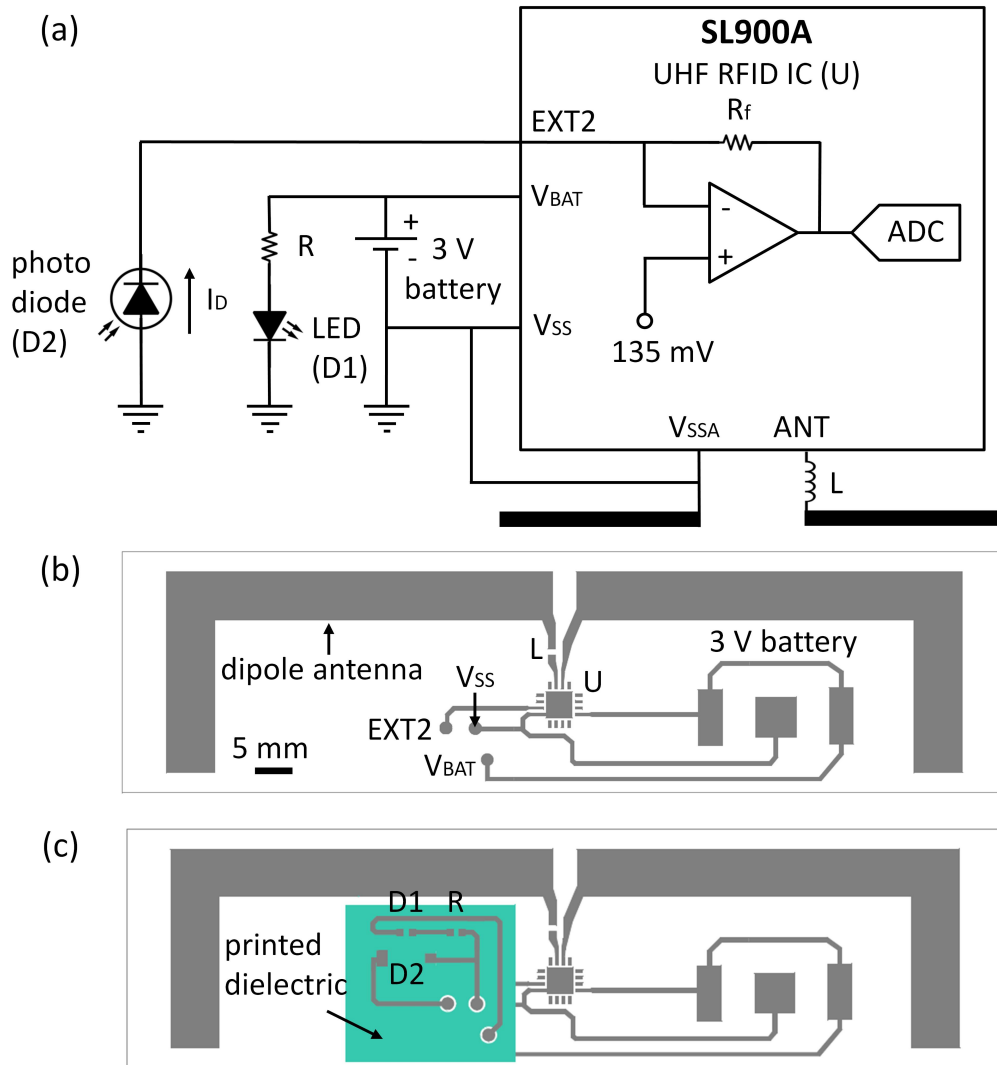


Figure 3.5 Wireless colour detector tag design illustrating a) schematic of sensing RFID tag; $R_f = 185 \text{ k}\Omega$, $R = 120 \text{ }\Omega$, $L = 39 \text{ nH}$. Image credit: photodiode, LED and inductor by Arthur Shlain, resistor by Michael Senkow, from the Noun Project. b) Printed design of colour detector tag, showing the first printed layer, and c) the second and third printed layers of the printed design. Tag dimensions = $110 \text{ mm} \times 30 \text{ mm}$.

The tag designs were printed onto various flexible substrates. A two-component silver epoxy conductive adhesive (186-3616 RS Pro Silver, RS Components), curable at room temperature in 24 h was used to mount and secure the various SMD components. A brightfield microscope (EMZ-8TR, Meiji Techno, Japan) was used for visual alignment of the components onto the printed tracks. Copper adhesive tape (3M Copper Foil Tape 1126, Digikey, USA) was used to secure the coin cell battery. Examples of the printed and assembled tags are shown in Figures 3.6 and 3.7 for the generic and colour detector tag designs, respectively.

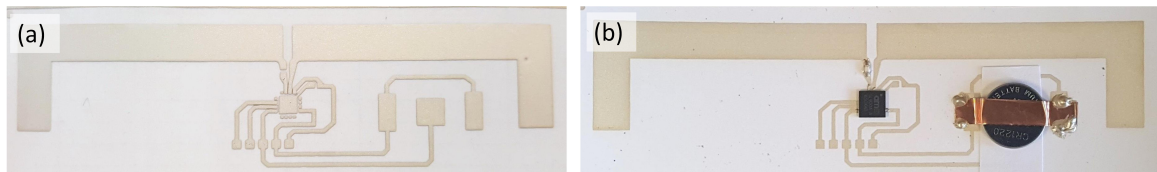


Figure 3.6 a) Printed generic SL900A tag and b) assembled printed tag with all components mounted. Tag dimensions = 110 mm \times 35 mm. Republished with permission of IOP Publishing Ltd. from [138]; permission conveyed through Copyright Clearance Center, Inc.

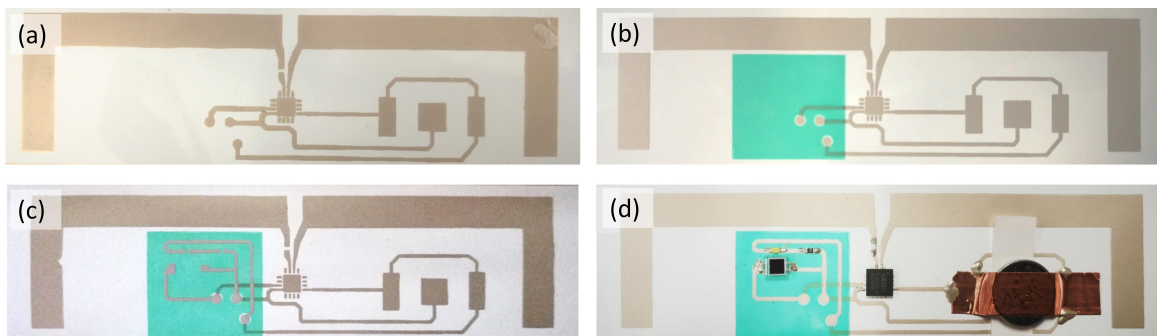


Figure 3.7 Printed wireless colour detector tag design, showing a) first printed layer, b) second printed layer (green dielectric), and c) third printed layer. d) Assembled printed tag with all components mounted. Tag dimensions = 110 mm \times 30 mm.

3.7 Wireless readout

Wireless readout of the sensing RFID tags was performed using the RFID reader development kit (AS3993-QF_DK_R Fermi reader, AMS, Austria), recommended for use with the SL900A. The reader kit consists of a monopole reader antenna and a

reader module, which are mounted onto a plate on an adjustable sliding clamp to enable read range measurements to be performed in a controllable set-up (Figure 3.8a). The height of the mounted reader antenna as well as the positioning for testing different tag orientations could easily be altered for extensive read range measurements to be performed (Chapter 6). The reader module has a USB interface for connection to a PC for detecting and analysing RFID tags using the AS3993 software and a graphical user interface (GUI) that forms part of the reader development kit (Figures 3.8b and c).

The power transmitted by the reader was 22 dBm, with the reader sensitivity set to the default value of -68 dBm. The reader settings were selected with Korea (917 to 920 MHz) as the region, as this falls within the standard South African frequency range for RFID (908 to 928 MHz). Instantaneous sensor readout could be performed directly through the user interface (Figure 3.9) for both temperature as well as for readout from external sensors connected to EXT1 and EXT2, where the ADC sensor value could be retrieved directly through the AS3993 reader user interface software.

The cool-LogTM custom command set allows for ease of sensor readout from the SL900A. Various parameters can be adjusted to optimise the sensor readout depending on the type of sensor connected and the sensor specifications. These settings are described in further detail in Chapters 5 and 6).

Modifications were made to the standard C++ user interface software for the reader development kit, to perform calculations directly on the sensor readout and enable the sensor value to be stored to a text file. Thresholding methods can be used to determine whether a result is positive or negative, or to establish the concentration or pH value, and to either provide instantaneous feedback to the user regarding the test results through a user interface or store the result for retrieval or analysis at a later stage. This approach was utilised for the real-world tests performed (Chapter 8) and allowed for data storage and traceability. The data acquisition process is error-free, as data are stored directly into a computer. Further data management can be implemented using standards for medical data handling, such as Health Level Seven (HL7) international electronic healthcare information standards [154].

3.8 Packaging

The sensing RFID tags were tested using different packaging configurations. Tests were performed using either bare tags (Chapter 4), tags housed in a poly(methyl methacrylate) (PMMA) enclosure (Chapter 5), and tags packaged into foldable cardboard box designs (Chapters 7 and 8).

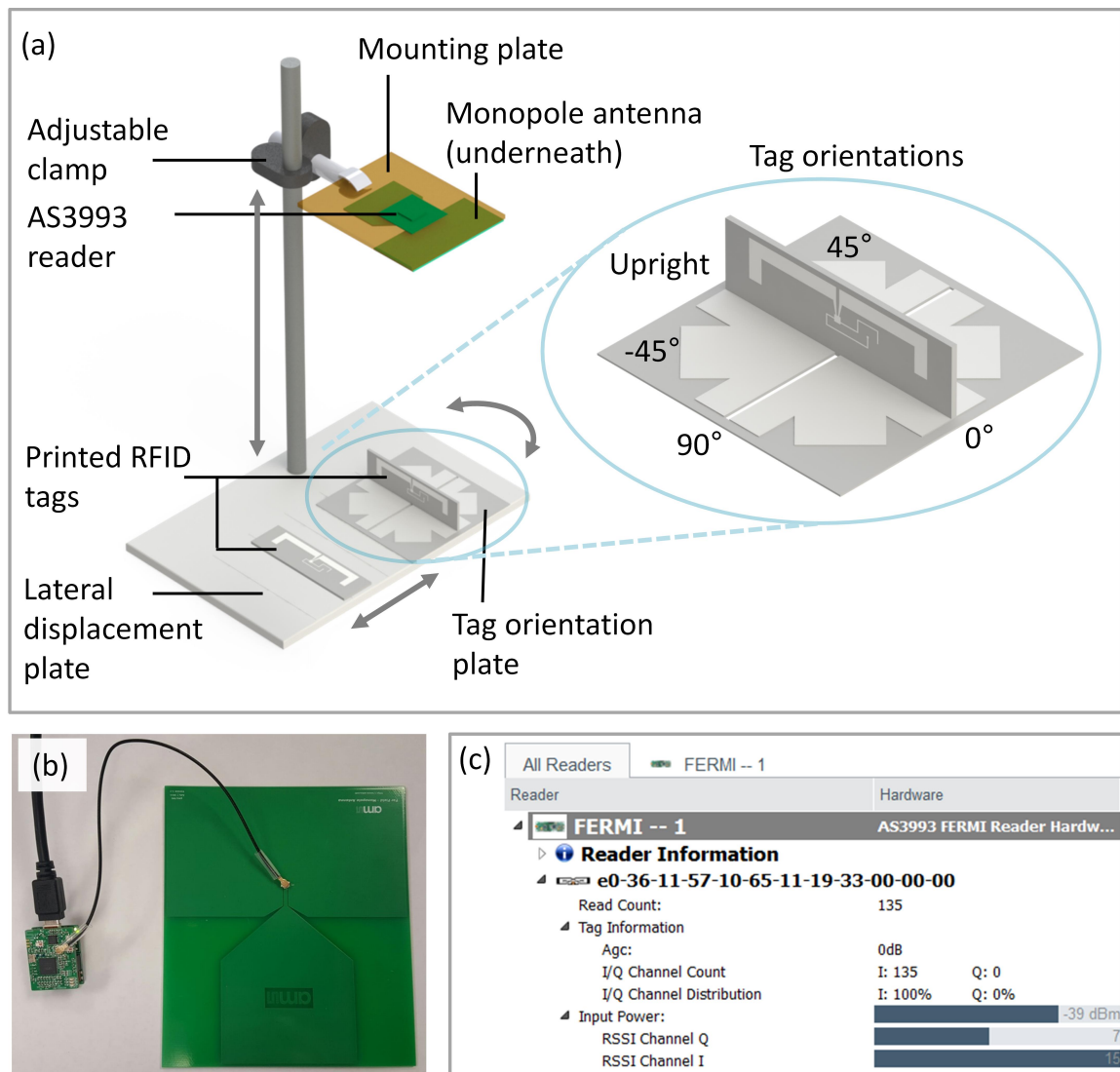


Figure 3.8 a) Wireless readout set-up. Read range measurements can be performed for tags in various orientations. Republished with permission of IOP Publishing Ltd. from [138]; permission conveyed through Copyright Clearance Center, Inc. b) The AMS AS3993 reader development kit with reader module and monopole antenna, connected via USB to a PC where tags can be scanned via c) the AMS AS3993 user interface.

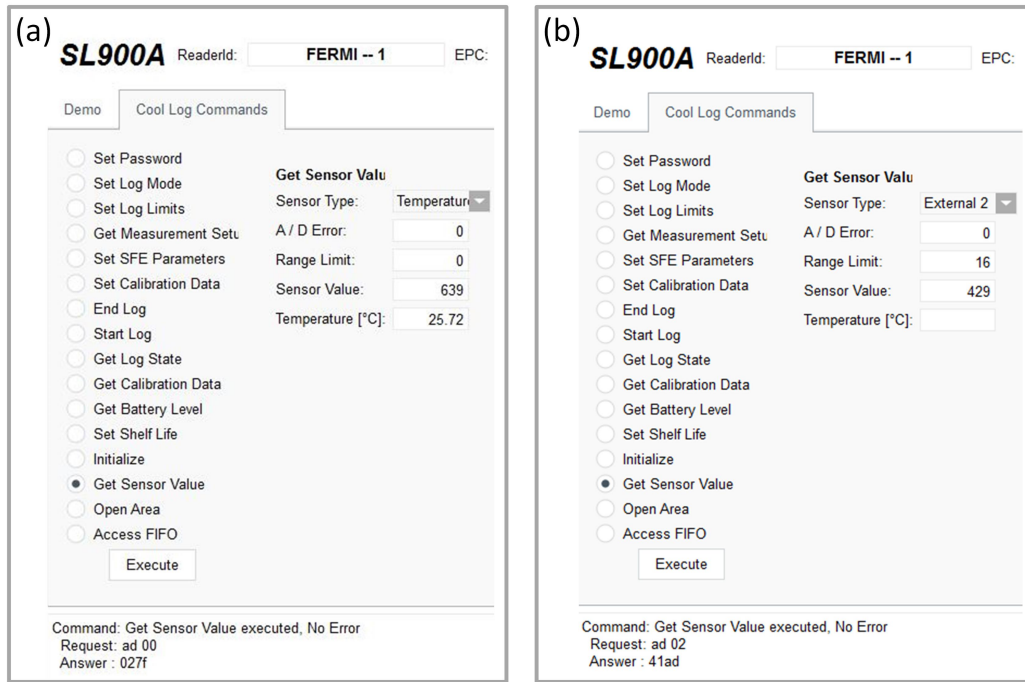


Figure 3.9 Example of sensor readout from printed RFID tags using AS3993 reader development kit software and GUI. a) Temperature readout where the measured sensor value output from the ADC is automatically converted to a temperature reading ($^{\circ}\text{C}$). b) Optical sensor readout from EXT2 which can be converted into a photo current value (mA) using a conversion calculation.

The goal was to integrate the printed tags into low-cost, maintenance-free and mass producible housing, as illustrated in Figure 3.1. Foldable cardboard box designs were thus explored as packaging solutions, as these are low-cost and disposable. This approach is also compatible with existing printing and packaging solutions that are currently available. The packaging designs were based on commercial design processes and technologies, which are extensively documented [155]. Die cutting, creasing and gluing are scalable processes that can be utilised to realise packaging solutions effectively.

In particular, local printing and packaging companies were approached as part of the development process to ensure that the solutions developed were feasible in terms of design scale up and the long term goal of local mass production (Chapters 7 and 9).

4 Substrates

This chapter is based on previously published work [138] and has been republished with permission of IOP Publishing Ltd., with permission conveyed through Copyright Clearance Center, Inc.

4.1 Overview

The objectives of this dissertation focus on the development of low-cost, maintenance-free and automated readout and connectivity solutions for POC diagnosis, with a major component being the investigation of different types of substrates onto which these components can be implemented. This chapter explores the printing and assembly of sensing RFID tags onto various low-cost, flexible substrates, towards the development of packaged printed functionality solutions.

Foundational work carried out demonstrated the sensing capabilities of the SL900A for fluidic detection on photo paper [32], but printing of the tag antenna has been limited to printed electronics substrates such as polyimide [153,156], with one example of printing onto cardboard packaging [157]. This chapter expands on existing investigations of SL900A-based sensing RFID tags by exploring the feasibility of the printing and assembly of these tags onto a variety of substrates that could be applicable in the development of low-cost POC diagnostic devices for health and environmental applications.

The substrates investigated varied in functionality, characteristics and cost. Substrates included specialised papers optimised for either paper-based diagnostics or printed electronics, low-cost, standard printing and packaging papers, adhesive vinyl substrates, and environmentally friendly materials. The print quality, including parameters such as resistance, roughness and print thickness, is presented in this chapter to illustrate the effect of the substrate on the printed result.

The selected substrates aid the implementation of low-cost, low-maintenance instrumentation solutions that could be realised using printed functionality components. The long-term goal could also be to integrate a low-cost yet reliable readout and

communication unit with paper-based microfluidics directly, thereby transforming a straightforward paper test strip into an automated, complete diagnostic device.

4.2 Methods

Characterisation of screen printed sensing RFID tags on 20 different substrates (Table 4.1) was performed. The generic SL900A tag design shown in Figure 3.4 was utilised, with the manual screen printing implemented as described in Chapter 3.

4.2.1 Substrates

Table 4.1 lists the substrates that were utilised. The main categories for substrate selection are: 1) suitability to paper-based microfluidic implementations (category PM), 2) suitability to printed electronics (category PE), suitability to low-cost, accessible, and practical uses, including both 3) direct application to flexible packaging (category FL) or 4) flexible sticker/adhesive formats that can be applied separately to a diagnostic device that may be manufactured on a different substrate (category FA), and 5) disposable, environmentally friendly biodegradable packaging (category BP). It should be noted that some substrates that have been specifically developed for printed electronics are also biodegradable. For truly environmentally friendly solutions to be realised, the disposability and biodegradability of all the inks and electronic components used would need to be considered. Costing of the different substrate categories varies with functionality and specialised properties. Costs are typically higher for specialised substrates that are suited to printed electronics or paper-based microfluidics, but vary substantially depending on the specific properties of the substrate.

Table 4.1 Overview of substrates grouped into categories according to their primary application.

Label	Substrate description	Substrate characteristics	Product	Manufacturer
Paper-based microfluidic substrates (PM):				
PM1	Chromatography paper	Porous, suited for fluidic control	Whatman No.1 CHR	GE Healthcare, UK
PM2	Chromatography paper with wax melted through	Barriers for fluidic control and containment	Whatman No.1 CHR with XER108R00749	GE Healthcare, UK
Printed electronics substrates (PE):				
PE1	Photo paper	Coated paper, suited to printed sensors, electronics, ink-jet printing	NB-RC-3GR120	Mitsubishi, Japan
PE2	Polyethylene-naphthalate (PEN) film	Smooth, transparent film suited to flexible electronic applications	Teonix Q65HA (125 μm)	DuPont Teijin Films, UK
PE3	Polyethylene terephthalate (PET) film	Smooth, transparent film suited to flexible electronic applications	Melinex 506 (125 μm)	DuPont Teijin Films, UK
PE4	Ultra-smooth electronics paper	High-definition patterning of printed electronics	Powercoat HD 230	Arjowiggins Creative Papers, France
PE5	Cellulosic electronics paper	High-throughput printed electronics	Powercoat XD 125	Arjowiggins Creative Papers, France
PE6	Smart printed electronics paper	High dimensional stability of printed electronics, non-porous surface coating	p_e: smart paper Type 1	Felix Schoeller Group, Germany

continued ...

... continued

Label	Substrate description	Substrate characteristics	Product	Manufacturer
Printed electronics substrates (PE):				
PE7	Smart printed electronics paper	High dimensional stability of printed electronics, hydrophilic nanoporous surface coating	p_e: smart paper Type 2	Felix Schoeller Group, Germany
PE8	Polyester primered film	Heat stabilized polyester film, acrylic primered	Kemafoil MTSL W	Coveme, Italy
PE9	Ceramic coated paper	Inorganic coated paper for electronics, low temperature sintering	Nano P60 paper	Printed Electronics Ltd, UK
Flexible low-cost substrates (FL):				
FL1	Standard printing paper	Readily available standard paper	Typek White Paper A4 80 GSM Premium	SAPPI, South Africa
FL2	Cardboard packaging	Readily available packaging	Typek White Paper packaging box	SAPPI, South Africa
FL3	Poly(methyl methacrylate) (PMMA)	Transparent, somewhat rigid, readily available plastic	AXSUHIC00-12500 1250I Acroglass XTUHI SHT – 1 mm	Maizeys Plastics, South Africa
FL4	Transparency/laser overhead projector film	Transparent and readily available film	17404081, Penguin Transparencies	Waltons, South Africa

continued ...

... continued

Label	Substrate description	Substrate characteristics	Product	Manufacturer
Flexible low-cost substrates with adhesive (FA):				
FA1	Transparent adhesive vinyl	Transparent film with adhesive	Grafitack Promo P100 Transparent Film	Grafityp Self-adhesive Products N.V., Belgium
FA2	Glossy adhesive vinyl	Glossy finish film with adhesive	Megarex D-MG Glossy Vinyl	X-Film, Germany
FA3	Matt adhesive vinyl	Matt finish film with adhesive	Grafitack 1106 Black Film	Grafityp Self-adhesive Products N.V., Belgium
Biodegradable packaging substrates (BP):				
BP1	Transparent, compostable, heat sealable film	Transparent, compostable, heat sealable	NatureFlex NVR	Futamura Chemical Co. Ltd, Japan
BP2	Transparent, compostable film	Transparent, compostable	NatureFlex NP	Futamura Chemical Co. Ltd, Japan

4.2.2 Characterisation of printed features

Print quality

Printed features were analysed using a brightfield microscope (EMZ-8TR, Meiji Techno, Japan) with different magnifications ($7\times$ and $45\times$) to assess the consistency of the printing, the edge irregularities and resolution of fine detail, specifically for the IC pads. A laser scanning microscope (LSM 5 Pascal, Carl Zeiss, Germany) was utilised to assess the thickness and uniformity of the printed features on different substrates. Surface roughness measurements were conducted using laser scanning microscopy (LSM) for both the substrate and the printed layer on the substrate to assess the effect of the substrate on the printed result. Three roughness measurements were conducted for each at a $200\times$ magnification, with surface roughness calculated using

the arithmetical mean roughness value (R_a). Six thickness measurements were also performed for each substrate using LSM. Measurements were performed across the antenna arms ($200\times$ magnification), with two devices analysed for each substrate. A theoretical wet print thickness of $28\ \mu\text{m}$ is expected from the screen mesh used, and a corresponding reduction in thickness of down to 30% can be expected for the dried ink thickness, resulting in expected print thicknesses of approximately $8.4\ \mu\text{m}$.

Electrical characterisation

Resistance measurements and subsequent sheet resistance calculations were carried out for printed features on different substrates. Figure 4.1 indicates the points at which the resistance measurements were conducted on each printed antenna using an LCR meter (LCR-8110G, GW Instek, Taiwan) to perform four probe resistance measurements.

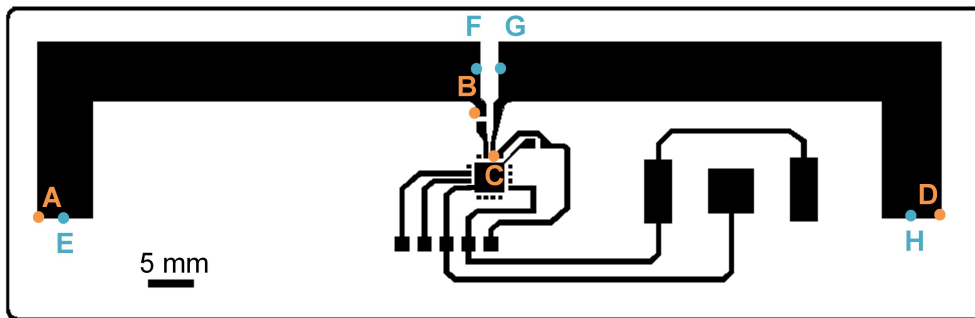


Figure 4.1 Tag design ($110\ \text{mm} \times 35\ \text{mm}$) based on development kit for printing onto different substrates. A to B and C to D show the longest path over which resistance measurements are made for each antenna arm, while E to F and G to H show the centre paths over which resistance is measured. Republished with permission of IOP Publishing Ltd. from [138]; permission conveyed through Copyright Clearance Center, Inc.

Two devices were characterised for each substrate, resulting in four resistance measurements for each substrate. The sheet resistance (R_s) values were calculated from the resistance measurements (R) using

$$R_s = R \times \frac{w}{l} \quad (4.1)$$

where w is the width (7 mm), and l is the length (63 mm) of the printed antenna arm design across which the four probe resistance measurements are performed. The

AG-800 silver ink used to print the devices has a sheet resistance of $<0.015 \Omega/\text{sq}$ for a $25 \mu\text{m}$ layer.

4.3 Results

Figure 4.2 shows selected examples of printed tags onto different substrates.

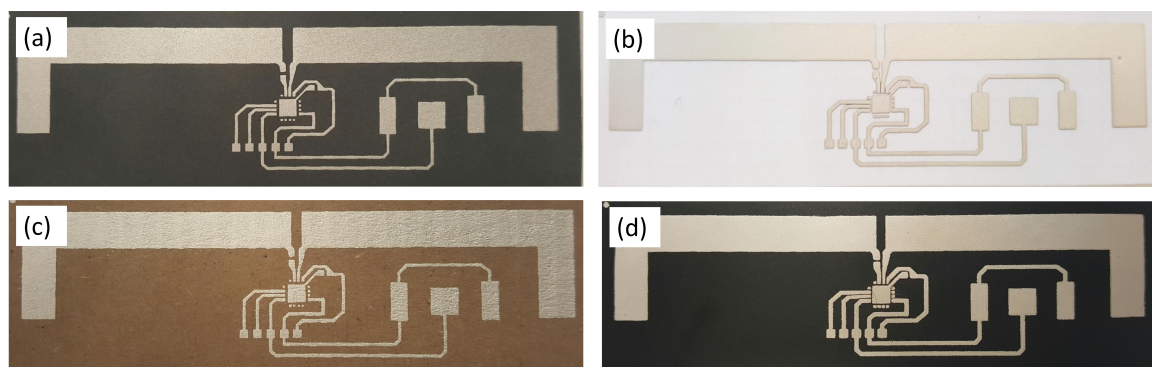


Figure 4.2 Examples of printed tags onto different substrate categories, namely a) PM2 - chromatography paper with wax melted through, b) PE9 - ceramic coated paper for printed electronics, c) FL2 - cardboard packaging and d) FA3 - matt adhesive vinyl. Republished with permission of IOP Publishing Ltd. from [138]; permission conveyed through Copyright Clearance Center, Inc.

Brightfield microscopy was used for visual assessment of print quality (Figures 4.3 and 4.4). LSM scans enabled surface roughness (Figures 4.5 and 4.6) and thickness measurements (Figure 4.7) to be obtained. Substrate and printed layer roughness and thickness were verified using surface profilometry (Form Talysurf PGI 820, Taylor Hobson, UK) for selected substrates and produced comparable results.

LSM scans at $200\times$ magnification produced surface profiles at the boundary between the substrate and the printed ink layer, to enable print thickness measurements to be made. Thickness measurements varied across substrates and different devices as a result of the manual screen printing process. The measured thickness across all substrates and devices (60 measurements in total) gave an average thickness of $7.82 \mu\text{m}$ ($\pm 3.27 \mu\text{m}$). The average thicknesses of the printed ink for all substrates ranged between $4 \mu\text{m}$ and $16 \mu\text{m}$, with large fluctuations from $1.5 \mu\text{m}$ to $23 \mu\text{m}$ noted in the PM substrates.

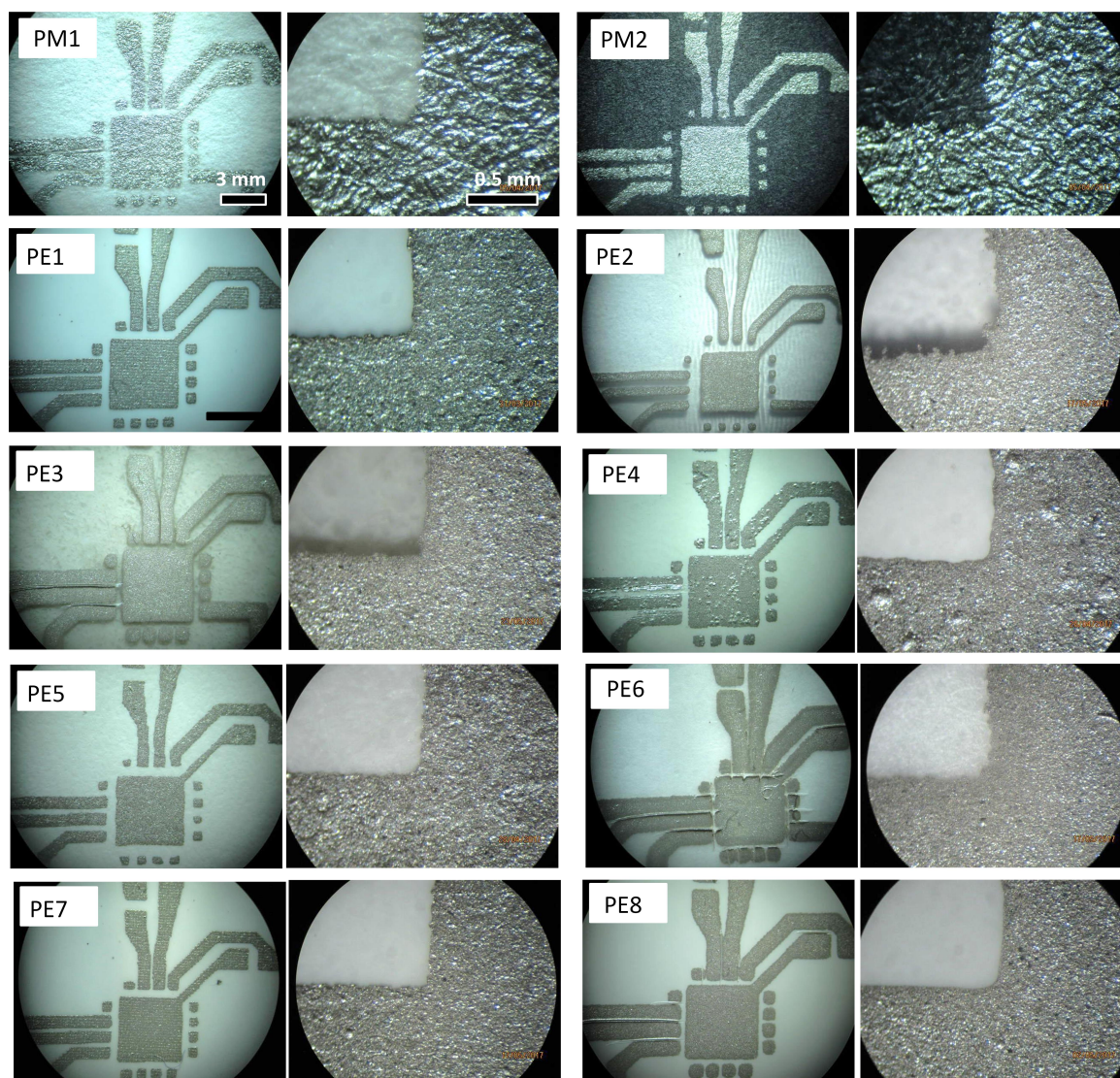


Figure 4.3 Brightfield microscopy images for RFID tags printed on to different substrates for paper-based microfluidics (PM1, PM2) and printed electronics (PE1 to PE8). Scale bars are indicated (top left). Republished with permission of IOP Publishing Ltd. from [138]; permission conveyed through Copyright Clearance Center, Inc.

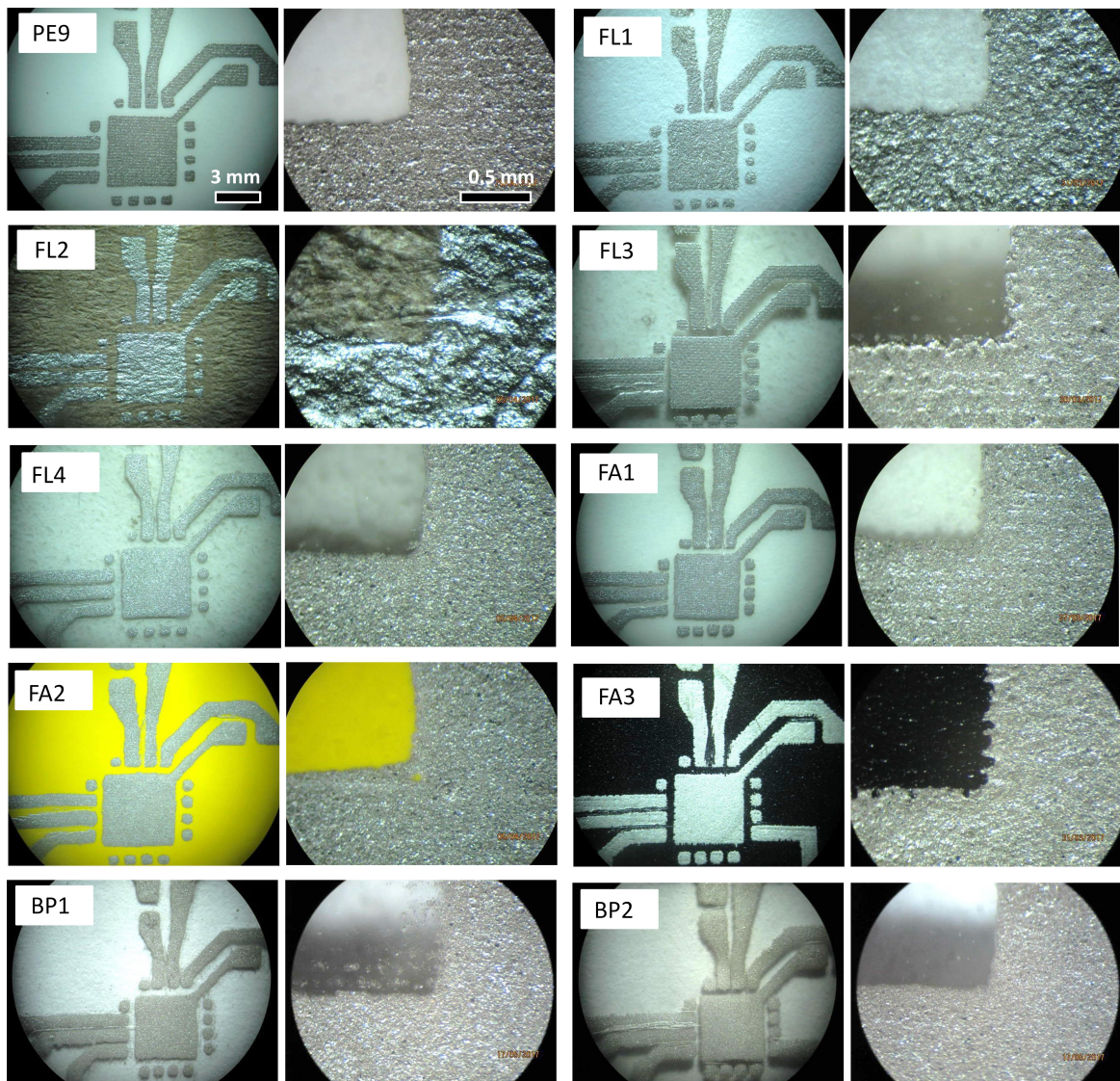


Figure 4.4 Brightfield microscopy images for RFID tags printed on to different substrates for printed electronics (PE9), flexible low-cost substrates (FL1 to FL4), flexible adhesive substrates (FA1 to FA3) and biodegradable substrates (BP1, BP2). Scale bars are indicated (top left). Republished with permission of IOP Publishing Ltd. from [138]; permission conveyed through Copyright Clearance Center, Inc.

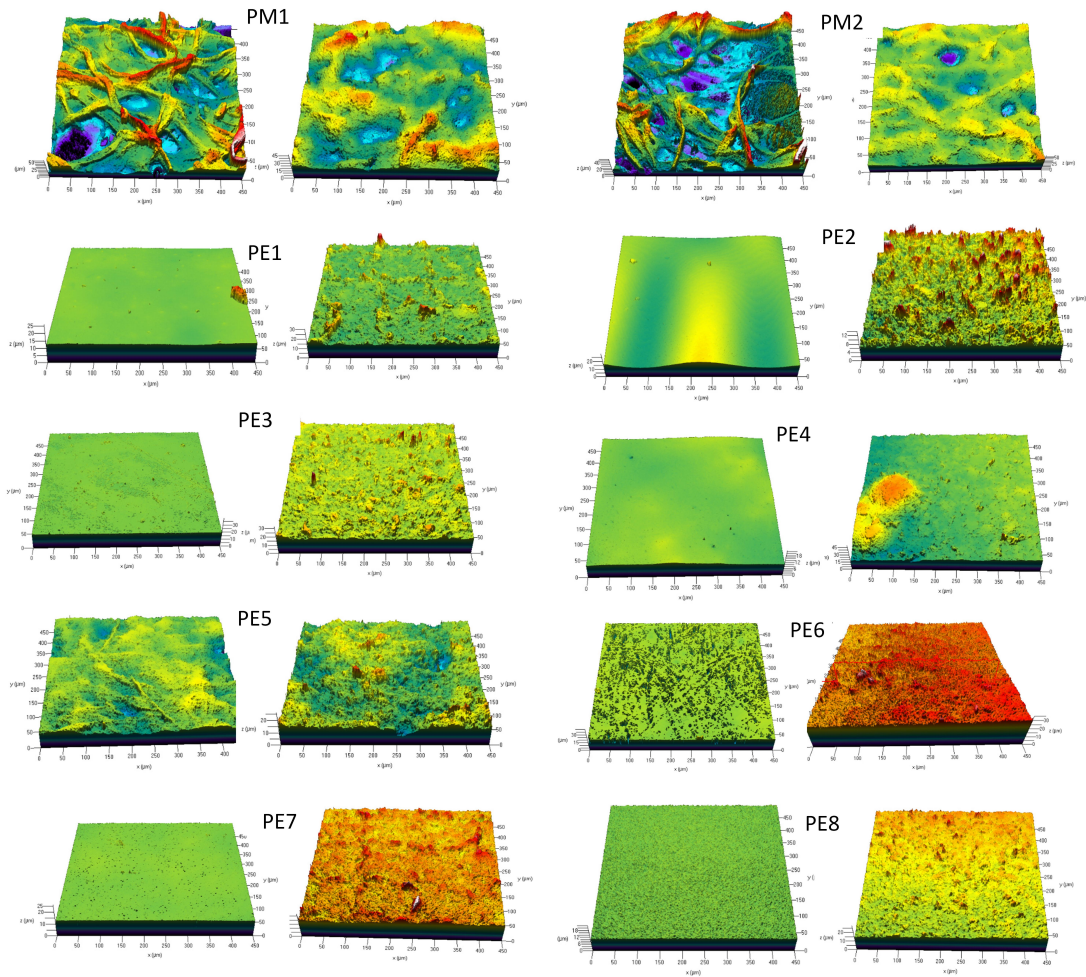


Figure 4.5 LSM images at 200× magnification for RFID tags printed on to different substrates and showing surface roughness for both substrate (left) and printed ink layers (right) for each substrate. The dimensions of the areas imaged are 450 μm × 450 μm with the height varying between 15 μm and 45 μm. Republished with permission of IOP Publishing Ltd. from [138]; permission conveyed through Copyright Clearance Center, Inc.

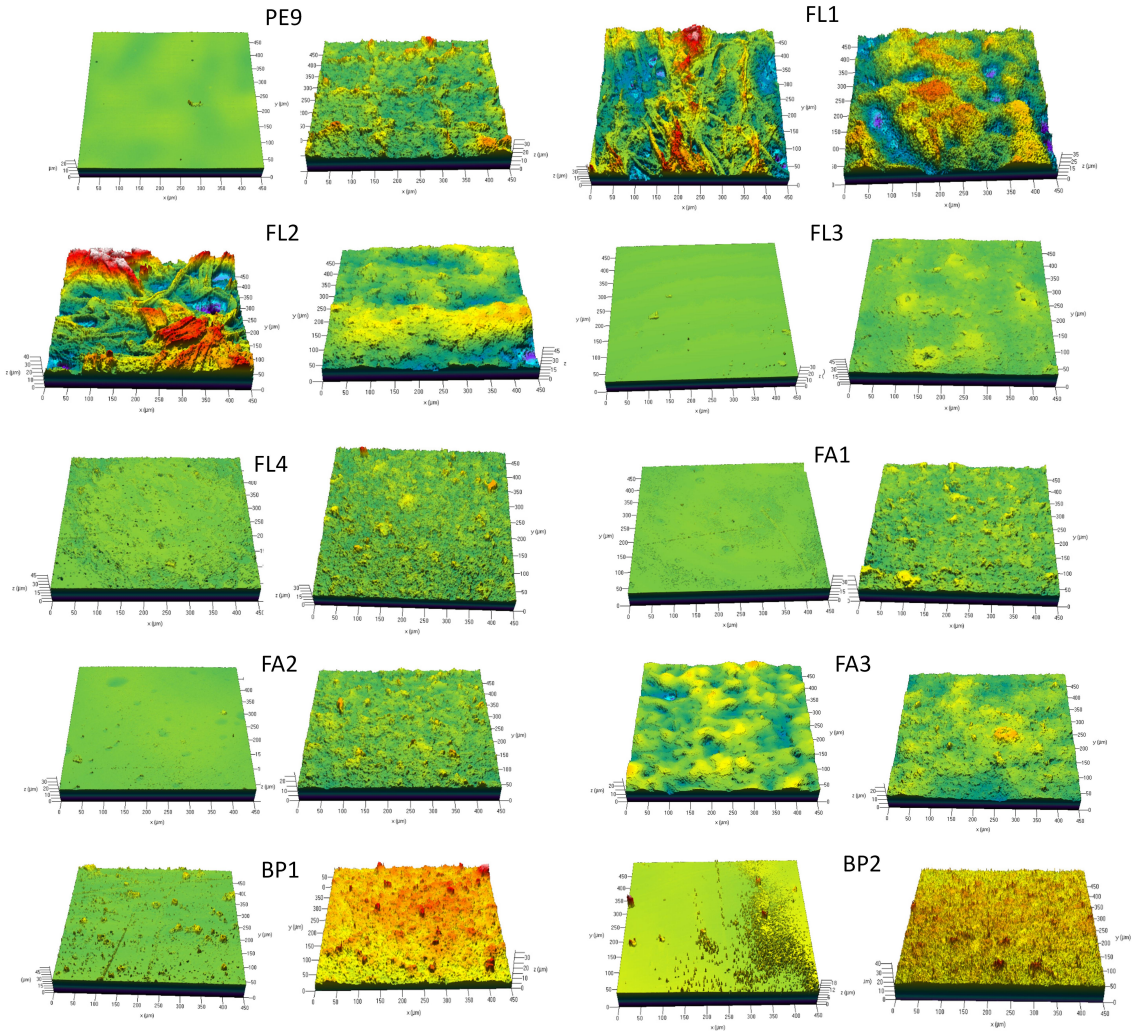


Figure 4.6 LSM images at $200\times$ magnification for RFID tags printed on to different substrates and showing surface roughness for both substrate (left) and printed ink layers (right) for each substrate. The dimensions of the areas imaged are $450\ \mu\text{m} \times 450\ \mu\text{m}$ with the height varying between $15\ \mu\text{m}$ and $45\ \mu\text{m}$. Republished with permission of IOP Publishing Ltd. from [138]; permission conveyed through Copyright Clearance Center, Inc.

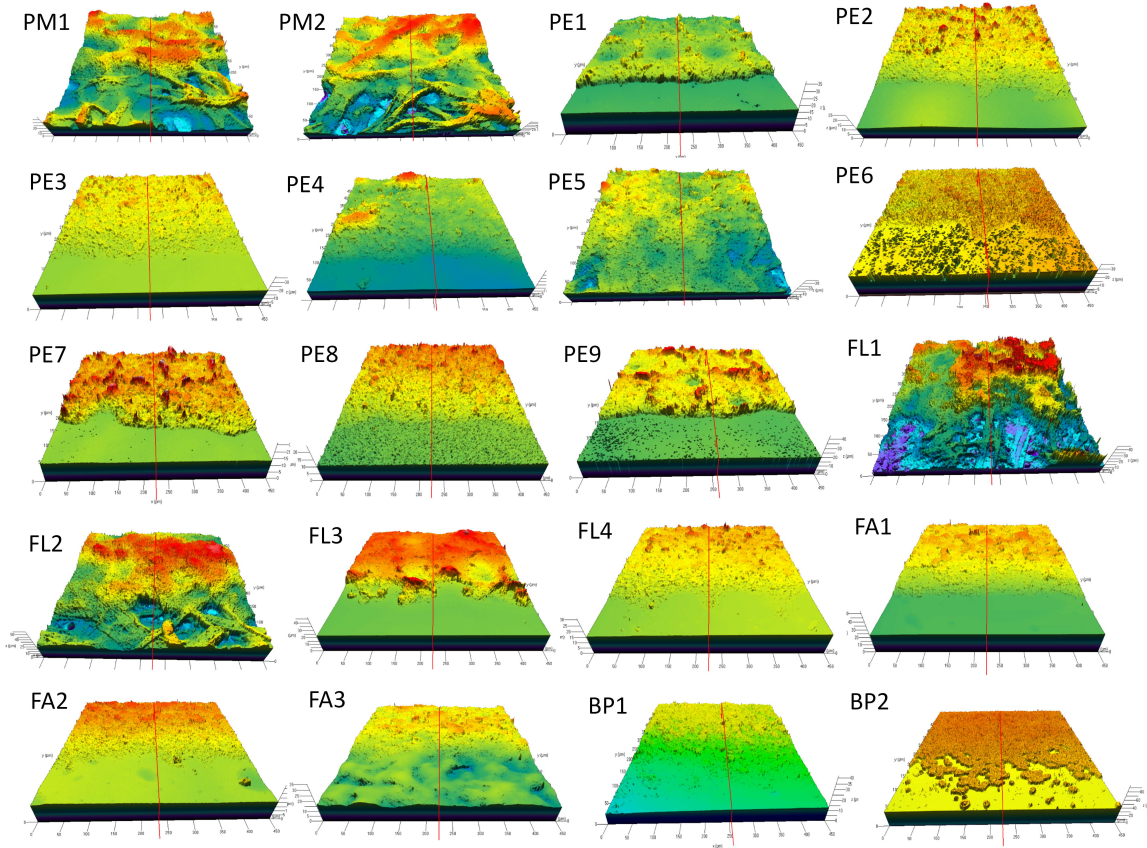


Figure 4.7 LSM images at $200\times$ magnification for RFID tags printed on to 20 different substrates and showing step profiles for the printed layer for each substrate. The dimensions of the areas imaged are $450\ \mu\text{m} \times 450\ \mu\text{m}$ with the height varying between $15\ \mu\text{m}$ and $45\ \mu\text{m}$. Republished with permission of IOP Publishing Ltd. from [138]; permission conveyed through Copyright Clearance Center, Inc.

Figure 4.8 summarises the roughness measurements obtained using LSM, along with sample brightfield microscopy and LSM images. Paper-based microfluidic substrates (PM) as well as printing paper and cardboard packaging (FL1 and FL2) produced the highest substrate roughness measurements, with the roughness of the print lower than the substrate as a result of the fibrous substrate being coated by the ink. Printed electronics substrate PE5 is a cellulose-based substrate with a roughness specification of $1.5 \mu\text{m}$, which is similar to the measured result and is rougher than many of the other specialised PE substrates. The printed layer on this and slightly rougher substrate FA3 is smoother than the substrate, with the ink coating the fibres and rough substrate surfaces. The majority of PE substrates and other smooth substrates in the FL and FA categories have very smooth substrates with roughness values well below $1 \mu\text{m}$, and corresponding print roughness values substantially higher than that of the substrate. Substrate PE4 has a large printed layer roughness arising from bubbles forming in the print. This is likely a result of the solvent phase in the ink that dissolves a binder component in the coating of the paper. This does not occur with aqueous ink and does not degrade the conductivity.

Sheet resistance measurements are also shown in Figure 4.8, with standard deviations across four resistance measurements are indicated for each substrate. Using the average thickness value of $7.82 \mu\text{m}$ obtained from LSM measurements across all tags, a theoretical calculated sheet resistance of $0.048 \Omega/\text{sq}$ was obtained. The average experimentally calculated sheet resistance for all substrates is $0.07 \Omega/\text{sq}$ ($\pm 0.057 \Omega/\text{sq}$). Many of the individual sheet resistance values fall within or close to this range, with large outliers being the BP substrates.

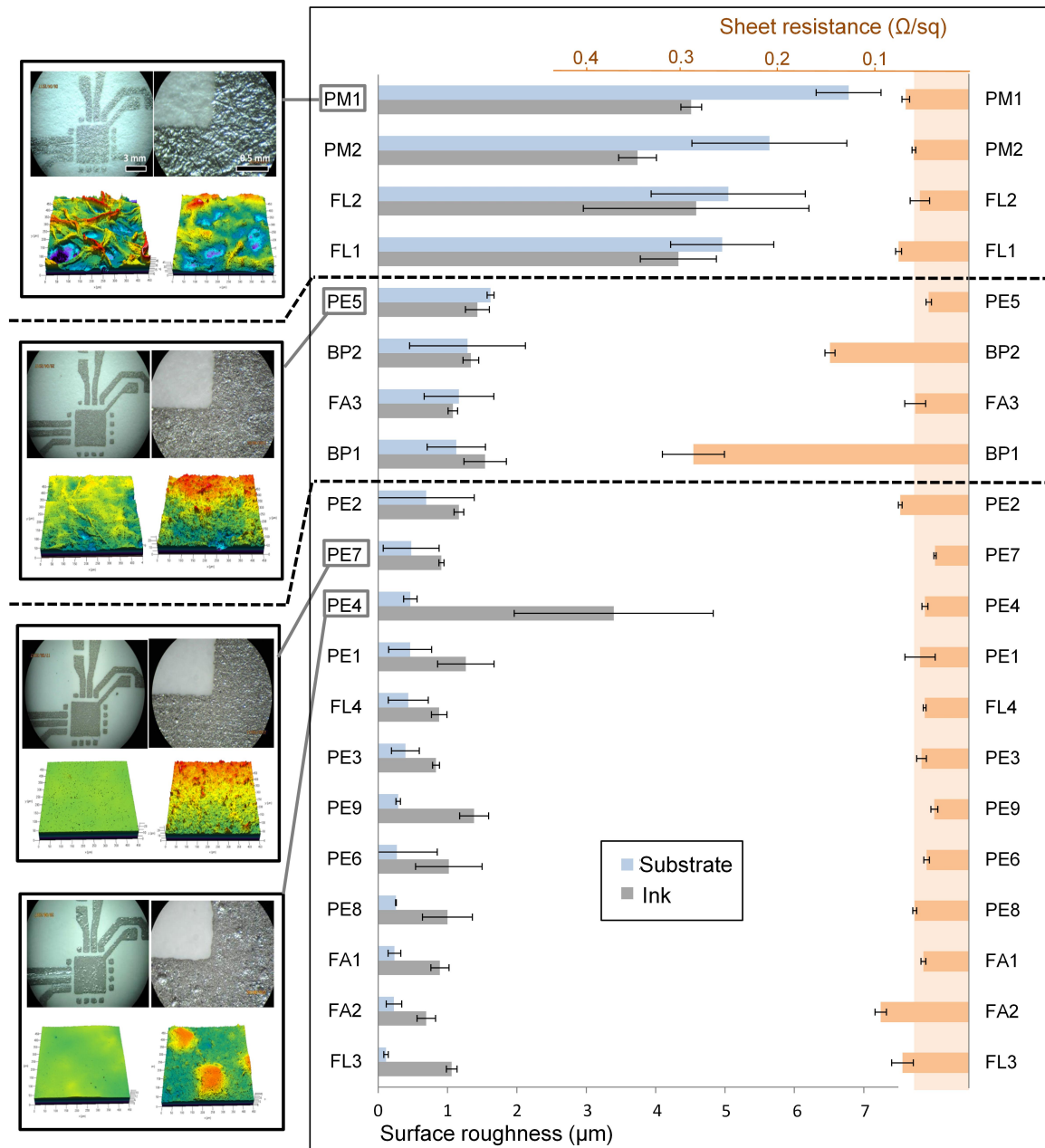


Figure 4.8 Substrate and print roughness measurements for various substrates along with corresponding sheet resistance values. Republished with permission of IOP Publishing Ltd. from [138]; permission conveyed through Copyright Clearance Center, Inc.

4.4 Discussion

This work illustrates the feasibility of implementing printed UHF RFID tags with sensing capabilities onto different substrates, with focus on low-cost POC diagnostic device development. A manual screen printing set-up and assembly process enables low-cost, rapid prototyping of devices which could be assessed in terms of print quality.

Surface roughness measurements for substrates and printed ink layers (Figure 4.8) showed two main trends: 1) fibrous substrates high in roughness had a smoother print layer, with the ink coating the fibres and filling the irregular spaces, and 2) smoother substrates resulted in print layers with increased roughness with values in the range of 1 to 1.5 μm , independent of the substrate roughness. Outliers in print quality such as PE4 highlight the need to consider the ink composition and its compatibility with the substrate being used to avoid print irregularities.

Printed thickness variations result from the manual screen printing process and variations in the substrate structures. Resulting sheet resistance values were comparable to the value provided for the silver ink on most of the substrates, but with large resistances noted for the BP substrates (Figure 4.8), where the extreme flexibility and warping of the substrates could affect the print uniformity and thus conductivity. However, paper-based substrates can be incinerated and thus biodegradability need not be a primary concern, and the substrate to be utilised should be chosen according to the desired properties for the application, be it fluidic, electronic or other. PE substrates generally have the lowest sheet resistance values as expected as these are designed specifically for printed electronics. Print quality does not have a direct effect on the resistances of the printed tags, but for fibrous substrates such as PM1, PM2 and FL2, this could result in increased ink coated surface areas, which contribute to improving the read ranges of these tags, as explored in Chapter 6.

The results indicate that a variety of low-cost substrates can be utilised as different packaging and label options for paper-based diagnostic tests. This work presents the feasibility of implementing such devices towards low-cost, integrated POC diagnostics, using straightforward fabrication techniques and realistic testing environments – as demonstrated in Chapter 6 – to illustrate the possibilities.

5 Detection

This chapter is based on work that has been submitted to Nature Scientific Reports as part of a manuscript that is awaiting reviewer feedback.

5.1 Overview

This chapter focuses on automated result readout for paper-based POC diagnostics. Manual result readout causes bottlenecks in clinic workflows and is prone to user error and consequent incorrect diagnoses. As highlighted in Chapters 2 and 3, paper-based tests typically have a visual or colorimetric readout and thus an automated colour detection solution is required. Related work has explored colour detection for paper-based assays [158], utilising camera-based and image processing solutions for quick response (QR) code and colorimetric analysis. This chapter explores the development of a printed colour detector solution using the SL900A IC to enable automated readout of colorimetric results from paper-based tests. Model LFTs were used with defined RGB, greyscale and CIE colourspace values to enable robust and repeatable assessment of the colour detector solution.

Various sensing applications using the SL900A IC have been showcased. Examples include SL900A based tags on polyimide substrates for temperature and relative humidity sensing using printed serpentine and interdigitated electrodes [159], as well as solutions implemented on a cardboard box using a commercial force sensor and opening detector for supply chain applications [157]. Environmental applications using an SL900A tag on a printed circuit board (PCB) have also been demonstrated for soil moisture sensing [160].

Colour detection examples using the SL900A include a multispectral assessment system on a PCB that incorporates an RGB colour sensor, infrared (IR) sensor and UV sensor with a microcontroller for switching between configurations [161]. An SL900A tag implemented on a flexible polyethylene naphthalate (PEN) film and using a printed photodiode for light detection has recently been demonstrated [162].

Work related to this dissertation demonstrates further example applications of printed SL900A RFID tags, including fluidic sensing [32] and temperature read-out [163]. This work demonstrated that sensing and communication solutions can be realised with simple circuitry, thereby lowering the cost and improving the robustness of the device, and making this well suited to the Southern African resource-limited clinic context.

5.2 Methods

5.2.1 Model lateral flow test devices

Twelve model LFTs with varying colour intensities were used to provide robust, repeatable and reusable tests with which to assess the performance of the wireless colour detector devices. The dimensions of the LFTs were 55 mm × 5 mm, with 12 different RGB colours to provide a range of red and pink intensity colours printed onto standard printing paper and mounted onto a backing card for rigidity. The test and control lines of varying colours were designed to have a 1 mm width. The model LFT colours were generated using DesignCAD [164], by setting RGB values individually for each colour (Figure 5.1a). Greyscale values (gsv) for the different model LFTs were calculated from the RGB values as follows:

$$gsv = (R \times 0.299) + (G \times 0.587) + (B \times 0.114) \quad (5.1)$$

This conversion allowed for the intensity or lightness trend of the colours to be used as a comparison to the measurements made. The CIE colour space [144] could also be utilized, where colour is represented in a 2D chromaticity diagram. Hue and saturation values of a colour, which make up the HSV (hue, saturation, value) and HSL (hue, saturation, lightness) colour space models, can also be derived from the CIE colour space [165]. By using the CIE colour space, specifically the CIELAB colour space, values for the lightness (L) (from white to black), as well as the red/green value (A) and yellow/blue value (B) of a colour can be defined [145]. The lightness values correspond closely to the trends of the greyscale values, and for the purposes of this work, the greyscale values for both the negative control sample (RGB = 255, 255, 255) and the lowest intensity sample (RGB = 128, 0, 0) were used for normalisation of the colour intensity measurements.

5.2.2 Colour sensing

Various photodiodes were initially explored based on suggested components for use with the SL900A [166], including the VTB8440BH photodiode (Excelitas Technologies, USA) and SFH 203 (Osram Opto Semiconductors GmbH, Germany) visible light and IR photodiode. To expand on this, different photodiode and LED combinations were investigated using the SL900A, including an RGB LED (KPTF-3216 PBVGSURKC, Kingbright, Taiwan) and RGB sensor (KPS-5130PD7C, Kingbright, Taiwan) with transistors (BSS138L, ON Semiconductor, USA) to allow for switching between different colour for both excitation and detection. The SPI interface of the SL900A was used for ease of testing in the initial experiments.

To streamline the colour detector solution for use with typical LFTs that utilise gold nanoparticles, the LED and photodiode combination selected was a 525 nm green LED (LTST-C190TGKT, Lite-On, Taiwan) and a silicon photodiode (SFH 2430, Osram Opto Semiconductors GmbH, Germany) with a spectral sensitivity between 400 and 900 nm, designed to resemble the sensitivity of the human eye. These IR and visible light spectrum photodiodes are used for various light sensor applications, and are low-cost and compact (4.5 mm × 4 mm × 1.2 mm), housed in a plastic SMD dual in-line packaging (DIP) format. The SFH 2430 has a radiant sensitive area of 7.02 mm², with a responsivity of 0.17 A/W and peak sensitivity at 570 nm. The relative sensitivity is greater than 80% for the wavelength range of 500 to 630 nm (Figure 5.1). This indicates that the photodiode has a high sensitivity in the range of wavelengths that are important in this work, including pink and red colours typically associated with standard gold nanoparticle-based LFTs, as described in Chapter 3.

Figure 5.1b shows the spectrum of the SFH 2430 photodiode, indicating the three cones for red, green and blue colour perception that fall within the spectrum. The wavelengths for the different model LFT colours used are also indicated. Model LFT numbers 9 to 12 fall directly within the red wavelength band, with wavelengths in the range of 648 to 766 nm [167], respectively, corresponding to a spectral sensitivity of between 30 and 75% for the photodiode, with darker red colours (e.g. LFT number 12) having lower sensitivities. White (LFT number 1) spans the visual spectrum of wavelengths. Similarly, pink colours, such as LFT numbers 2 to 8, are made up of red, green and blue colours and are non-spectral, meaning they are not defined by a single wavelength [168], and cover a range of wavelengths. Dominant and complementary wavelengths for non-spectral colours can be determined using the CIE 1931 colour space [144], and for light pink colours as used in this work, would be expected to be between 580 and 700 nm, and 495 and 520 nm, respectively, corresponding to spectral sensitivities of 60% or higher for the SFH 2430 photodiode. This again highlights

the suitability of the SFH 2430 photodiode for detection of LFT colours, with high sensitivity to lighter pink and red colours. This is illustrated in Figure 5.1b, where the wavelength ranges of the model LFT colours are broadly indicated in orange.

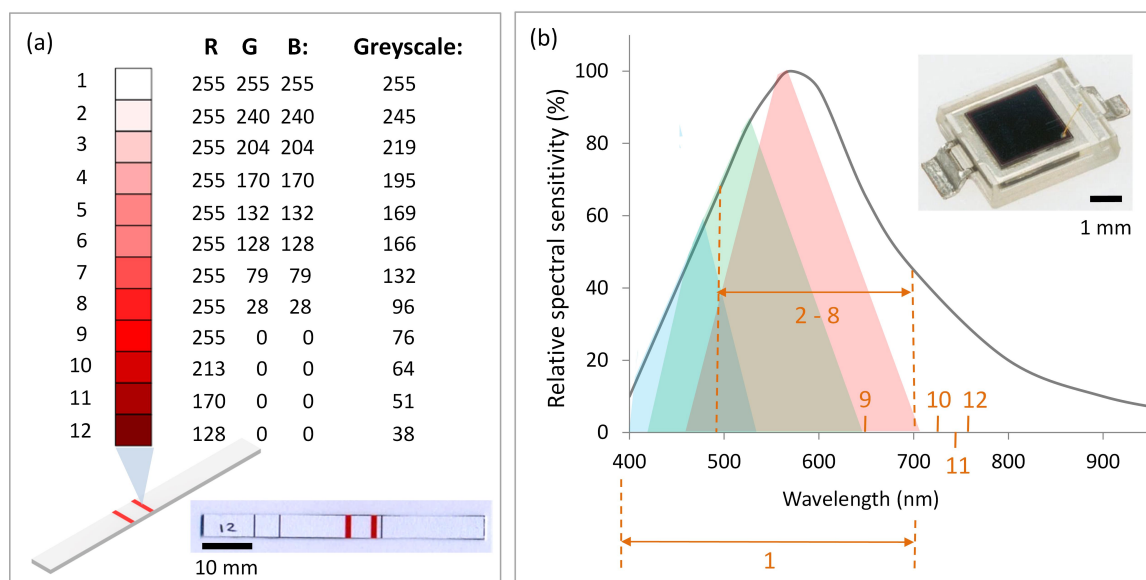


Figure 5.1 a) RGB and greyscale values (rounded up) of the model LFT colours used for testing the developed colour detector tags, and b) spectrum of SFH 2430 photodiode indicating wavelength ranges of cones (red, blue, green shaded areas) for colour perception, along with the wavelengths of the model LFT colours. Model LFT numbers 9 to 12 are each defined by a specific wavelength as indicated. Numbers 1 to 8 are not defined by a unique dominant wavelength, and the range of dominant and complimentary wavelengths are shown instead.

5.2.3 Colour detector tags

The SL900A tag design for colour detection shown in Figure 3.5 was utilised, with the manual screen printing and assembly of components implemented as described in Chapter 3. The designs were printed onto either a white vinyl adhesive film (800 Premium Cast, Avery Dennison, USA) or a transparency/laser overhead projector film (17404081, Penguin Transparencies, Waltons, South Africa) to demonstrate the functionality on low-cost, flexible substrates that could easily be incorporated into packaged devices.

First, light intensity measurements were carried out using a handheld commercial light meter (Goldilux Autoranging Light Meter, MIT, South Africa) and compared to sensor values captured from the SFH 2430 photodiode using one of the tags (Tag 4). The LED on the tag was not used; instead, a separate LTST-C190 LED was positioned over a range of distances away from the tag in both ambient conditions and inside a cardboard box, providing a controlled lighting environment for testing. Using this approach, the functionality and working range of distances for the LED/photodiode combination could be determined.

The photocurrent was calculated from the measured light meter values, using a spectral sensitivity of 6.3 nA/lx for the photodiode as provided in the SFH2430 dataheet. These values were compared to the photocurrent values obtained from the measured ADC sensor values from the SL900A for the same lighting conditions.

Instantaneous sensor readout of EXT2 through the user interface was performed, with the feedback resistor value (R_f) set to 185 k Ω . The feedback resistor can be set to one of five values: 185, 400, 875, 1875 or 3875 k Ω . Alternatively, the autorange function of the SL900A can be used to automatically select an R_f value that provides unsaturated measurements within the ADC input voltage range [161].

The limits of the ADC input voltage are V_{ref} and $2V_{ref} - V_{o1}$, with default values of $V_{o1} = 0$ V and $V_{ref} = 310$ mV used in this work, giving a range of 310 to 620 mV, and a photocurrent detection range from 45.24 nA to 2.62 μ A with $R_f = 3875$ k Ω and $R_f = 185$ k Ω , respectively. Other detection ranges can be achieved by adjusting the values of V_{o1} and V_{ref} , selectable in 50 mV steps from 160 to 610 mV, enabling a minimum detectable current of 32.3 nA and a maximum of 5.86 μ A [161]. This enables the user to set a specific resolution and range.

The equation used to determine the photocurrent, I_D , from the ADC sensor values, $sens$, is calculated as follows using the default values for V_{o1} and V_{ref} [166]:

$$I_D = ((sens \times (V_{ref} - V_{o1})/1024 + V_{ref}) - 135mV)/R_f \quad (5.2)$$

5.2.4 Experimental set-up

Next, the colour detector tags were assembled in a PMMA enclosure to provide a rigid and repeatable test set-up for the experiments, as well as enabling low-cost, rapid prototyping and assembly of devices. A cardboard box with lining entirely in white vinyl and impervious to external ambient light was used to provide uniform and consistent lighting conditions in which to test the devices (Figure 5.2). The PMMA structure consisted of of five transparent 1 mm thick PMMA layers (AXSUHIC00125001250I Acroglass XTUHI SHT 1 mm, Maizeys Plastics, South Africa). Cut-outs were designed

to house and align the model LFTs and the various SMD components. The layers were stacked together using M3 screws, with the layout shown in Figure 5.2. Future developments would utilise cardboard to create the housing as well as the insert for alignment of the LFTs (Chapter 7).

The tag devices were tested in the PMMA housing, which provided a default spacing of 2 mm between the LFT and LED/photodiode set-up. To assess the effect of the spacing on the measured sensor readout values, the PMMA housing was modified to create 1 and 4 mm spacings for Tag 4.

Once the spacing was optimised for the colour detector set-up, six different tag devices – three on transparency (T) and three on adhesive vinyl (V) – were tested in the PMMA housing inside the box.

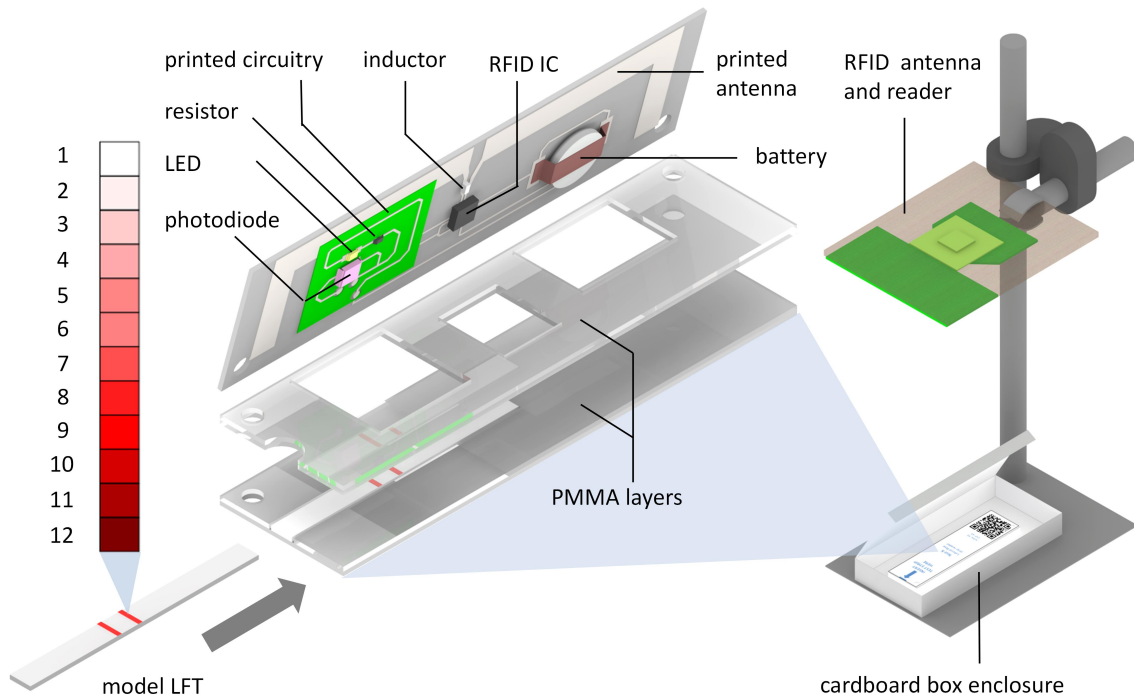


Figure 5.2 Wireless colour detector tag design showing the stacked PMMA housing layers, the sensing RFID tag design and components, as well as the reader set-up used to perform experiments.

Each colour detector tag was tested 5 times using 12 model LFTs with varying colour intensities. Sensor values were captured through the RFID reader user interface as described in Chapter 3, using an average over a 30 s period as a stable sensor readout result for each test. The results obtained were compared to those obtained for the model LFTs using the commercial portable LFT reader. The commercial reader employs LED excitation and photodiode detection for fluorescence and colorimetric detection, with excitation ranges from 365 to 660 nm and emission ranges from 460 to 720 nm.

5.3 Results

5.3.1 Colour readout

Table 5.1 displays the light intensity measurement results obtained using the commercial light meter compared to sensor values captured from the photodiode using Tag 4. Office lighting is typically defined as between 320 and 500 lx, which corresponds to the measurements made using the light meter for ambient lighting. The LED has a dominant wavelength at 525 nm and a luminous intensity of 71 to 450 mcd. Using the equation to relate luminous intensity, I_v , in candelas (cd) to illuminance, E_v , in lx using the distance, d , from the light source in metres (m):

$$E_v = \frac{I_v}{d^2} \quad (5.3)$$

and assuming an isotropic source, this would result in several 100 lx at 10 mm up to more than 10000 lx at 1 mm for the lower intensity range. For these ranges, this would translate to photocurrents within the range of 0.63 to 6.3 μA for the photodiode (photodiode spectral sensitivity of 6.3 nA/lx), indicating that a distance of several mm between the LED and photodiode would be a workable range. This can be observed in Table 5.1, where the sensor readout provides a linear range for an LED distance of between 4 and 8 mm inside the cardboard box (ADC readout), which are realistic test conditions.

The saturated sensor values that are read out wirelessly correspond to the calculated photocurrents using the light meter measurements that are above the short circuit photocurrent of 6.1 μA for the SFH 2430, as indicated by the values in bold in Table 5.1.

Figure 5.3 shows the effect of spacing between the LFT and LED/photodiode on the measured sensor readout values. As expected, larger distances resulted in lower sensor values and ranges, but these still fell within the sensor detection range. However, the dynamic range for the sensor values was lower for the larger spacing, making the distinction among colours more challenging. A spacing of 2 mm between the LFT and LED/photodiode resulted in the largest dynamic range for the photodiode sensor readout values (Figure 5.3, Table 5.2) and this spacing was used in the development process moving forward.

Table 5.1 Comparison of light meter readings (lx) with ADC sensor readout values from tag photodiode for different distances in mm (D) between the LED and photodiode and with the LED off (X). Calculated photocurrent values (μA) are also presented.

D	Ambient				Cardboard box			
	Light meter	ADC	Photo current		Light meter	ADC	Photo current	
			Light meter	ADC			Light meter	ADC
X	457 ± 8	640 ± 49	2.88	1.99	0	0	0	0.95
10	413 ± 5	294 ± 39	2.60	1.43	201 ± 1	0	1.27	0.95
9	441 ± 10	387 ± 29	2.78	1.58	289 ± 3	0	1.82	0.95
8	482 ± 5	548 ± 25	3.04	1.84	366 ± 1	0	2.31	0.95
7	627 ± 2	703 ± 40	3.95	2.1	507 ± 2	100 ± 1	3.19	1.11
6	649 ± 2	854 ± 24	4.09	2.34	564 ± 1	222 ± 2	3.55	1.31
5	871 ± 2	933 ± 26	5.49	2.47	650 ± 1	565 ± 6	4.10	1.87
4	1057 ± 4	1023	6.66	2.62	830 ± 1	1023	5.23	2.62
3	1277 ± 12	1023	8.05	2.62	1065 ± 2	1023	6.71	2.62
2	1599 ± 8	1023	10.07	2.62	1490 ± 5	1023	9.39	2.62
1	1862 ± 26	1023	11.73	2.62	1757 ± 6	1023	11.07	2.62

5.3.2 Colour detector tag performance

Testing of the six wireless colour detector tags in the PMMA housing was carried out under inconsistent lighting conditions within different laboratory and office spaces to assess the effectiveness of the cardboard box in sealing the tag devices from external light. Figure 5.4a shows an example of a tag device in the PMMA housing from which the sensor values were captured. Figure 5.4b shows the wireless sensor readout values

obtained directly from the ADC of the SL900A for each device over the range of test strip colours. Measurements were normalised to the negative control sample (LFT number 1, RGB = 255, 255, 255), and referenced to the lowest greyscale value (LFT number 12, RGB = 128, 0, 0) for ease of comparison to the results obtained using the commercial reader (Figure 5.4c). Table 5.2 provides a summary of the colour detector tag test results. The presented results are for Tag 4, with the exception of the final row, which shows averages across all tags measured for a 2 mm spacing.

The performance of two colour detector tags: the most repeatable with the lowest standard deviation (Tag 4), and the least repeatable with the highest standard deviation (Tag 2), compared to the commercial LFT strip reader was assessed for three selected model LFT colours (Figure 5.5a). The grey shaded lines show the resulting range of measurements for both the most repeatable and least repeatable tags. The colour readout trends are similar for different colours when comparing the commercial reader with the most and least repeatable tags, and the colour readout results fall within distinct bands for the three LFT colours (3, 6, 9) spaced across the 12 model LFT range, showing feasibility for minimal semi-quantitative colour readout.

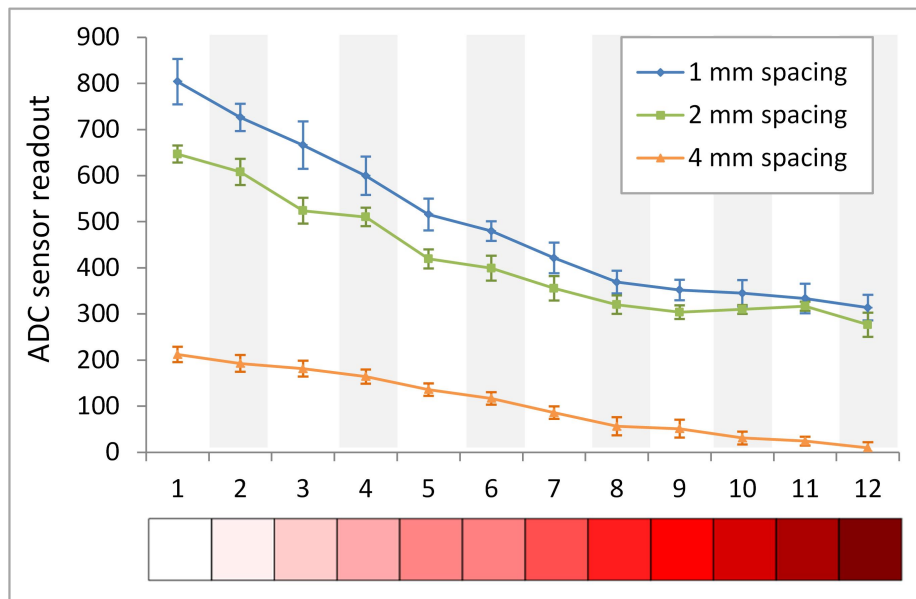


Figure 5.3 Sensor readout for variations in distance between LED/photodiode and LFTs for Tag 4.

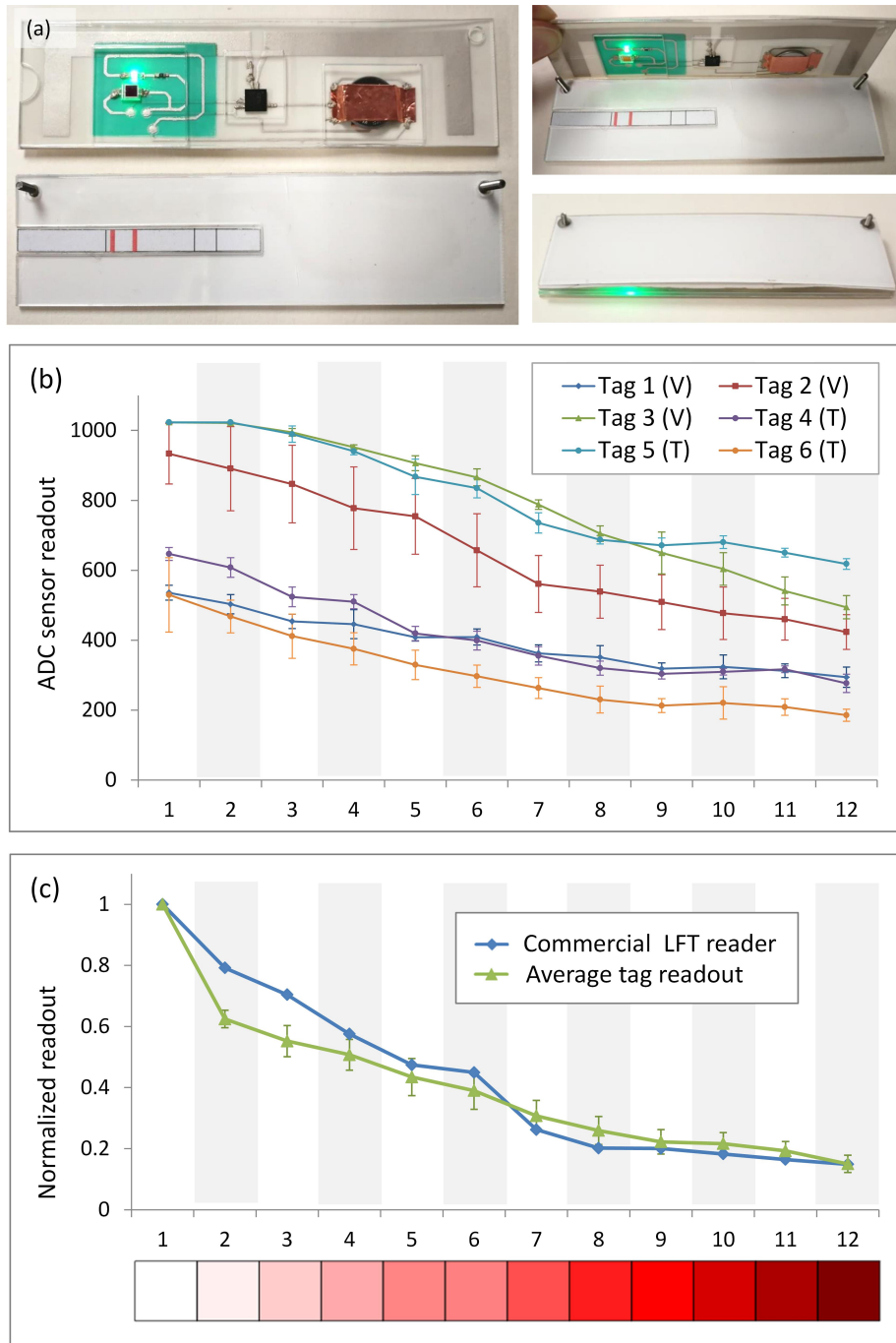


Figure 5.4 a) Example of assembled wireless colour detector device in PMMA housing. b) Sensor values obtained directly from the ADC for each of the six tag devices for the different model LFT colours, with standard deviations shown across each of five tests. c) Normalised average wireless colour detector readouts compared to commercial reader results.

Table 5.2 Summary of results showing sensor value ranges from ADC and corresponding photocurrent values for different measurement set-up configurations.

Device / measurement set-up	ADC readout	Photocurrent (μA)
• Ambient light	172 ± 74	1.23
• Ambient light with LED on	280 ± 70	1.40
• Tag device in black box (LED off)	0	0.95
• Tag device in black box (LED on)	0	0.95
• Tag device in housing in black box (LED off)	0	0.95
• Tag device in housing in black box (LED on)	667 ± 2	2.04
• Tag device with LFTs (1 mm spacing)		
<i>Lightest colour</i>	804 ± 49	2.26
<i>Darkest colour</i>	314 ± 27	1.46
• Tag device with LFTs (2 mm spacing)		
<i>Lightest colour</i>	647 ± 18	2.00
<i>Darkest colour</i>	277 ± 26	1.40
• Tag device with LFTs (4 mm spacing)		
<i>Lightest colour</i>	212 ± 17	1.29
<i>Darkest colour</i>	10 ± 3	0.96
• Average of all tag devices with LFTs (2 mm spacing)		
<i>Lightest colour average</i>	782 ± 237	2.22
<i>Darkest colour average</i>	382 ± 160	1.57

The results from the most repeatable colour detector tag that exhibited colour readout values closest to those from the commercial reader (Tag 4) are shown for five selected model LFT colours (Figure 5.5b). Clearly distinguishable ranges for colour readout values are discernible, particularly for lighter LFT colours (2,4,6), illustrating a higher degree of quantitative readout for top performing devices.

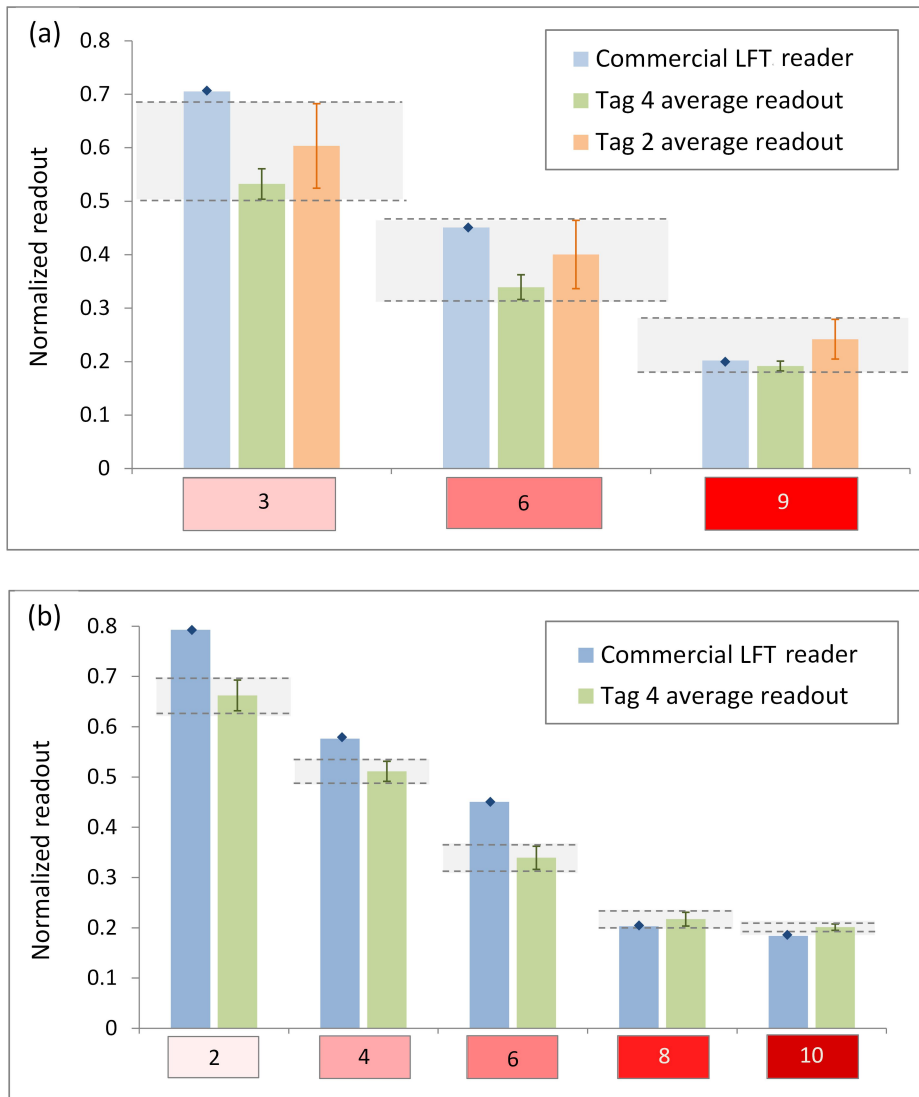


Figure 5.5 Wireless colour detector readouts compared to commercial ESEQuant reader results for a) most repeatable (Tag 4) and least repeatable (Tag 2) devices using three different model LFT colours, and b) colour detection for Tag 4 for five different model LFT colours. The grey shaded lines show the range of measurements across the least and most repeatable colour detector devices, highlighting correspondence to commercial reader results and distinct readout ranges for each colour.

5.4 Discussion

Colorimetric detection in paper-based diagnostic devices remains a challenge, and has been extensively reviewed [11]. Improvements are required for both diagnostic test implementation and colour detection. From a colour detection perspective, this chapter focuses on a low-cost solution to automate result readout. The colour detection results obtained were comparable to a commercial LFT reader and enabled result capture and communication through RFID, where the latter will be explored in more detail in the following chapter (Chapter 6). The colour detector could already be utilised for screening and semi-quantitative test readout requirements.

The results indicated successful semi-quantitative distinction between different model LFT devices. Variations in the measured colour intensity results for a single device range from 1 to 15% (Figure 5.4b). These large variations are a result of the currently manual assembly methods, where positioning of the SMD components affects the results. In addition, the battery voltage affects the intensity of each LED and thus the measured sensor value. The tag substrate (transparency or vinyl) does not appear to have an effect on the sensor readout, as this differs across devices on varying substrates (Figure 5.4b). Calibration methods can be implemented in future to account for these inter-device inconsistencies. Normalisation of the measured sensor values to the negative control sample as well as referencing of the results to the lowest intensity sample already assist with this process and could be extended to incorporate additional reference colours for calibration, yielding more accurate and quantitative colour detection capabilities if and where required.

Currently, the wireless tag devices show fair repeatability and usability for semi-quantitative colour detection. Inconsistent testing environments and lighting conditions were used throughout the testing, but the cardboard box housing ensured that these effects were negligible on the colour detection results. Figure 5.5a illustrates that a clear distinction can be made between different colours even when taking into account devices that have large standard deviations for colour readout values. For devices that perform similarly to the commercial LFT reader, a higher level of quantitation can be achieved, with the highest sensitivity for lighter colours (Figure 5.5b), which is where manual readout errors are most likely to occur.

The green LED used is well-suited to the long-term application for detection of colloidal gold on LFTs. Different colour light sources can be investigated, including white light sources, to provide a broader detection spectrum. This is useful where this work is extended to different paper-based test formats utilising different chemistries and is explored further in Chapter 8. The SFH 2430 photodiode is well-suited for detection of the model red and pink colours, with higher sensitivity to lighter pink

colours (Figures 5.4c and 5.5b), where distinct colour values are obtained for visually similar colours (e.g. LFT 5 and 6). The SFH 2430 provides a large dynamic range for the sensor measurements obtained, without adjusting the parameters in the SL900A ADC. Future work could entail the investigation of different light sources and photodetectors to find the optimal sensitivity range. In addition, parameters in the SL900A ADC can be adjusted to provide an optimal dynamic range for the sensor being utilised, allowing for more sensitive sensor readout.

In the current design, default settings were employed along with a 2 mm spacing between the LED/photodiode and LFT. The characterisation of spacings in conjunction with ADC settings could be investigated to produce optimal results for the light source and sensor combination implemented.

LFT formats could be extended to the commonly available LFTs packaged in plastic cartridges, as explored in Chapter 8, or alternative housings. In the long term, the colour detector system could be applied to paper-based tests with customised form factors.

Based on the results presented in this chapter, a paper-based, scalable packaged design was developed and tested using both the model and real-world LFTs to assess the functionality of the wireless colour detector devices further.

6 Communication

This chapter is based on previously published work [138] and has been republished with permission of IOP Publishing Ltd., with permission conveyed through Copyright Clearance Center, Inc. Sections of this work are based on [112] and have been reproduced with permission from the Rapid Product Development Association of South Africa.

6.1 Overview

This chapter focuses on the communication of results and information from paper-based POC diagnostics. Data capturing is typically performed manually in resource-limited clinic settings, introducing immense challenges in the tracking of samples and results between the clinic and laboratory [1]. Storing and back-up of results and data are problematic [50], and can cause delays and errors in the recording of patient results. Automated digital data capture and communication would be optimal to enable result storage, as well as the ability to access, share and file results. As discussed in Chapters 2 and 3, the connectivity of paper-based diagnostics has been explored through printed antennas and RFID technologies. This chapter explores wireless communication using the SL900A to readout and transmit information and measured sensor values that could potentially be obtained from paper-based diagnostic tests.

This work builds on literature in which the characterisation of printed UHF RFID antennas on different paper, cardboard and flexible substrates has been explored [110, 111, 169], along with the manufacture of printed smart tags to balance reliability and cost [170]. Extensive characterisation of SL900A-based tag antennas has been presented [153, 161, 171].

Initial tests included printed antennas on paper substrates to extend the read ranges of existing RFID tags, as well as the printing and assembly of RFID and NFC tags onto paper substrates to demonstrate functionality for paper-based solutions. Next, the work focussed on SL900A-based RFID tag characterisation and performance.

Tags printed and assembled onto different substrates (Chapter 4) were assessed to demonstrate the wireless communication capabilities of the tags and suitability to resource-limited clinic settings. Read range measurements were performed for both the detection of the tags and readout of sensor values. Tags were tested in both passive and semi-passive modes, as well as with a load attached to assess the practical functionality of the tags. Varying orientations of the tags to the reader were also tested to evaluate the non-ideal test situations that may occur in real-world testing environments.

6.2 Methods

6.2.1 Printed RFID tags

The mounting of existing commercial RFID tags or inlays onto printed lines on paper substrates was explored to assess the read range enhancement of the tags that was achievable. This work was carried out with a local RFID company (Techsolutions (Pty) Ltd., South Africa), using a handheld RFID reader (CSL101, Convergence Systems Limited, Hong Kong) with a frequency of 915 MHz and an J42 sticker inlay (Impinj, USA) with dimensions of 15 mm \times 8 mm. Printed lines with a width of 1 mm and lengths ranging from 100 to 160 mm were printed onto photo paper (NB-RC-3GR120, Mitsubishi Paper Mills Ltd, Germany) using a Dimatix DMP 2831 materials printer (Fujifilm, Japan) and conductive silver ink (NPS-JL silver nanopaste, Harima Chemicals, Japan). The ink was cured in an oven at 120°C for 2 h. The inlay sticker was then mounted over the printed line and read range measurements were performed.

To illustrate wireless communication capabilities utilising printed devices further, RFID tag designs, including NFC and UHF examples, were printed, assembled and tested (Figure 6.2). The NFC tag antenna design was based on one of the tags from the the AS3955 NFC IC development kit (AS3955-WL_DK_ST, AMS, Austria), namely the 23 mm \times 38 mm coiled design. The NFC IC package size is 3 mm \times 3 mm \times 0.9 mm. The dimensions of the contact pads are 0.4 mm \times 0.25 mm, with a spacing of 0.25 mm between the pads. An insulating bridge was designed (yellow strip in Figure 6.2a) to enable a connection to be made from the outer antenna coil to the NFC IC over the antenna loop.

Various printed UHF RFID tag antenna designs were explored utilising an RFID IC (SL3ICS1002/1202 UCODE G2XL, NXP Semiconductors, Netherlands) mounted onto the terminals of printed antennas. Antennas included a UHF RFID design

reproduced with permission from NXP as well as a design based on the AD-224 (Avery Dennison, USA). The latter design was also investigated for use with the SL900A IC as it obviated the need for an additional matching inductor. Further details can be found in related publications [32, 112]. In related work, printed inductors have also been explored [172] and could be used with the SL900A. NFC and UHF RFID tag designs were inkjet printed onto photo paper using the same methods and materials as for the printed lines in the above paragraph. A design based on the reference design of the SL900A development kit was also manually screen printed, as described in Chapter 3.

After printing, the devices were assembled by mounting the NFC and UHF RFID ICs and other SMD components, as described in Chapter 3. Additional components used were a strip of insulating polyimide adhesive film (HB830-25, Hi-Bond Tapes Ltd., UK) to create a bridge and a 2.2 μF SMD decoupling capacitor (CGA4J1X7R1V225M125AE, TDK Corporation, Japan) to extend the read range, in addition to a green SMD LED and a 39 nH SMD matching inductor, as described in Chapter 3. The design, manufacture and testing of some of the tags are summarised in Figure 6.2. An Impinj Speedway Revolution R420 reader (Impinj, USA) was used, as well as a reader antenna provided by local South African RFID company Synertech (Pty) Ltd. (PATCH-A0025, RFID Patch Antenna, 860 to 960 MHz, circular polarization, Poynting Antennas (Pty) Ltd., South Africa) for initial tag testing, along with the Impinj MultiReader software, to visualise the effective reading and read range of the printed RFID tags. Testing was also carried out using the AS3993 development kit reader, as described in Chapter 3.

6.2.2 Antenna characterisation

Initial antenna characterisation was carried out using an SL900A tag antenna printed onto an adhesive vinyl substrate (FA1, Table 4.1 in Chapter 4). The antenna was connected to a E5071C ENA Vector Network Analyzer (Agilent Technologies, USA) via two U.FL cables mounted to the antenna terminals using conductive silver epoxy, and connected to a SMA coaxial cable to enable the reflection coefficient or S11 parameters to be measured. The monopole reader antenna from the development kit could also be connected to the Network Analyzer for S12 parameters to be measured as an indication of the power transmitted from the reader to the tag. S12 parameters were measured for different distances and different angular positions of the tag from the reader antenna (as illustrated in Figure 3.8 in Chapter 3), with the distances ranging from 5 to 25 cm.

Antenna characterisation for SL900A devices on flexible substrates has been carried out in detail [153]. Characterisation was not carried out in further detail in this work, as this required sophisticated equipment and peripherals which were not accessible, as well as the use of a custom short-open-load-through (SOLT) calibration kit [153,173]. For this work, practical read ranges were deemed a more relevant performance criterion to assess the functionality of the tags in real-world settings.

6.2.3 Read range measurements

Read range is the most important RFID tag performance characteristic, and is defined as the maximum distance at which an RFID reader can detect a backscattered signal from a tag [97]. The read range is affected by the tag response threshold, tag orientation, and the material surrounding the tag. The read range, R , can be calculated using

$$R = \frac{\lambda}{4\pi} \sqrt{\frac{G_t G_r P_r \tau PLF}{S_t}} \quad (6.1)$$

where λ is the wavelength (using a frequency of 915 MHz) and S_t is the sensitivity of the SL900A IC, which is the minimum received power required to activate the chip. G_t and G_r refer to the gain of the tag antenna and the reader antenna, respectively. PLF is a factor that takes into account the polarization mismatch between the reader antenna and the tag antennas, and can be assumed to be 0.5 (−3 dB) [153,161], while τ is the power transmission coefficient, which is a factor that takes into account the losses related to mismatching between the chip and the antenna, and can be calculated as

$$\tau = \frac{4R_c R_a}{|Z_c + Z_a|^2} \quad (6.2)$$

where R_c and R_a are the chip and antenna resistance, respectively, and Z_c and Z_a are the chip and antenna impedance, respectively [97,174]. Improved impedance matching results are obtained as τ approaches 1 [97].

Read range measurements were carried out using the AS3993 development kit reader, as described in Chapter 3 and shown in Figure 3.8. The reader antenna used was the monopole from the development kit with a gain of 2.2 dBi (G_r). The power transmitted by the reader is 22 dBm, providing an effective isotropic radiated power (EIRP) of 24.2 dBm assuming no cable losses. The reader sensitivity, S_r , was maintained at the default setting of −68 dBm. Assuming a tag antenna gain, G_t , of 1 dBi

as measured previously for a PCB-based SL900A dipole [153, 171] and $S_t = -7$ dBm, a theoretical read range of 750 mm would be expected using equation 6.1 for tags in passive mode. The tag sensitivity is calculated using the wake up power of the SL900A IC of 0.2 mW in passive mode.

Shorter read ranges would be expected as the theoretical read range value assumes perfect matching between the chip and the antenna, but different real parts of the impedance of the antenna and chip cause mismatching, lowering the value of τ [162]. The path loss, PL , is a function of λ and the distance between the tag and reader, and can be calculated using

$$PL = 10 \log\left(\frac{\lambda^2}{(4\pi r)^2}\right) \quad (6.3)$$

where r is the distance between the reader and tag antenna [175, 176]. Assuming a distance of 0.5 m between the RFID reader and tag, an example of the RFID link budget, which takes into account the various gains and losses in the system [177], can be estimated. Using a distance of 0.5 m, $PL = -25.6$ dB (equation 6.3). The forward link, FL , or power incident on the tag is defined by

$$FL = EIRP + PL = 24.2 \text{ dBm} - 25.6 \text{ dB} = -1.4 \text{ dBm} \quad (6.4)$$

With the wake up power of the chip being -7 dBm in passive mode, the FL has enough power to power on the tag IC. The reverse or return link, RL , or the power received by the reader from the backscattered tag signal is determined using the power incident on the tag, PT , the modulation loss, ML , and PL by

$$RL = PT + ML + PL = -1.4 \text{ dBm} - 10 \text{ dB} - 25.6 \text{ dB} = -37 \text{ dBm} \quad (6.5)$$

This assumes $ML = -10$ dB, as this value is typically -6 dB or worse and is a function of the antenna design. This indicates that the reader can detect the incoming tag signal of -37 dBm, as the reader is more sensitive (-68 dBm). However, this does not take into account any additional losses that may be present in the system or that may be introduced by the manually assembled tags on different substrates. Figure 6.1 illustrates the tag and reader set-up with various parameters for the different calculations.

The received signal strength indicator (RSSI) is an indicator of the signal strength returned from a tag to the RFID reader, and can be estimated theoretically by RL (equation 6.5) [176]. The RSSI can be used to estimate the distance between a tag and a reader antenna practically. Both read ranges and corresponding RSSI values were recorded for the tags tested in this work.

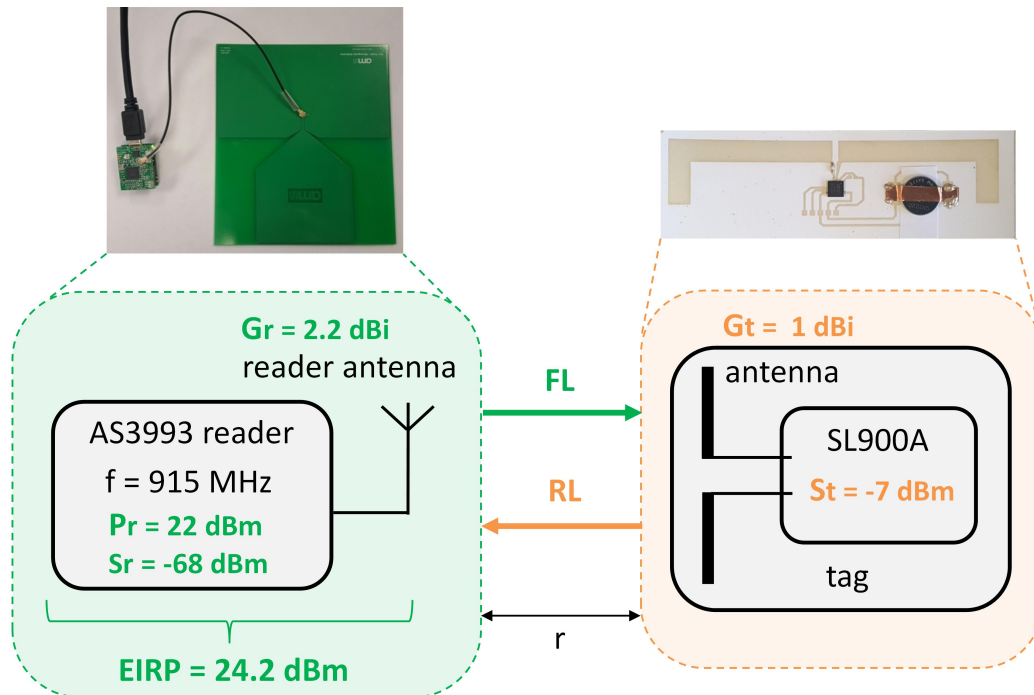


Figure 6.1 Tag and reader set-up with values used to calculate theoretical read range and RFID link budget.

The tags tested were based on the generic SL900A tag design shown in Figure 3.4 in Chapter 3. Although the ideal value of the matching inductor would vary according to the substrate used, and consequent input impedance, the value of 39 nH was implemented for all tags, as per the design implemented for the tag development kit. This allowed for relative comparisons to be made across all substrates, and eliminated the need for specialised antenna optimisation software and characterisation equipment that would be required to calculate the matching inductor values for each printed antenna.

In addition to read range measurements for tag detection, the maximum distance for successful readout of the temperature sensor value (on-board the SL900A IC) from the tag was also recorded. Three devices were tested for each type of substrate – both with and without a battery. For each tag scanned, the corresponding RSSI was recorded. The screen printed RFID tags were compared to PCB devices of the tag antenna as a benchmark, including the SL900A development kit (CB1) and a milled PCB of the tag antenna manufactured and assembled in-house (CB2).

Individual tags for eight selected substrates (Table 6.1) were analysed to determine the effect of the distance between the tag and reader on the RSSI values (Figure 6.5). RSSI values over distance were also tested with a load connected to the SL900A for each tag to simulate a practical application, towards an integrated POC diagnostic solution. This entailed components being attached to both the EXT1 and EXT2 pins of the SL900A IC mounted onto the tag, as resistive and optical sensor inputs, namely a 100 k Ω resistor (RS Pro, RS Components, South Africa) and an optical sensor (VTB8440B photodiode, PerkinElmer Optoelectronics, USA), respectively, as well as a 575 nm green LED (TLLG4400, Vishay, USA) connected between the battery supply for potential user feedback or displaying of results. The components were assembled on a bread board and connected to the tag via wires and a 4-pin PCB header (26-60-4040, Molex, USA). The EXT1, EXT2, V_{BAT} and V_{SS} pins on the tag design of Figure 3.4b were extended to the edge of the tag using copper tape and insulation tape as a bridge where required, enabling the header to make contact with the tag and connecting to the external load circuitry.

To understand the practical functionality of the printed tags further, read ranges for different tag orientations were also recorded using the test set-up shown in Figure 3.8 in Chapter 3 to emulate real-world, non-ideal testing conditions.

Table 6.1 Selected tag substrates for performing further practical functionality testing.

Substrate	Description
CB1	Development kit PCB: benchmark device for comparing to printed devices
CB2	Milled PCB: benchmark manually assembled device for comparing to printed devices
PE3	Printed electronics substrate: performs well with large read ranges achieved
PM2	Chromatography paper with wax: typically used for paper-based microfluidics
PE1	Photo paper: standard substrate for printed electronics, particularly inkjet printing
FA2	Adhesive substrate: large variations in read range performance
FL4	Transparency: low-cost substrate, poor performance without battery
PE6	Printed electronics substrate: shorter read ranges recorded

6.3 Results

6.3.1 Printed RFID tags

Read range enhancement using an existing inlay with printed silver tracks was demonstrated. The read range for the RFID inlay alone was measured as 50 mm. When attached to the printed tracks, read ranges of over 4 m were achievable for printed lines of 150 mm in length. This demonstrated substantial read range extension of existing tag stickers, which are mass producible and low in cost, through simple printed lines on paper substrates, where a small modification enables a significant improvement in the read range capability.

NFC and UHF RFID tag designs as shown in Figure 6.2 were manufactured, assembled and tested to illustrate the functionality for wireless communication of data stored on the tags. For the NFC tags, a Samsung Galaxy S6 smart phone in NFC-enabled mode was used as the reader. When a tag is detected, the phone displays text information that was stored on the tag prior to scanning the tag. Various data formats can be written to the tag, including website links. NFC has very short read ranges, up to only a few centimetres depending on the system parameters, and for the manufactured prototype in Figure 6.2a, the mobile phone needed to be in very close proximity to the tag (almost contacting) to allow for detection of the tag.

For the SL900A tags using the reference development kit antenna design, read ranges of up to 2 m would be expected in ideal conditions and in battery-assisted mode, with over 1 m for passive mode (without a battery). Successful scanning of tags using the Avery Dennison antenna design was demonstrated for read ranges between 100 and 200 mm, while for the reference dipole design, read ranges of approximately 400 mm were achievable in passive mode using the AS3993 reader (Figure 6.2b). When the tag is in range of the reader antenna, the green LED on the tag is illuminated using the RF field. The sensing capabilities of the SL900A IC enable the instantaneous readout of temperature using the development kit software. The optimal read range specifications assume that there is perfect matching between the tag and antenna, but as a result of the thin printed layers achieved with inkjet printing, there is a mismatch between the impedances of the antenna and the RFID chip, as well as poor antenna gain. In addition, the flexible photo paper substrate and consequent bending of the antenna could also hinder the achievable read range.

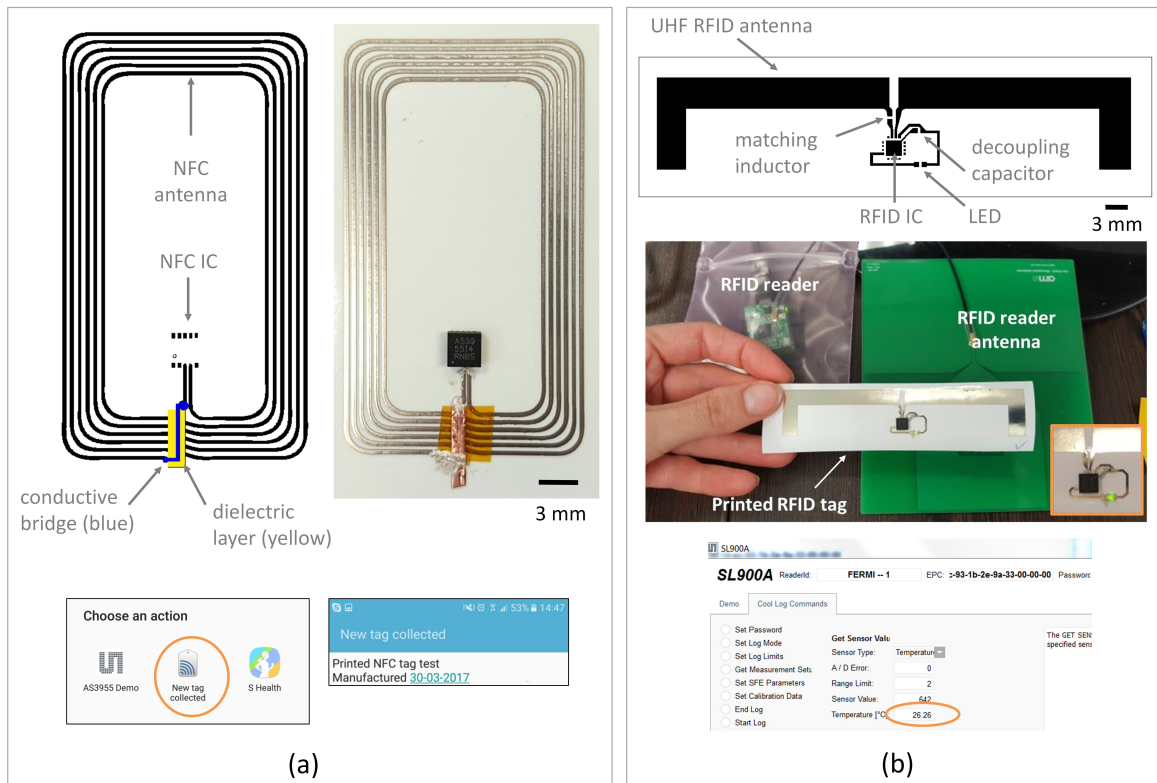


Figure 6.2 a) NFC tag design and printed, assembled tag device tested using a smart phone as a reader. b) SL900A UHF RFID tag design and printed, assembled tag device tested using AS3993 reader and antenna. Scale bars are indicated in each case. Reproduced from [112] with permission from the Rapid Product Development Association of South Africa.

6.3.2 Antenna characterisation

The input impedance of the dipole antenna at 915 MHz was measured as $20 + j68.5 \Omega$. The dipole was designed to match the real part of the impedance of the SL900A IC. Differences in the measurements are likely as a result of the substrate, printed ink and imperfect mounting of the cables onto the printed antenna. Using the theoretical input impedance of $31 - j305 \Omega$ for the SL900A IC [152], the matching inductor value of 39 nH as per the design compensates for the imaginary part as required.

For different tag distances and orientations to the reader, the power ranges from -26.8 dB for 5 cm to -32.5 dB for 25 cm at 915 MHz, with similar power levels obtained for different orientations at the same distance. As expected, the power decreases as the distance between the tag and reader increases. Further antenna

characterisation was not performed, as a differential measurement set-up must be used for a symmetric feed to be realised. An unsymmetric feed introduces common mode currents that cause stronger radiation than the original radiation of the antenna [173]. To perform balanced reflection coefficient measurements, a differential port must be formed, and a custom-built calibration kit must be used to shift the reference plane of the measurement directly to the dipole. As accurate measurements could not be performed, the characterisation focused on read range measurements, as this is the most important performance characteristic for RFID tags.

6.3.3 Read range measurements

Read range measurements were carried out for SL900A tags printed and assembled onto various substrates, as described in Chapter 4. Read range measurements were also performed for colour detector tags that were assembled and tested, including those tested inside PMMA housing and a cardboard box, as described in Chapter 5.

Various substrates

Examples of tags printed and assembled onto various substrates used for the read range testing are shown in Figure 6.3.

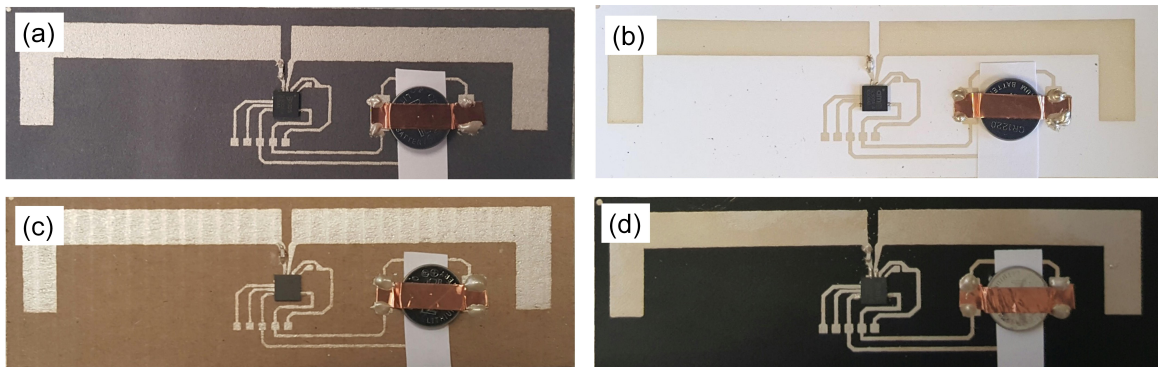


Figure 6.3 Examples of tags assembled onto different substrate categories as in Chapter 4, Table 4.1, namely a) PM2 – chromatography paper with wax melted through, b) PE9 – ceramic coated paper for printed electronics, c) FL2 – cardboard packaging and d) FA3 – matt adhesive vinyl. Republished with permission of IOP Publishing Ltd. from [138]; permission conveyed through Copyright Clearance Center, Inc.

Figure 6.4 shows the read range measurements obtained using the set-up shown in Figure 3.8 in Chapter 3. The maximum read ranges and RSSI values were recorded

for each tag. Read ranges between 75 and 300 mm were measured for tags in passive mode (average of 212.1 mm for tag detection (± 78.9 mm) and 177.5 mm for temperature readout (± 66.8 mm)), and between 150 and 400 mm for battery-assisted mode (average of 352.4 mm for tag detection (± 137.4 mm) and 300.8 mm for temperature readout (± 96.7 mm)), excluding the benchmark development kit device (CB1), which had slightly higher read ranges of more than 900 mm with a battery connected. Longer read ranges are achieved in battery-assisted mode, as expected, and variations in the read ranges for the same substrate can be noted as a result of manual fabrication and assembly of the individual tags. The average RSSI values recorded for the various tags range from -44 to -40 dBm for passive mode and -54 to -47 dBm for tags in battery-assisted mode. Large variations in RSSI values can be noted for PE4, potentially as a result of the print quality affecting the tag measurements.

Read range results were also performed by Synertech with a commonly used commercial RFID reader (Impinj Speedway Revolution R420, Impinj, USA), circularly polarized reader antenna (SF-1101, Flexiray, Czech Republic) with a gain of 0 dBi, and with region setting for South Africa. The reader settings were adjusted in the software and included a reader transmit power of 26 dBm and a receive sensitivity of -70 dBm. The results showed that all printed tags were functional with read ranges between 170 and 510 mm obtained for tags in passive mode, and between 313 and 863 mm in battery-assisted mode. RSSI values obtained ranged from -46 to -39 dBm for passive tags and -63 to 46 dBm for battery-assisted tags. Longer read ranges were obtained compared to the development kit reader measurements as a result of the difference in reader antenna properties and settings.

The results for the eight selected substrates to evaluate the effect of distance between the tag and the reader on RSSI values obtained are shown in Figure 6.5. RSSI values over distance results are shown for three modes: passive, battery-assisted, and battery-assisted with a load connected.

Read ranges for different tag orientations were recorded. The default 0° orientation provides optimal read range results, but in a practical situation the tag orientation could vary. The set-up used for the orientation tests is shown in Figure 3.8, with the results presented in Figures 6.6 and 6.7, and summarised in Figure 6.8, to illustrate the overall effect of the tag orientation on the readability of the tags.

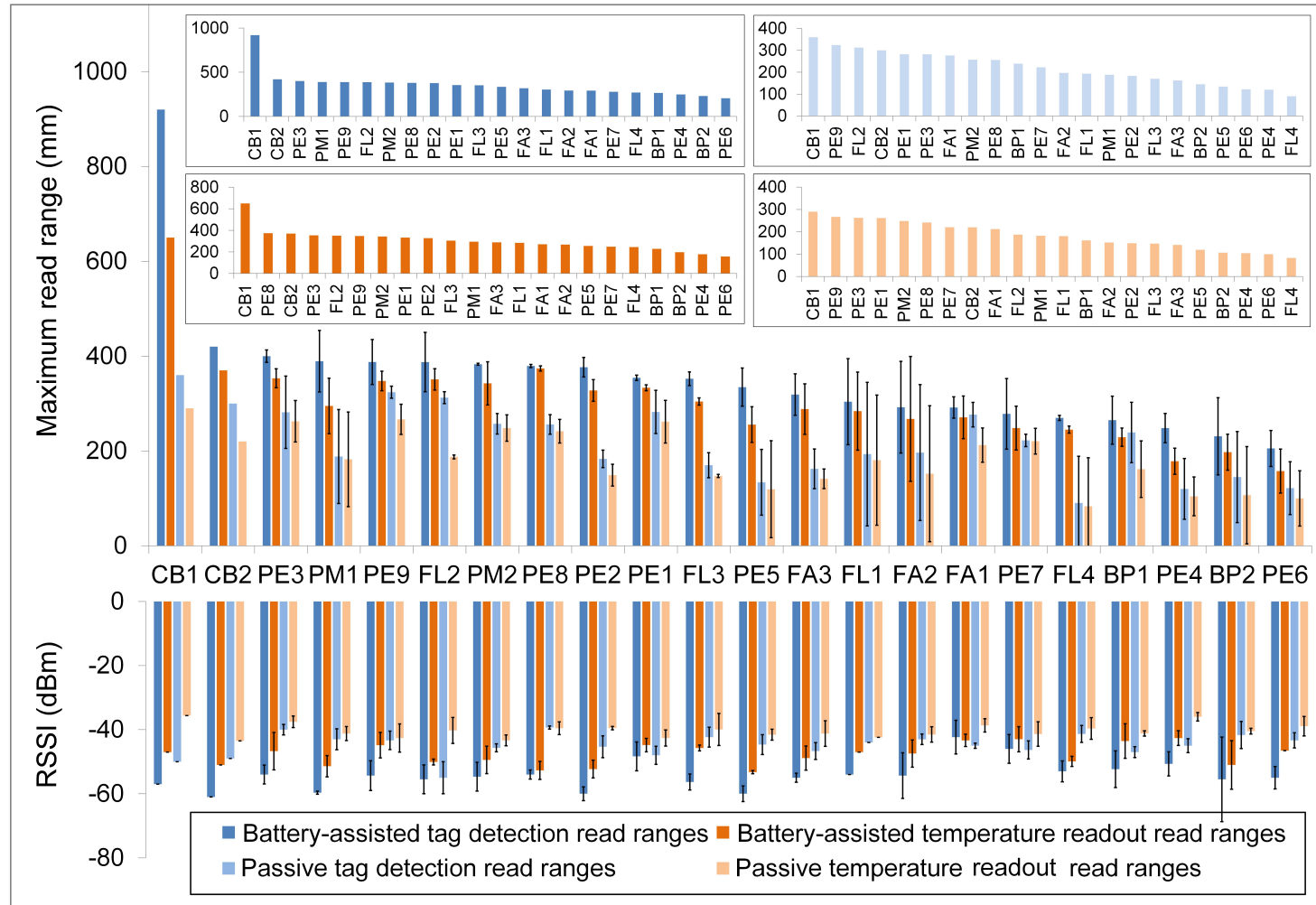


Figure 6.4 Maximum read ranges and RSSI values recorded for three tags per substrate type. Battery-assisted and passive modes were investigated, for both tag detection (blue) and sensor readout (orange). Insets show ordering of read ranges from highest to lowest across the substrates for each of the tag readout modes. Republished with permission of IOP Publishing Ltd. from [138]; permission conveyed through Copyright Clearance Center, Inc.

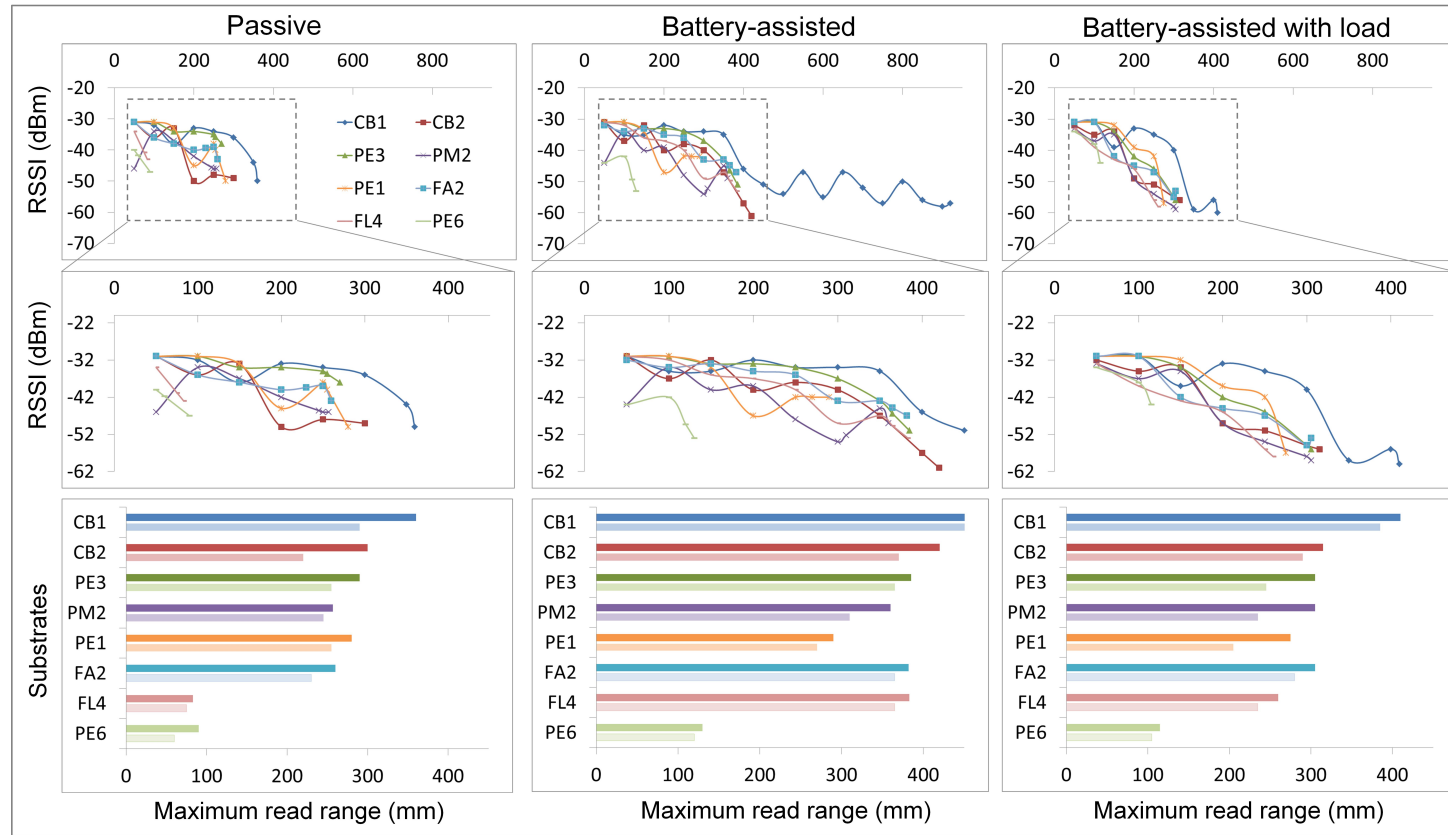


Figure 6.5 RSSI over distance with maximum read ranges for individual tags of selected substrates to illustrate practical functionality in passive and battery-assisted modes, as well as with a load connected. Republished with permission of IOP Publishing Ltd. from [138]; permission conveyed through Copyright Clearance Center, Inc.

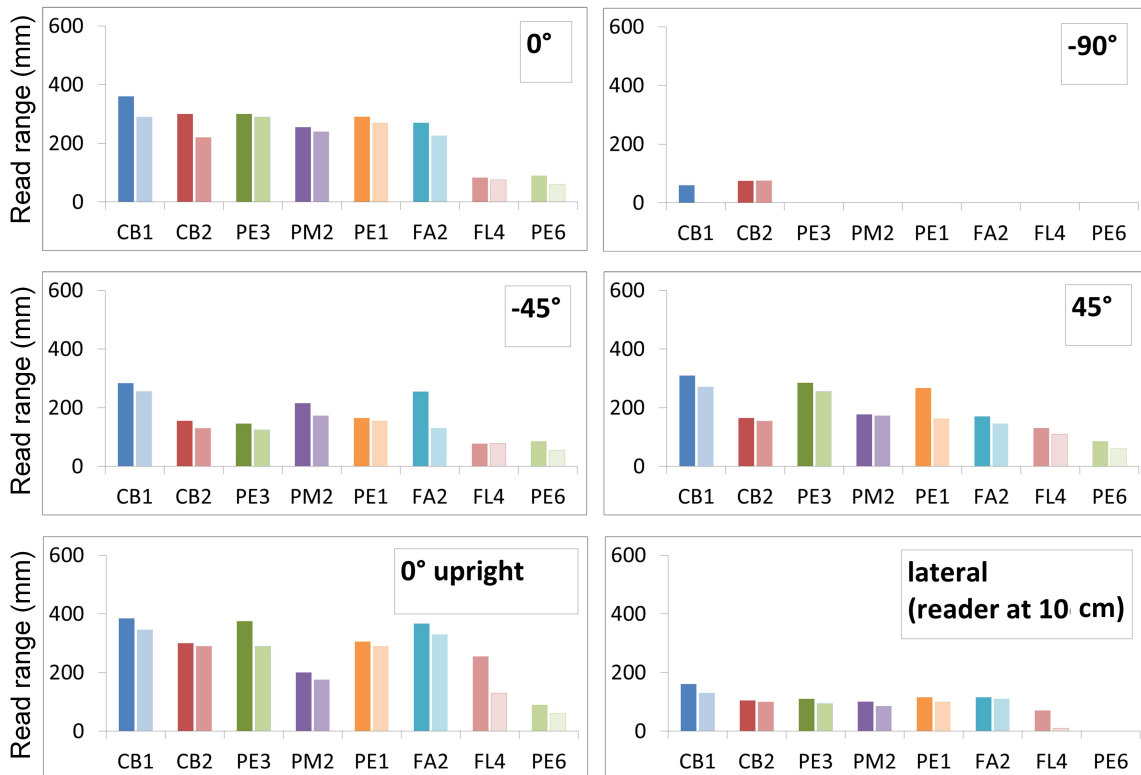


Figure 6.6 Maximum read range results for different tag orientations for eight selected substrates in passive mode. Maximum read ranges for successful detection are shown in darker colours and corresponding maximum read ranges for successful temperature read-out in lighter colours. Republished with permission of IOP Publishing Ltd. from [138]; permission conveyed through Copyright Clearance Center, Inc.

Colour detector in PMMA housing

As an addition to the extensive read range measurements for tags assembled on different substrates, the maximum battery-assisted mode read ranges at which the photodiode sensor values could still be read out wirelessly through the RFID reader user interface were recorded. Six vinyl and transparency tags, as described in Chapter 5, were used to perform the read range measurements. Tags were tested with and without the PMMA enclosure, as well as inside the PMMA enclosure and the cardboard box sealed from external light (as described in Figure 5.2). When tested in the housings, the tags retained at least 50% of the read ranges achievable for both transparency

and adhesive vinyl substrates (Table 6.2), with longer read ranges achievable using tags printed and assembled onto adhesive vinyl substrates.

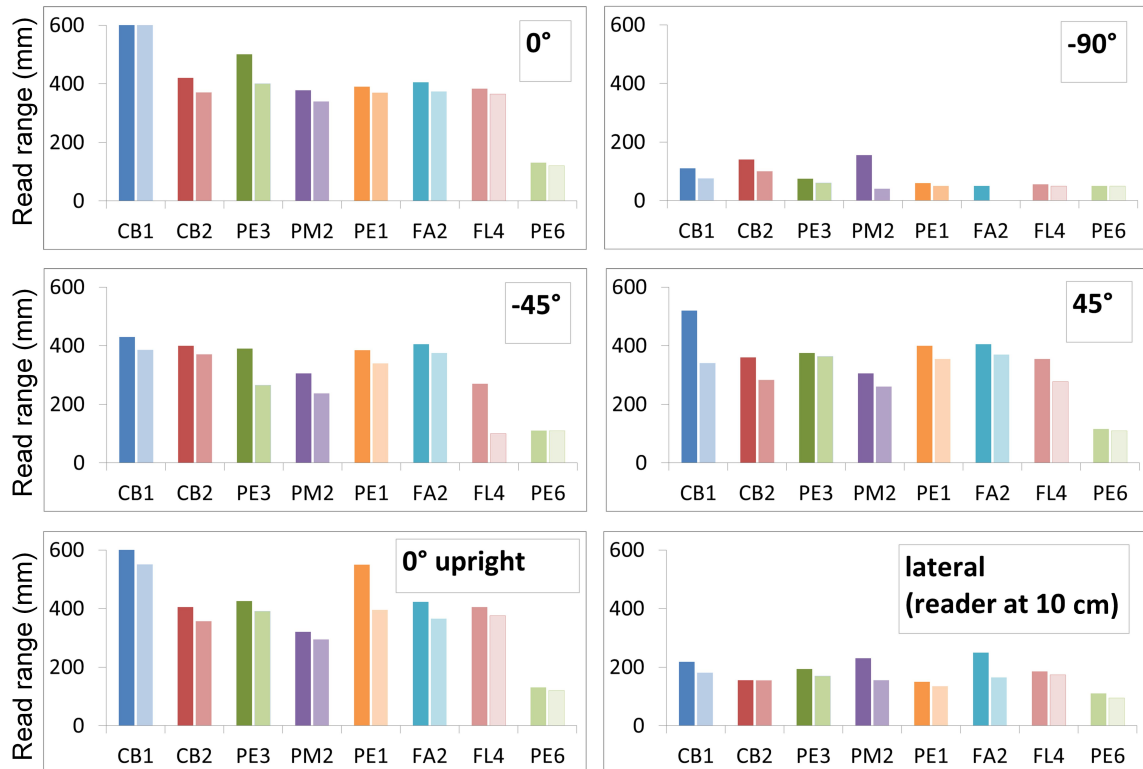


Figure 6.7 Maximum read range results for different tag orientation for eight selected substrates in battery-assisted mode. Maximum read ranges for successful detection are shown in darker colours and corresponding maximum read ranges for successful temperature readout in lighter colours. Republished with permission of IOP Publishing Ltd. from [138]; permission conveyed through Copyright Clearance Center, Inc.

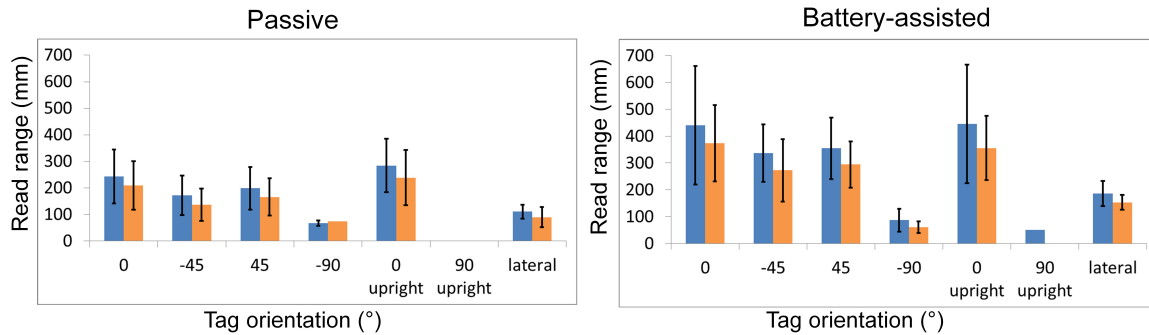


Figure 6.8 Summary of tag orientation results across eight different substrates. Average maximum read ranges for successful detection (blue) and temperature readout (orange) are shown to illustrate the trends for varying orientations in both the passive and battery-assisted modes. Republished with permission of IOP Publishing Ltd. from [138]; permission conveyed through Copyright Clearance Center, Inc.

Table 6.2 Maximum read range measurements for three colour detector tag devices for each substrate. Average read ranges are shown with standard deviation across the tag devices.

Substrate	Read ranges (mm)		
	Tag only	Inside PMMA housing	Inside PMMA and cardboard box
Transparency tags (T)	56.67 ± 7.64	40.00 ± 5.00	23.33 ± 7.64
Vinyl tags (V)	118.33 ± 7.64	76.67 ± 10.41	53.33 ± 18.93

6.4 Discussion

Functional RFID tags were demonstrated through the wireless communication of information stored on the RFID ICs to a mobile phone or a PC (Figure 6.2). This information could include the type of test, serial number, manufacture date and expiry date for POC tests. Initial antenna characterisation was carried out, but more detailed measurements were not performed for this work. With the various substrates tested, characterising antennas for each substrate would be difficult, particularly in using manual mounting techniques for the connectors, which would also affect the accuracy of the measurements. Extensive read range measurements were performed as

these are most important in terms of the performance and practical implementation of the wireless communication, rather than focusing on optimisation parameters for the antennas or transmission speeds.

All 60 printed tags tested were operational, with minimum read ranges of 75 mm achieved in passive mode (Figure 6.4). This is adequate for the purposes of the intended POC diagnostic applications for contactless and contamination-free communication of results from the test device. Maximum read ranges for the development kit in this work were approximately 900 mm in battery-assisted mode and 360 mm in passive mode, and used as a comparative baseline. The theoretical maximum read range calculated for the set-up in this work was 750 mm. Shorter read ranges would be expected in practice as a result of various factors.

Other research that utilised the SL900A and carried out optimisation of the antenna design and impedance matching achieved read ranges between 800 and 1100 mm in passive mode [153, 159, 161, 162]. In all cases, the theoretical read ranges were longer than those achieved in practice. In these works, tags are generally implemented on optimal substrates using high-precision printing techniques, and each with different antenna and reader settings. The development kit tag and reader manufacturer reports a read range of up to 2 m achievable in battery-assisted mode, but this can be affected by a number of parameters including the antenna gain, antenna polarization, output power, reader sensitivity, transponder (SL900A IC) and antenna type, which are not specified for this result. Variations in the read range and RSSI values in this work can also be attributed to the manual printing and assembly procedures, as well as environmental factors as the tags were tested in a standard laboratory, where reflections in the RF signal can occur. Impedance mismatch and poor antenna gain can be caused by printing, and could be improved by printing thicker, more uniform layers [162]. The printing technique used can also affect the performance of the RFID tag, but can still produce reliable tags [178], which is the ultimate goal of this work.

Individual tags for selected substrates were tested to investigate the variation in signal strength received as a function of distance, and showed a decrease in RSSI as the distance increased (Figure 6.5). Typical RSSI ranges utilised by Synertech include a -80 dBm cut-off, where a tag is typically no longer classified as readable, and a maximum received signal strength of a tag of -20 dBm as a standard measure of performance. RSSI values between -35 and -30 dBm are considered to be indicative of high performance tags, but are often difficult to achieve in real-world conditions. The RSSI values recorded for the various tags in this study range from -60 to -35 dBm, with all values still well within the acceptable performance range. The sensitivity of the reader will affect the RSSI values recorded, as an increase in sensitivity will allow for weaker tags (lower RSSI values) to be recorded.

Trends in the RSSI values and resulting maximum read ranges for the selected substrates are comparable for the passive, battery-assisted, and battery-assisted with load scenarios. Read ranges are shorter with a load connected than in semi-passive mode with a battery, but tag performance is adequate, with read ranges in excess of 100 mm achievable with a load comprising an LED and two sensor inputs. This showcases sufficient functionality for practical applications. The power settings of the reader will affect the measurements, where an increase in 3 dB doubles the power, and thus increases the read range. This will be an important consideration for practical implementations in clinics, where power could be restricted and a trade-off should be made between acceptable read ranges and resource constraints, along with cost.

The tag orientation, angle and placement all play a role in the read ranges achievable, as seen from Figures 6.6, 6.7 and 6.8. An orientation of 0° is optimal for all tags, while -90° upright results in the poorest tag performance, with only the development kit tag (CB1) detected in battery-assisted mode. Lateral displacement of tags also resulted in poor tag performance, particularly for antenna reader heights exceeding 200 mm, where most tags could no longer be detected for any displacement distance tested. In practical settings, tag orientation is an important consideration, but could be implemented in such a manner that the scanning set-up adheres to a range of tag orientations that would produce a working result.

Colour detector tags on vinyl substrates resulted in average read ranges of more than 50 mm even when assembled inside the PMMA housing and the cardboard box (Table 6.2). Future work focusing on the optimisation and automation of printing and assembly of tag devices could enable longer read ranges to be achieved. More powerful RFID readers and reader antennas could also be investigated, along with optimisation of the tag antenna design. Read range enhancements of more than 200% have been showcased for SL900A-based devices using a photovoltaic panel for energy harvesting [171].

This work confirms that for acceptable read ranges of approximately 50 mm, reliable RFID readout can be achieved for tags printed onto different substrates with colour detection capabilities and suited to POC diagnostic applications.

7 Packaging and integration

This chapter is based on work that has been submitted to Nature Scientific Reports as part of a manuscript which is awaiting reviewer feedback.

7.1 Overview

This chapter focuses on the integration of the components detailed in the previous chapters, including substrates, colour detection and communication. Packaging of these components into a solution suited to POC diagnostic applications in resource-limited settings is key for the developments made thus far to be effective.

As discussed in Chapter 3 and illustrated in Figure 3.1b, automated wireless readout devices need to be integrated and packaged into robust, low-maintenance and low-cost solutions. Paper or cardboard packaging implementations are advantageous in terms of cost, disposability and suitability to printed functionality and were thus explored as potential solutions. Components for printed functionality can either be printed directly onto the packaging itself, or printed onto adhesive vinyl substrates that could be applied onto the packaging. This includes both printed electronic capabilities for colour detection and wireless communication, and printing of graphics, where user guidelines can be included. Product information, reference colour charts, user instructions, and QR codes are examples of printed graphics that could be included on the packaged device for ease of use and for providing information to the user.

Large-scale production processes exist for printing as well as paper and cardboard packaging, and could be utilised as a basis for the design and prototyping of packaged solutions. These processes are available locally, and a number of printing and packaging companies were approached to provide insights and expertise on the design and manufacturing processes that are typically followed. This enabled the most simple yet functional solutions to be realised as an initial integrated solution, with the potential for future scale up and mass production. Costing of the devices for automated and large-scale production could then also be mapped, and is discussed in more detail in Chapter 9.

Various packaging designs were explored, with a first version tested using model LFTs to assess the functionality of the devices. Colour detection and wireless communication of the results were demonstrated using the packaged, integrated wireless readout devices to illustrate their potential for real-world POC diagnostic testing.

7.2 Methods

7.2.1 Packaging designs

To expand on the promising results obtained from the wireless colour detector tags using the PMMA housing (Chapter 5), an initial scalable packaged design was developed towards a mass producible solution (Figure 7.1). This design utilises standard commercial large-scale printing and packaging designs and methods, where print designs are provided for the front and reverse. The design enables sheet-to-sheet printing of the functional tag devices and graphics. Once printed, individual devices are cut out or stamped, electronic components assembled, and the device folded with a cardboard insert to house the LFTs and retain the shape of the box. The insert differs depending on the test format used, i.e. whether it is a bare LFT or an LFT in a plastic cassette housing, or a different test strip, providing a modular cardboard packaging solution.

Figure 7.1a shows the design that houses the printed and assembled electronics (inside of box), and the design with graphics printed on the reverse (outside of box), including product information, user instructions and a QR code (Figure 7.1c). Up to four devices can fit onto a single A4 (297 mm × 210 mm) sheet (Figure 7.1b and d), and sealing and folding instructions are illustrated with numbered steps (Figure 7.1e) to create an assembled box (Figure 7.1f). The boxes are cut out along the black perimeter lines shown in Figure 7.1e) and the cut-out is then creased along the lines marked in pink and blue. Creasing can be done manually using a scalpel to lightly score the lines for ease of folding the box into shape. Folding and gluing of the box are performed by following the steps numbered 1 to 7.

Site visits to local packaging companies and investigations into packaging design and production processes that have been extensively documented [155] enabled a number of packaging designs to be conceptualized. The goal was to use standard packaging manufacturing techniques, as described in Chapter 3, section 3.8.

Further consultations with a local packaging company (Merrypak, South Africa) based on these designs resulted in the development of a matchbox-style cardboard box design with a cardboard insert as the first packaged solution to be tested using the wireless colour detector tags. The matchbox-style design (Figure 7.2) was printed

in a single-sheet format (one sheet for the outer sleeve and one sheet for the inner tray) on white glossy cardboard (King Pearl Design 210 GMS, Stationery and Print, South Africa) and manually cut out, creased, folded and glued for the prototypes used in this work. Graphics were printed on the outer sleeve to provide product information such as the test type, manufacture and expiry dates, as well as user instructions and a QR code for electronic information.

The dimensions of the outer sleeve (Figure 7.2a) are 141 mm × 46 mm × 21 mm. The outer sleeve and inner tray can each be printed onto an A4 sheet, or for larger-scale production, numerous designs could be printed on larger sheets or rolls. The box is designed to be closed at one end when folded. This provides an automatic stop when the user pushes in the tray. Some text is printed on the reverse of the sleeve (Figure 7.2b) as a guideline to the user and for positioning the colour detector RFID tag correctly when applying the label to the box. The inner box or tray is based on a typical matchbox inner tray design (Figure 7.2c), but is slightly lower on one end (15 mm) to ensure that it does not contact the electronic components of the RFID tag and that there is sufficient clearance. The dimensions of the inner tray are 120 mm × 45 mm × 20 mm, with the width and height slightly smaller than the outer sleeve design for ease of sliding the tray in and out of the sleeve. The length of the inner tray is shorter than the length of the outer sleeve so that when the tray is completely pushed in there is an additional 20 mm ledge to cover the inner tray. This is to prevent external light from affecting the colour intensity measurements. The insert design is highlighted by orange dashed lines (Figure 7.2c) and is positioned inside the tray as shown. This design will vary depending on the test format to be used, so that the test can be positioned correctly to align with the colour detector components and securely held in place.

The printed and assembled RFID tags, as shown in Figure 3.7 in Chapter 3, were mounted on the boxes prior to assembling the packaged devices. The inserts for the tray component of the box were made from lightweight 10 mm thick cardboard packaging (Kimmoboard, Kimmo (Pty) Ltd., South Africa) and were cut to size using a jigsaw. The cut-outs were covered with white vinyl as a protective layer, with an additional 1 mm thick vinyl-covered cardboard layer mounted on top and a custom cut-out for the specific test format used, such as cassette or test strip. A flexible vinyl ribbon with an arrow was attached under the insert to assist with pulling the tray out to insert a test. The dimensions of the final packaged reader devices are 141 mm × 46 mm × 21 mm.

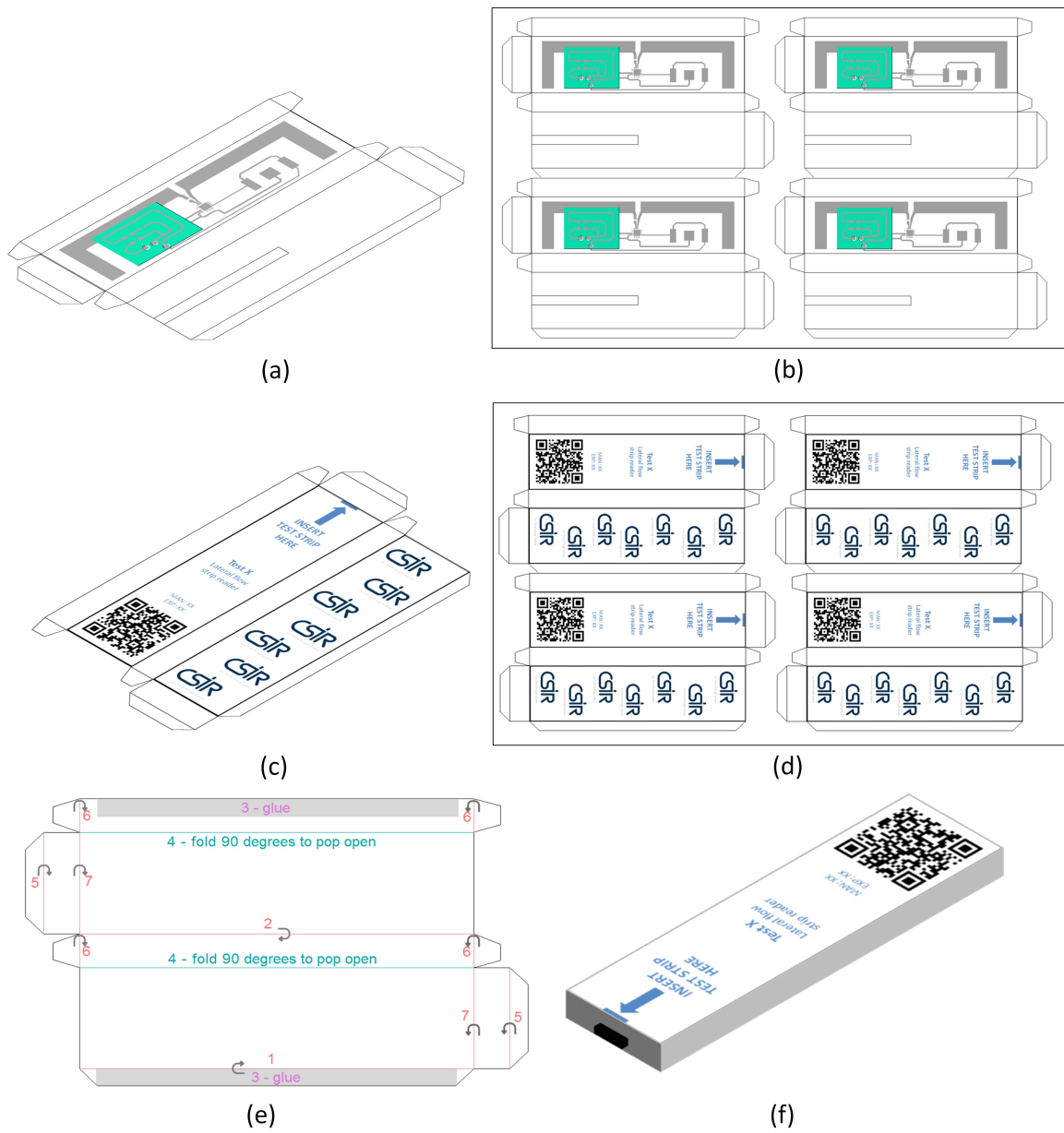


Figure 7.1 Scalable packaging designs for printed wireless colour detector modules. a) Front (inside) printed electronics design, b) reverse (outside) graphics design, c) sheet format of design for printing, d) folding instructions with assembly steps numbered (black lines = cut, pink and blue lines = crease), and e) complete assembled device.

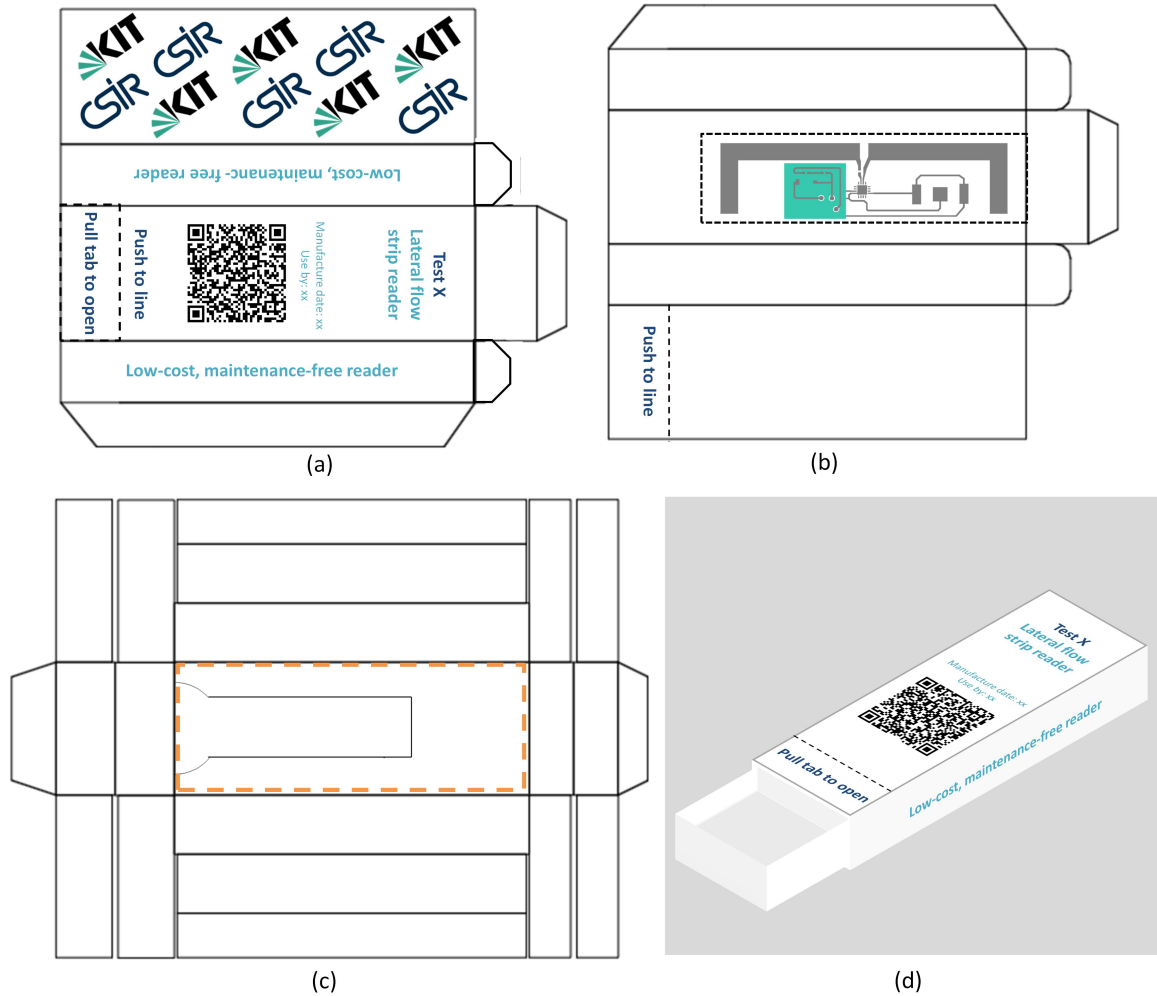


Figure 7.2 Scalable matchbox style packaging designs for printed wireless colour detector modules. a) Outer sleeve design with graphics and device information included to be printed in three colours. b) Reverse or inside of sleeve design, with alignment graphics for housing the printed colour detector tag and electronics. c) Inner tray design showing the placement and design of the insert (surrounded by orange dotted rectangle), and d) assembled box with inner tray that slides in and out of the sleeve.

For automated production, existing commercial printing and packaging methods including die cutting are feasible, in which print designs are provided for the front and reverse in large sheet formats. Once printed, automated cutting, creasing and gluing are carried out to produce the cardboard box packaging. The inserts can be made separately and placed into the tray once the box is assembled, or alternatively, could also be designed and manufactured to form part of the inner tray design. The insert can then be folded and glued in such a manner that it provides a rigid structure inside the tray. Several insert concepts were explored with Merrypak, but for the ease of developing an initial prototype, the inserts were produced separately for this design.

7.2.2 Integrated device testing

Five packaged low-cost wireless reader devices were tested using the 12 model LFT devices described in Chapter 5. The LFTs were housed in plastic LFT cassettes (MICA-125 DCN plastic cassette, 1 hole, Diagnostic Consulting Network, USA) to emulate real-world, commercially available LFT formats that would typically be tested in resource-limited clinic settings. The cassette dimensions are 20 mm × 69.75 mm × 5.25 mm and are designed to accommodate standard LFT strips with dimensions of 4.5 mm × 60 mm. Each of the 12 model LFT cassettes was tested inside the packaged reader devices. Sensor values were captured through the RFID reader user interface as described in Chapter 3, using an average over a 30 s period as a stable sensor readout result for each test. The results were compared to those obtained using the commercial LFT reader as well as ImageJ results obtained using the scanned image of the LFTs, as described in Chapter 3 and illustrated in Figure 3.3.

Read range measurements were performed using the set-up and parameters as described in Chapters 3 and 6. The maximum read ranges at which the photodiode sensor values could still be read out wirelessly through the RFID reader GUI were recorded. Read range measurements were performed on ten colour detector tag devices assembled into the cardboard boxes, and with LFT cassettes inside the cardboard boxes. The read ranges were recorded with the battery connected to emulate real-world testing conditions for these devices, as the LED is currently driven using the battery.

7.3 Results

7.3.1 Packaging designs

Figure 7.3 shows the manufacture and assembly of the initial packaging design explored for this work. Sheet-to-sheet printing with manual assembly of components was demonstrated towards the long-term goal of a low-cost, maintenance-free packaged device for POC testing. The matchbox-style packaging prototype used for testing the colour detector tags with model LFT devices housed in plastic cassettes is shown in Figure 7.4. Flexible adhesive vinyl tabs were mounted into the inner tray under the insert with an arrow to indicate to the user to pull the tab to slide out the tray, into which a test could then be placed.

7.3.2 Integrated device testing

Figure 7.5 shows an example of a packaged reader device with a model LFT cassette and colour detector tag used for testing. An inside view of the box along with the closed, fully assembled box are shown. The results from five packaged devices compared to results obtained using both the commercial LFT reader and ImageJ are presented in Figure 7.6. The results were normalised to the white test strip ($RGB = 255, 255, 255$) for ease of comparison.

The performance of two packaged reader devices: one with the smallest variations in measurements and colour readout values that were closest to the commercial reader (Device 5), and one with the largest variations in measurements (Device 4), compared to both the commercial LFT reader and ImageJ results was assessed. The results show that semi-quantitative colour distinction is possible using the packaged readers for three selected model LFT colours (Figure 7.7a). The grey shaded lines show the resulting range of measurements for the tags with the smallest and largest variations in measurements, highlighting correspondence to the commercial reader and ImageJ results and distinct readout ranges for each colour (Figure 7.7a). The results of the packaged reader device with the smallest variations in measurements (Device 5) do not always fall within the same range of values as the commercial reader and ImageJ results (Figure 7.7b), particularly for darker colours, but have distinct ranges with small standard deviations, enabling discrimination to be made among colours. For darker colours, e.g. 8 and 10, colour discrimination is more distinct for Device 5 than for the commercial reader and ImageJ analysis.

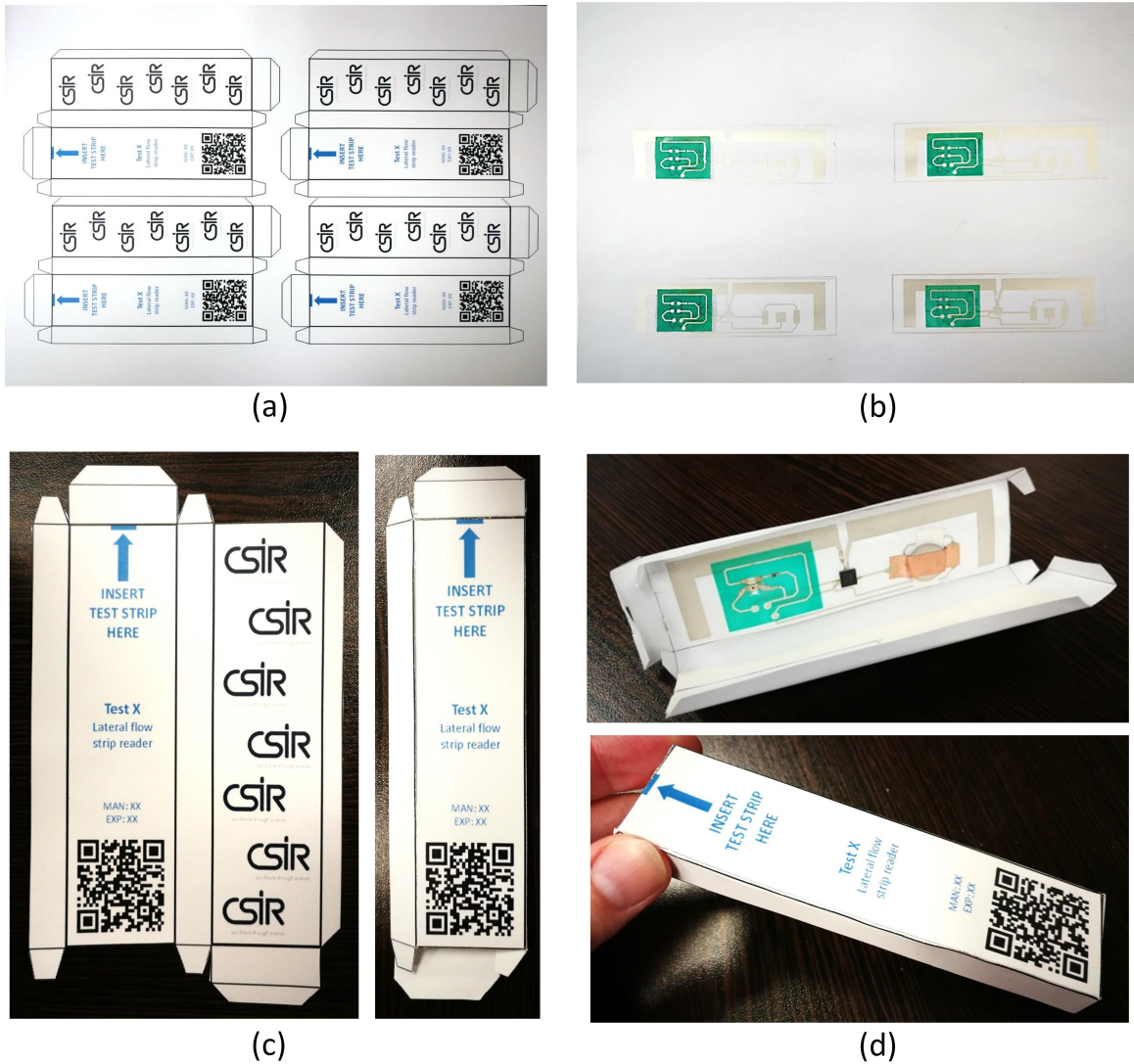


Figure 7.3 Initial prototypes for scalable, packaged reader devices, showing a) sheet-to-sheet printed graphics (outside of device), b) sheet-to-sheet printed electronics (inside of device), c) individual devices cut out, folded and glued, and d) assembled circuitry folded into final packaged device.

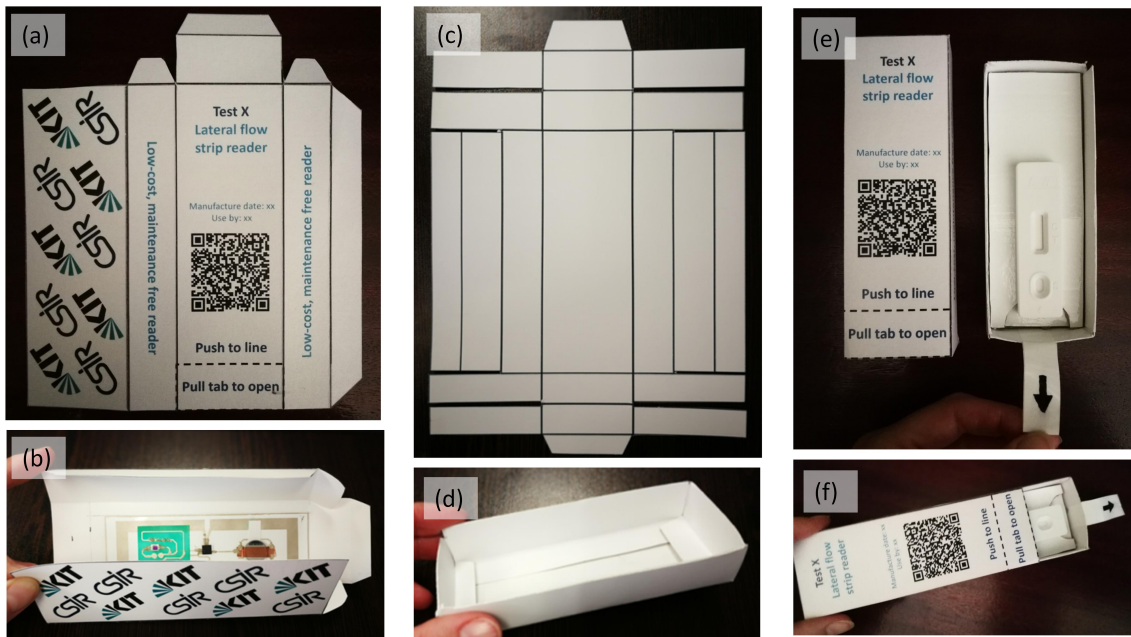


Figure 7.4 Matchbox-style boxes with a) an outer sleeve with printed graphics with b) printed electronics mounted on the inside of the sleeve before being folded, c) and d) inner tray design, e) folded and glued outer sleeve and inner tray with cardboard insert for positioning the LFT cassette inside the tray, and f) complete assembled packaged reader device with tab for sliding the tray in and out of the sleeve.

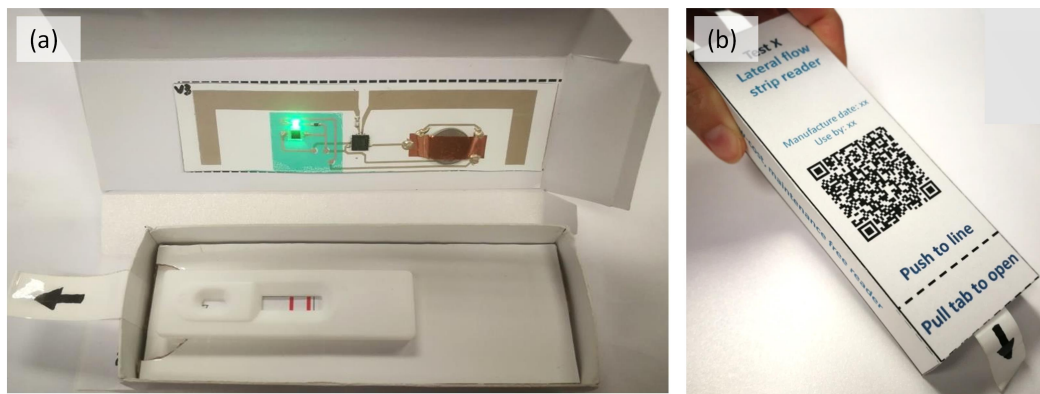


Figure 7.5 a) Inside view of packaged reader with model LFT cassette positioned inside tray of box using custom insert, and b) complete assembled and folded packaged device.

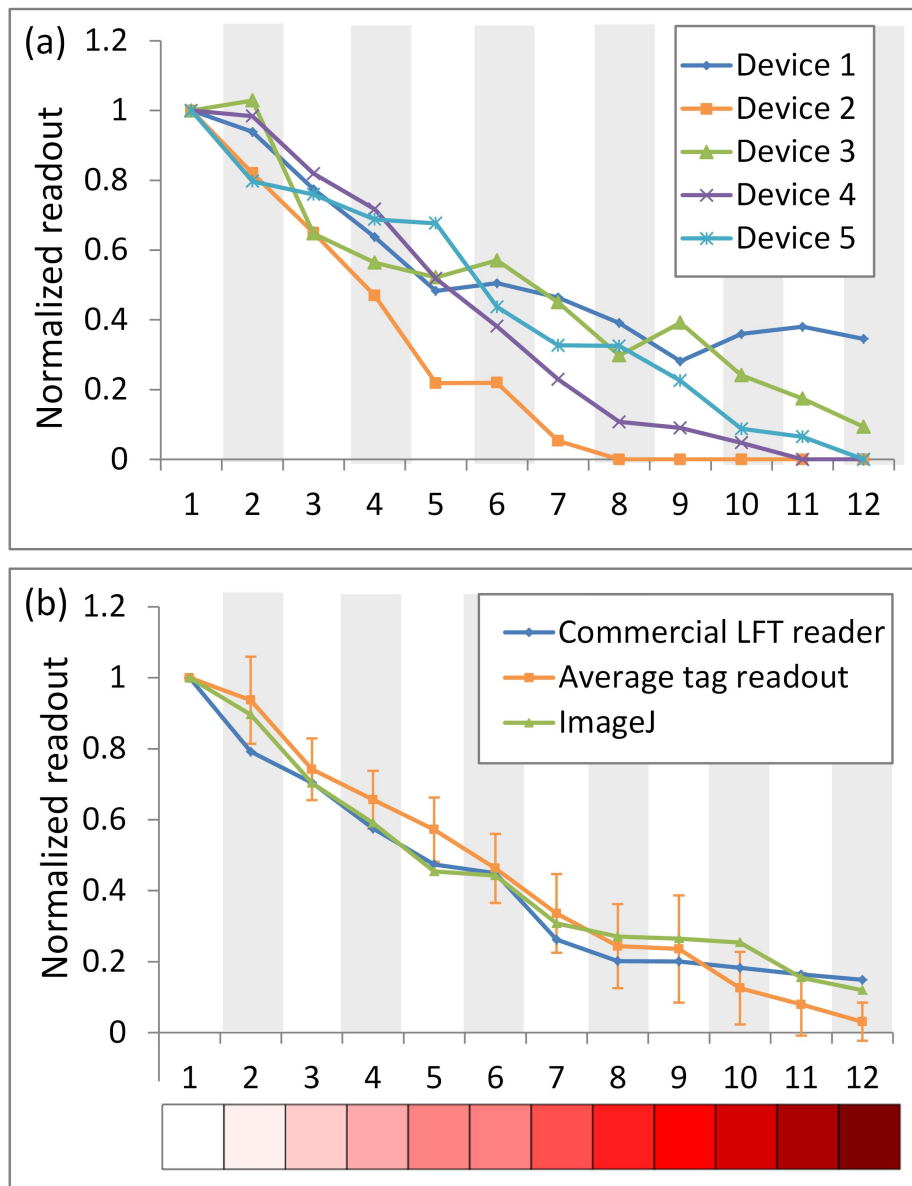


Figure 7.6 a) Normalised readout from five packaged reader devices for model LFTs in plastic cassettes and b) normalised average results for model LFTs in plastic cassettes for all packaged readers compared to commercial LFT reader results and ImageJ analysis results.

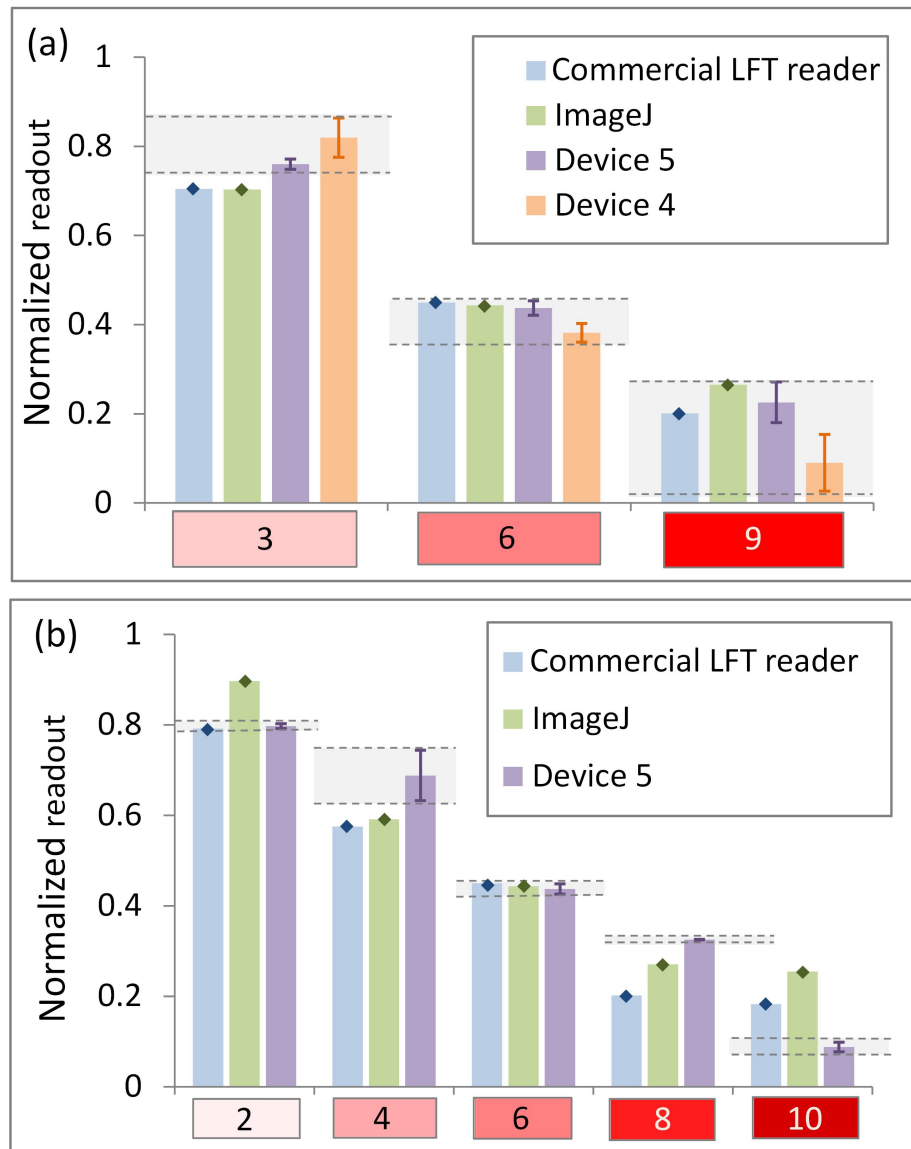


Figure 7.7 a) Packaged reader devices with smallest (Device 5) and largest (Device 4) variations compared to commercial LFT reader and ImageJ results for three different model LFT colours (numbers 3, 6, 9). b) Packaged reader device with smallest variation (Device 5) compared to commercial reader and ImageJ results for five different model LFT colours (numbers 2, 4, 6, 8, 10).

Read range measurements carried out for the packaged low-cost wireless reader devices varied between 35 and 180 mm, with an average of 97.5 mm (\pm 51.6 mm). Automated data capturing occurs when the packaged reader device is scanned using the RFID reader, as described in Chapter 3. Direct feedback is provided via a GUI and the sensor values are stored in a text file.

7.4 Discussion

Figure 5.4c shows that the commercial LFT reader results and the ImageJ results align closely. As a result of maintenance challenges with the commercial reader, ImageJ analysis of scanned images of LFT devices was used as a reference against which to compare the results obtained from the packaged reader devices for real-world testing in Chapter 8.

The colour detection results obtained for model LFTs in plastic cassettes under inconsistent testing environments and lighting conditions enabled result capture and communication through RFID, and were comparable to the image analysis results obtained using both the commercial reader and ImageJ analysis. The results were also comparable to the initial tests carried out using model LFT devices in the repeatable PMMA enclosure set-up (Chapter 5).

Variations were observed in the measured colour intensity results for a single packaged reader device, and are again attributed to the manual assembly methods used, in which the positioning of the SMD components affects the results. Furthermore, the battery voltage affects the intensity of each LED and thus the measured sensor value.

The average read ranges for wireless communication of the results were just under 100 mm. As discussed in Chapter 6, these would be adequate read ranges for use in clinic environments, as envisaged for these devices, and are close to the read ranges of 100 mm or more achieved in Chapter 6 for tests performed with a load connected.

Successful packaging of printed and assembled detection and wireless communication components on a low-cost vinyl adhesive substrate has been demonstrated. The components were effectively integrated into a matchbox-style, collapsible and foldable cardboard box format for readout of colour results from paper-based diagnostic tests. The packaging is low cost and can be manufactured using existing printing and packaging production processes, enabling local manufacture and distribution.

Based on the positive performance of the packaged low-cost wireless reader devices for model LFTs, the demonstrated functionality of the devices was extended to real-world rapid tests, as explored in Chapter 8.

8 Real-world tests and usability

This chapter is based on work that has been submitted to Nature Scientific Reports as part of a manuscript that is awaiting reviewer feedback.

8.1 Overview

This chapter focuses on applying the developed packaged low-cost wireless reader devices to real-world testing environments. Chapter 7 detailed the design and functionality of the integrated packaged device for testing with model LFT strips. For the packaged solution to be applicable to resource-limited clinics, real-world tests and testing environments need to be investigated to assess the practical functionality of the developed devices. Different real-world test formats were explored, and an initial usability study was carried out to assess the performance of the packaged solution in practical conditions.

As discussed in Chapter 2, there are a number of commercially available portable reader devices for LFTs. The limitations of these existing solutions were highlighted, and include high cost, vulnerability to theft, maintenance and power requirements, and single test format use. The packaged device developed in this work provides a modular solution, adaptable to various paper-based test formats. As an initial example, different single-use LFTs were used with the device to read out a colour result wirelessly. Furthermore, pH test strips were investigated and formed part of a preliminary usability study, as user friendliness is a REASSURED requirement.

Usability testing is an important consideration in the early stages of prototype development, enabling identification of user needs and potential functional problems to allow for usability errors to be designed out while the solution can still be modified. This work utilises tools such as the modified System Usability Scale (SUS) [179] and the After Scenario Questionnaire (ASQ) [180] to provide ratings of the device usability and user satisfaction.

The results presented illustrate adequate functionality of the packaged wireless colour detector devices for different real-world tests, enabling semi-quantitative read-

out to be obtained repeatably. Simple calibration techniques were implemented to further improve the result readout. Usability studies showed that the devices were intuitive for handling and performing measurements, given minimal instructions, showing promise for future development of the packaged low-cost wireless reader devices.

8.2 Methods

Packaged reader devices utilising colour detector tags printed on white adhesive vinyl were assembled and tested using the RFID reader set-up described in Chapter 3. Three different real-world test types and formats were explored, and included yes/no and semi-quantitative LFTs, along with a paper strip test format. In each case, sensor values were captured through the RFID reader user interface as described in Chapter 3, using an average over a 30 s period as a stable sensor readout result for each measurement performed. An initial usability study was formulated to enable participants to assess the functionality of the packaged devices in real-world settings and provide suggestions for improvements in future prototype development.

8.2.1 Real-world tests

Yes/no LFTs

Commercial rapid tests (Clicks ovulation test, Clicks Pharmacies, South Africa) were used as initial yes/no real-world tests (Figure 8.1). These are qualitative test strips housed in plastic cassettes that are used to predict when there is a surge in luteinizing hormone (LH) levels in urine. A female urine sample was collected and immediately tested using the dropper supplied with the rapid test kit to introduce the sample to the cassette and run the test. Negative urine samples were tested in the cassettes to produce a control line. For each cassette, the wireless colour detector device recorded sensor readouts for the dry or unused test, negative test line and positive control line.

Semi-quantitative LFTs

LFTs developed and manufactured at the CSIR, South Africa, for the detection of *E. coli* in contaminated water samples were utilised as semi-quantitative real-world tests (Figure 8.2). Dilutions were made from cultured bacteria using a phosphate buffer to obtain different bacteria concentrations. For testing purposes, three LFTs were run for each sample concentration or colony-forming unit (cfu) per ml. The samples tested in this study included the phosphate buffer (negative control), tap

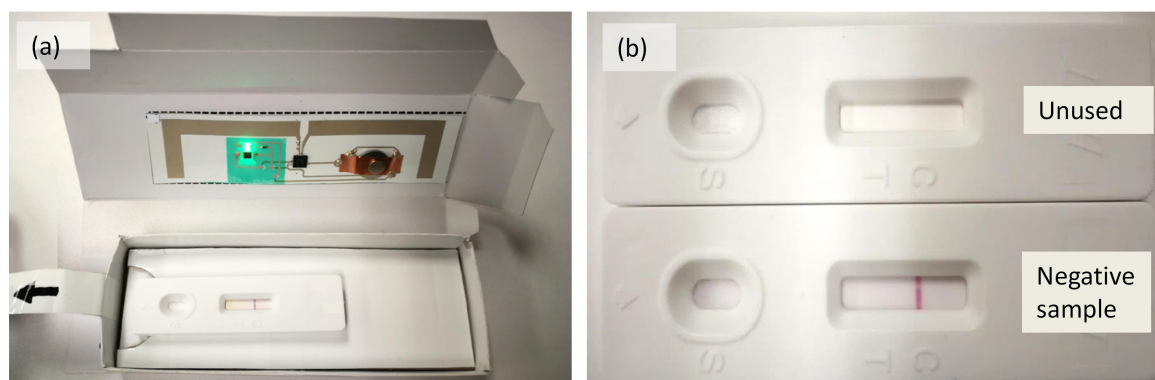


Figure 8.1 a) Inside view of packaged reader with rapid test cassette positioned inside tray of box using custom insert. The printed and assembled colour detector tag is mounted on the inside of the sleeve of the box. b) Example of rapid tests showing a dry, unused test and a test with negative sample.

water, 3×10^6 cfu/ml, 3×10^7 cfu/ml, 3×10^8 cfu/ml and a black test line created using a permanent marker on an unused LFT, as an additional calibration sample. The 3×10^7 cfu/ml concentration is visually darker than the 3×10^8 cfu/ml concentration as a result of the hook effect, in which excess antibodies or antigens in the test cause false-negatives or false low results [181]. The LFTs were scanned (Figure 8.2b) and ImageJ analysis was performed, as described in Chapter 3, as a baseline with which to compare the results obtained using the packaged reader devices.

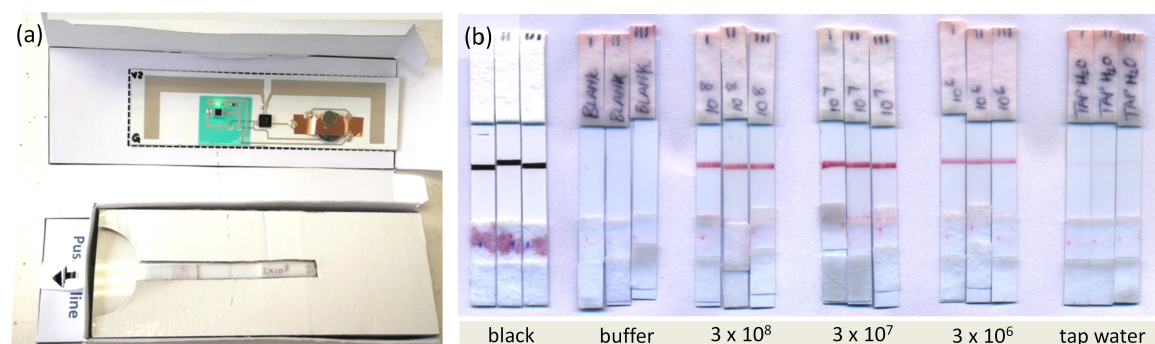


Figure 8.2 a) Inside view of packaged reader with LFT positioned inside tray of box using custom insert. b) Scanned image of tested LFT devices, including dry test strips with black line as reference for potential future calibration purposes.

Different test formats

To investigate different test formats, home-use pH test strips (Clicks alkaline/acid pH test strips, Clicks Pharmacies, South Africa) were utilised. These test kits are supplied with a colour chart to determine pH values in the range of 5.5 to 9.5 (Figure 8.3b). The pH 6, 8 and 9 solutions were made from a pH 7 neutral standard, using a pH meter (pHscan30L Pocket pH, Bante Instruments, China) to confirm the pH values.

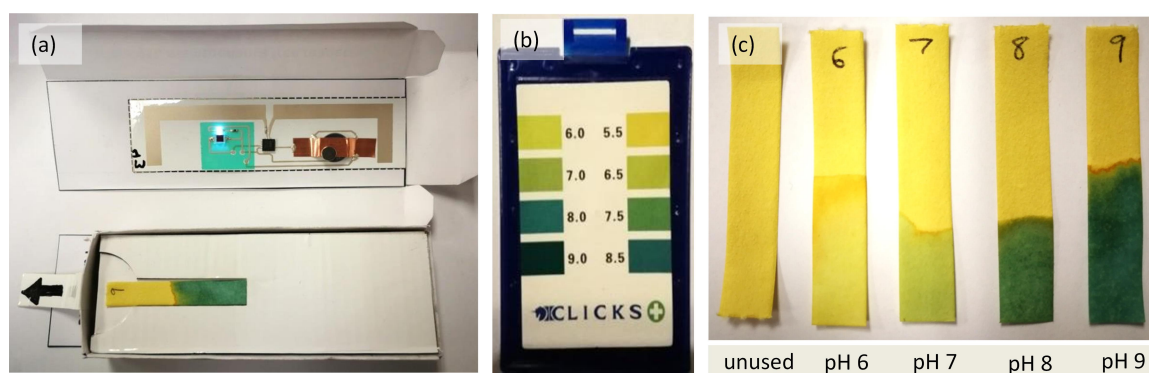


Figure 8.3 a) Inside view of packaged reader with pH test strip positioned inside tray of box using custom insert. b) Colour chart provided with the pH test strip kit and c) pH test strips dipped into samples with different pH values as indicated.

8.2.2 Usability

An initial usability study was formulated to assess the packaged wireless colour detector devices. Ethics approval was obtained from the CSIR Ethics Committee. All research was performed in accordance with the relevant guidelines and regulations. Informed consent was obtained from all participants.

Six participants aged between 27 and 62 were asked to assess the devices through a questionnaire that was formulated (Appendix B), and to perform a user test using the pH test strips to assess the functionality of the packaged reader devices in real-world conditions. One of the participants was a retired nurse, while one had no previous experience with medical devices or rapid tests.


A brief background was presented to the participants, explaining the purpose and end goal of the packaged reader devices. The participants were provided with a user guide (Figure 8.4) and were requested to carry out a practical test with the pH test


strips. The test involved dipping a pH test strip into a sample of their choice and determining the pH value of the sample. The participants were asked to read out the resulting pH value manually using the colour chart provided as part of the commercial pH test strip kit. The participants then placed the test strip in the packaged reader device and scanned the device to obtain an automated readout of the pH value through a user interface on the monitor of a PC to which the RFID development kit reader was connected. Both the effectiveness (how many attempts it takes for the participant to successfully obtain a result from the packaged reader device) and the efficiency (how long it takes for the participant to complete the task) were recorded.

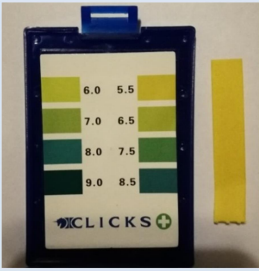
Once the test was completed, the participants answered a questionnaire to assess the usability of the packaged reader devices and note areas of improvement in future developments. The questionnaire was established based on studies for home healthcare devices [182, 183]. Specifically, usability was assessed using the modified SUS [179], comprising ten questions, each with a five-point scale answer. The SUS score is calculated from the sum of the answer scores. Satisfaction was assessed using the ASQ [180], consisting of three questions, each with a seven-point answer. The ASQ score is calculated from the average of the answer scores. General operational characteristics of the reader devices were also assessed using the questions utilised by UNICEF for the assessment of LFT kits [184]. Users were also encouraged to provide additional feedback and comments regarding the overall appearance and handling of the packaged reader devices to gain insights as to where and how improvements should be made. The questionnaire is included as part of this dissertation in Appendix B.


USER GUIDE: Low-cost reader


- 1** Pull out the sliding tray using the tab with arrow:


- 2** Dip one end of the yellow test strip into a sample container (1, 2, or 3) for 1 - 2 seconds:


- 3** Compare the test strip colour to the colour chart and read out the pH value:


- 4** Place the test strip into the slot in the sliding tray of the box:


- 5** Slide the tray back in up to the dashed line:


- 6** Scan the device at the green reader connected to the computer. Click the "Execute" button on the screen and see the result pop up:

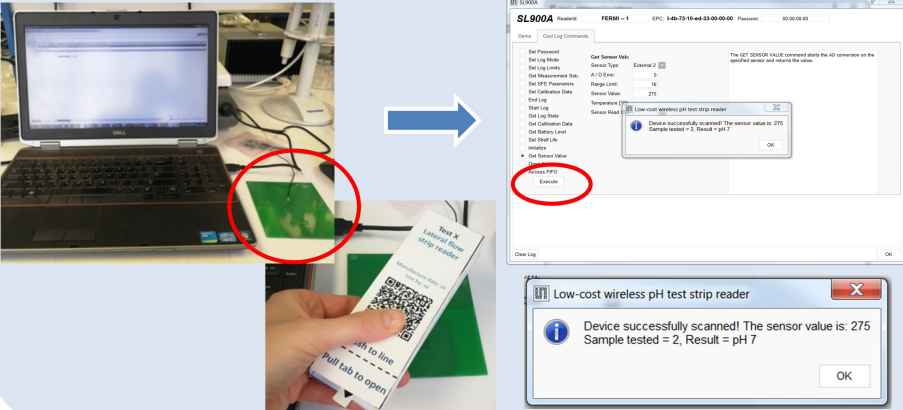


Figure 8.4 User guide provided to participants for the usability study.

8.3 Results

8.3.1 Real-world tests

Yes/no LFTs

Five packaged reader devices were tested, with three different rapid tests analysed per reader. The results were normalised to the dry unused test, and enabled clear distinctions to be drawn between the negative and positive test results (Figure 8.5).

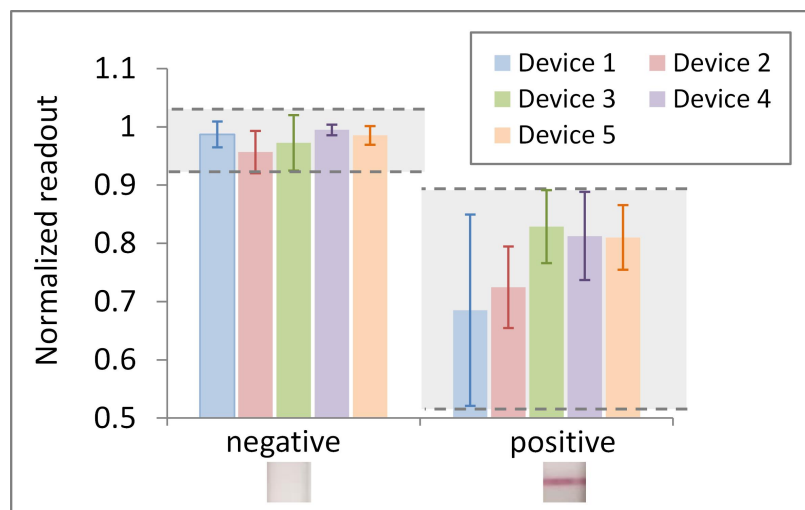


Figure 8.5 Average normalised results for negative and positive test results for five tags, along with test results for each individual tag, each tested with three rapid test cassettes. The shaded areas indicate the range of measurements across the packaged wireless colour detector devices, highlighting distinct readout ranges for positive and negative test results.

Larger variations are present in the readout for positive results, and are primarily caused by the positioning or alignment of the control line relative to the detection mechanism inside the box. However, clear distinctions can be made between the negative and positive results, with no readout errors present across all tests and packaged reader devices for a threshold value of 0.89. Threshold values can be optimised through more extensive testing, and individual thresholds can be determined for each device.

Semi-quantitative LFTs

Six packaged reader devices were tested, with three LFTs assessed for each sample concentration. The results were normalised to the dry, unused tests for each reader device. The results are presented from the lowest signal (buffer) to the highest (3×10^7 cfu/ml) for ease of analysis and trend comparisons (Figure 8.6). Across all packaged reader devices, a clear distinction can be made between a negative and positive test result. Thresholding can again be used to determine whether a test result is negative or positive. With a threshold setting of 0.65, an 11.11% error is obtained (two false positives using Device 1) across all devices and repeats tested.

Two packaged reader devices were compared to the ImageJ results to demonstrate that semi-quantitative analysis is possible (Figure 8.6b). Device 4 had the smallest variations across measurements ($\pm 6\%$) and similar trends and values to the ImageJ reference results, while Device 2 had the largest variations across measurements ($\pm 15\%$) and values that were further from the ImageJ reference values. The results indicate that semi-quantitative analysis is possible for discriminating among different concentrations of *E. coli*.

Distinct ranges are defined for Device 4 for each concentration, with no errors. The values also fall within the range of the ImageJ reference values for each concentration. Uncertainty exists in the discrimination between 3×10^8 cfu/ml and the darkest 3×10^7 cfu/ml concentrations, but for discrimination between more faint signals, the results indicate a clear distinction between concentrations. For Device 2, the results do not fall within the same range of values as the ImageJ results, but distinct ranges are defined for each concentration, enabling discrimination between different concentrations. Device 2 is less sensitive than Device 4, as a clear distinction can only be made between 3×10^6 and 3×10^7 cfu/ml (darkest colour) effectively, with some uncertainty in the discrimination between 3×10^6 and 3×10^8 cfu/ml as well as between 3×10^8 and 3×10^7 cfu/ml.

Different test formats

Commercial pH test strips were used to test a different test format with the packaged wireless colour detector devices, and to perform initial usability studies. Five packaged reader devices were tested, each with six tests per pH value. In each case, pH test strips from two different test kits were used (three from one, three from the other) to incorporate variations in the test strip colours across test kits. A new strip was tested each time. The test results were normalised to the dry, unused test strip (yellow colour), which also assists in accounting for variations in colour from one test kit to

another, where significant visual differences can be noted across test kits. pH solutions of 6, 7, 8 and 9 were tested. Distinct ranges were obtained without errors for pH 6, 7 and 8, with uncertainty in the discrimination between pH 8 and 9 (Figure 8.7a). Visually, the differences between pH 8 and pH 9 are more difficult to discern than the differences between the lower pH values. This indicates that the uncertainty in the discriminations between pH 8 and pH 9 read out from the packaged reader devices is a result of these visual similarities. The discrimination between lower pH values is more distinct for the packaged reader devices (Figure 8.7), as these are also more visually distinct.

8.3.2 Usability

Based on the results of Figure 8.7a, pH solutions of 6, 7 and 9 were utilised for the usability study to ensure that the devices could correctly determine the pH value. Calibration was performed on the individual devices for each pH value in the usability tests. Numerous measurements were performed for each pH value, from which threshold values were determined (Table 8.1). As an example, the pH results for devices with the lowest error (Device 1) and highest error (Device 5) are illustrated in Figures 8.7b and c. Distinct ranges can be defined for Device 1, while Device 5 exhibits a large uncertainty (overlap) between the different pH values (orange highlights in Figure 8.7c). The thresholding approach can be optimised through more extensive testing of individual devices to ensure that minimal errors are produced.

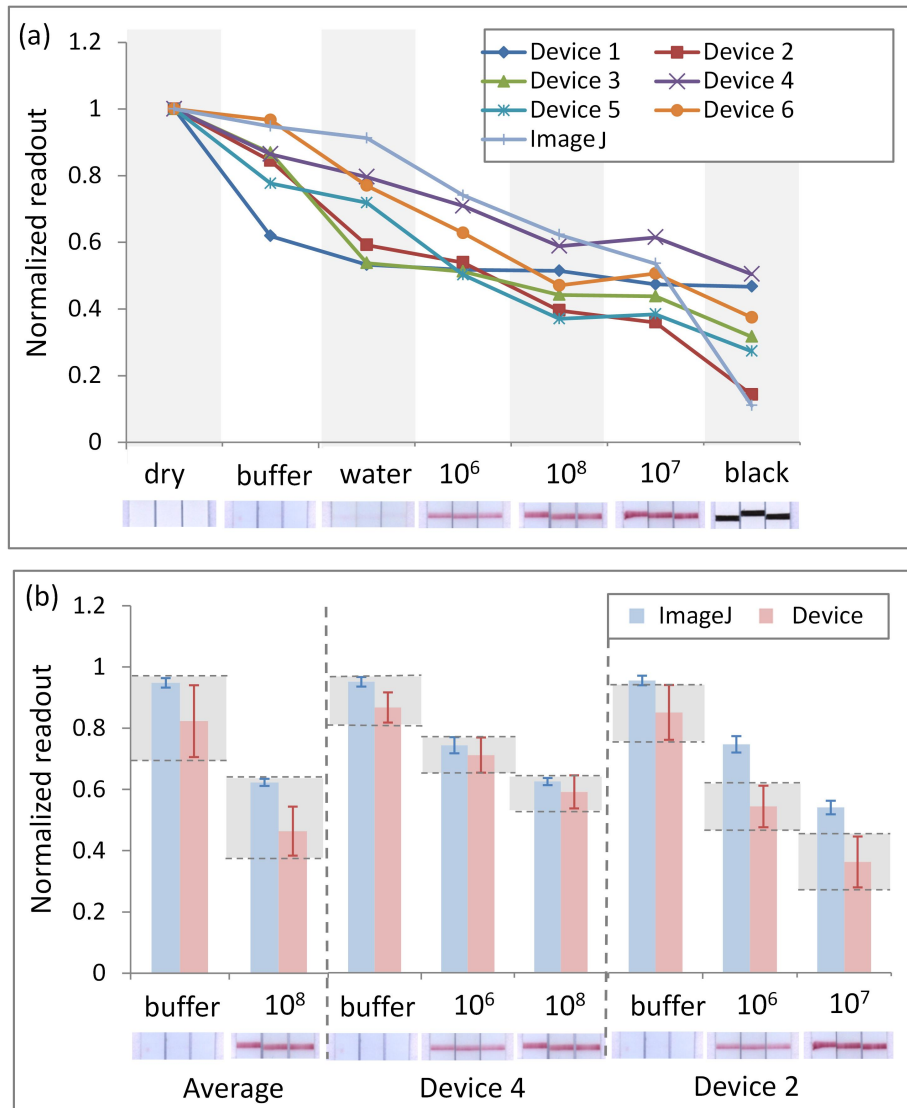


Figure 8.6 a) Normalised results for six packaged reader devices compared to normalised ImageJ results (average over three LFT readings) for different bacteria concentrations (cfu/ml). b) Normalised results for average over six reader devices compared to normalised ImageJ results to show distinction between negative (buffer) test strips and concentrations of 3×10^8 cfu/ml, along with device with smallest variations (Device 4) and largest variations (Device 2) compared to ImageJ results for three different *E. coli* concentrations. The shaded areas indicate measurement ranges across packaged wireless colour detector devices, highlighting distinct readout ranges for different bacteria concentrations.

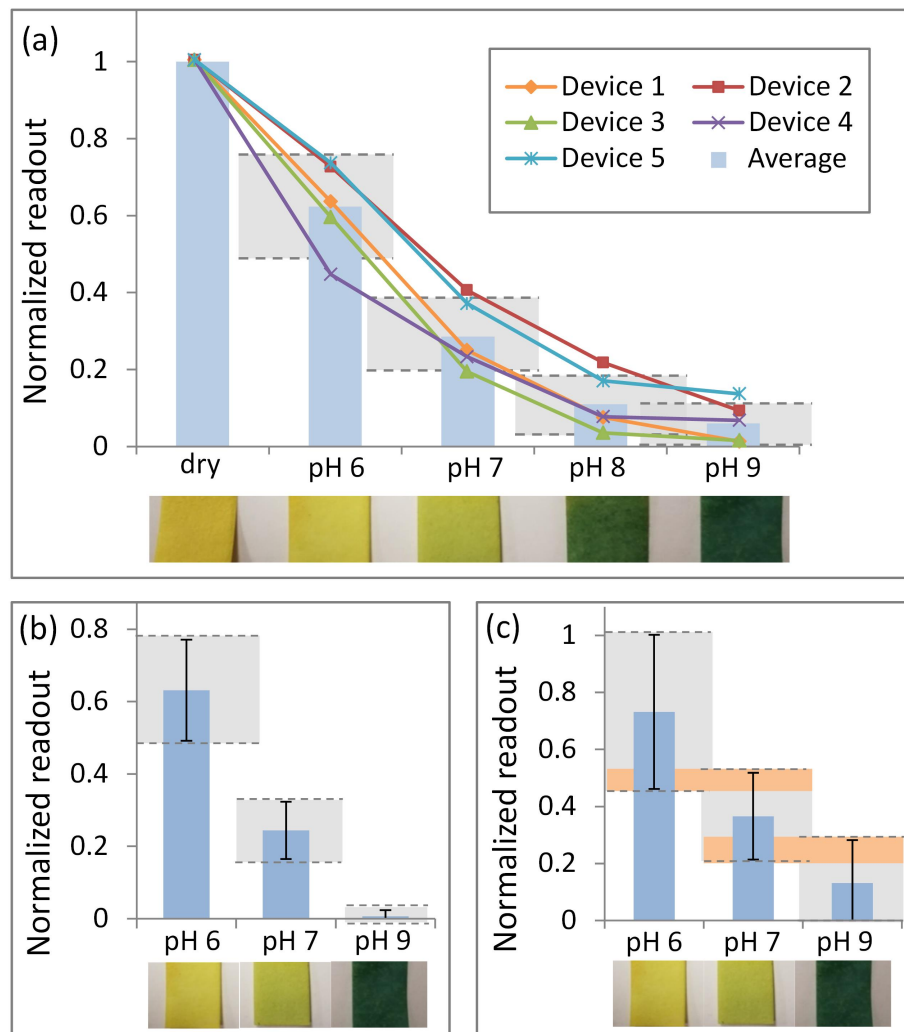


Figure 8.7 a) Normalised results for five packaged wireless colour detector devices, with each pH value tested six times, along with average results indicating distinct ranges obtained for each pH value. Threshold results for pH readout for device with b) lowest errors (Device 1) and c) highest errors (Device 5).

Table 8.1 Calculated thresholds and errors for different pH values for individual devices.

Device number	pH 6	pH 7	pH 9	% error
1	> 0.6	0.15 – 0.6	< 0.15	0
2	> 0.63	0.18 – 0.63	< 0.18	12.5
3	> 0.35	0.04 – 0.35	< 0.04	4.2
4	> 0.55	0.12 – 0.55	< 0.12	8.3
5	> 0.55	0.2 – 0.55	< 0.2	20.8

Participants performed pH test strip analysis using both a manual colour chart readout and the automated packaged low-cost wireless reader solution (Figure 8.8). A total of eight tests were carried out by the six participants. In all cases, participants required only one attempt to obtain a result from the device (effectiveness = 1). The average time for users to perform the task (efficiency) was 35 s (\pm 20 s) for the manual readout and 5 s (\pm 3 s) for the automated readout. The total time required to complete the task for both the manual and automated readouts, including gaining an operational understanding of the device via the user guide and wetting a test strip in a selected sample, was 2 min 20 s (\pm 30 s). Among the tests carried out, two manual colour chart readout results were correctly interpreted, while six automated results using the packaged reader devices were correctly read out. Table 8.2 compares the manual and automated readout of pH values using the colour chart from the test kit and the packaged wireless colour detector devices, respectively. The readout time is calculated as a percentage of the total time required to complete the task, including sample preparation, and both manual and automated readout. The readout time using the automated devices is approximately seven times faster than performing manual readout, and only accounts for 3.5% of the total time taken to perform the complete pH test usability task.

According to the questionnaires completed by the participants, the average usability score using the SUS was 84.17 (\pm 6.23) out of 100 and the overall satisfaction score using the ASQ was 6.39 (\pm 0.39) out of 7. In general, the users were satisfied with the usability of the packaged reader devices, with the main challenges identified on the box sliding mechanism, the positioning of the test strip in the insert and the positioning of the tray inside the sleeve for correct alignment.



Figure 8.8 a) Participant carrying out usability test by following the user guide instructions for manual readout of pH values, and b) automated readout using the packaged reader device as part of the usability test, with the result displayed on a PC monitor via a user interface once scanned using the RFID reader.

Suggestions for improvements included using a different form factor for the box, with either a flap or lid for the box that opened at the top, or a reduction in the size of the form factor. The alignment of the sliding mechanism was highlighted as the main concern. Although the overhanging part of the outer sleeve was implemented to ensure isolation from external light interference, this would not necessarily be required in future versions, as more extensive calibration could be carried out for individual devices.

Most of the participants reported that they felt the device could be used between 5 and 20 times, with one stating that they thought it could be used between 20 and 50 times. All participants felt that a device could be used more than once, but not more than 50 times.

Table 8.2 Comparison of manual and automated pH value readouts obtained from initial usability testing.

Parameter	Manual readout	Automated readout
Effectiveness (no. attempts)	1	1
Readout efficiency (s)	35 ± 20	5 ± 3
Readout time (%)	25	3.5
Correct readout (%)	25	75

8.4 Discussion

The packaged wireless colour detector devices show promise for effective readout of real-world tests in inconsistent testing environments and lighting conditions (Figures 8.5 to 8.7). Results for semi-quantitative tests were comparable to image analysis results obtained using ImageJ (Figure 8.6). Moreover, the initial usability tests suggest that the current format can already be utilised for screening and semi-quantitative test readout requirements (Figure 8.7). The packaged wireless colour detector allows for various paper-based test formats to be analysed, providing a modular solution that contributes to the low-cost, accessible nature of the approach.

Variations were observed in the measured colour intensity results for a single packaged reader device, and are a result of the currently manual assembly methods, in which the positioning of the SMD components affects the results. Furthermore, the battery voltage affects the intensity of each LED and thus the measured sensor value. Calibration methods have been implemented to account for these inter-device inconsistencies through normalisation of the measured sensor values to the dry or unused test strip, and could be extended to incorporate additional reference colours for calibration, yielding more accurate and quantitative colour detection capabilities. Automated matching of the reference measurements captured from an individual device to the unique device identification number (specific to the RFID IC) when a device is scanned could improve the readout accuracy.

A green LED was used for the LFT devices, as it is well suited to the detection of colloidal gold, while white LEDs were implemented for the pH test strips to provide a broader detection spectrum, and could be extended to other paper-based tests that utilise various colours. The printability of the devices onto low-cost substrates –

specifically for packaged solutions – was explored in Chapter 4, and offers the potential to align with current printing and packaging processes (Chapter 7).

Future versions of the colour detector devices will focus on improvements in the packaging designs, based on the feedback collected from the usability study. For a similar form factor to the one presented in this chapter, the inner tray would be designed to be flush with the outer sleeve in future iterations, or possibly have a raised edge to prevent external light from interfering if this proved to be problematic. Different form factors with a lid or flap on the top or the side of the box device could also be further explored, building on the initial designs presented in Chapter 7.

The participants of the user study felt that the current packaged devices could be reusable several times before functionality became compromised and the device would need to be discarded. For large-scale, automated production of the devices, as explored in the following chapter, it would be expected that the devices would be more robust with the potential to be used up to several hundred times.

Users were generally satisfied with the usability and functionality of the packaged reader devices. Issues regarding the mechanical components will likely be addressed by mass production, with prototypes currently being manually assembled, while other aesthetic and functional inputs will be considered in the next iteration of prototypes. In production, quality checks could be performed to eliminate devices in which functionality is compromised, and to calibrate individual devices extensively for different test formats.

The results of the usability study show that automated readout using the packaged reader devices is a simple process, as the users only required one attempt to perform the task correctly (Table 8.2). The devices are user friendly with minimal training required for the participants to operate the packaged colour detector devices correctly. In a clinic environment, the use of these devices could potentially be incorporated into existing training processes, as extensive and specialised training would not be necessary and thus the existing workflows would not be substantially burdened. In addition, the modular solution enables various test formats to be utilised, while the operation of the packaged colour detector device remains the same, further reducing the training requirements.

The real-world test results and outcomes of the usability study show promise for effective, semi-quantitative readout under real testing conditions, with little user training required. This aligns well with the REASSURED principles and provides a foundation on which to build low-cost, mass producible and deployable solutions, as will be discussed in the next chapter.

9 Scalability

Parts of this chapter are based on work that has been submitted to Nature Scientific Reports as part of a manuscript that is awaiting reviewer feedback.

9.1 Overview

This chapter explores the scale up and cost reduction of the different processes and components utilised to realise the packaged low-cost wireless reader devices. The development presented in previous chapters was carried out with the aim of producing devices that are mass producible and distributable at a low cost while demonstrating functionality and usability, towards achieving REASSURED POC diagnostic solutions. Although not specifically part of this work, initial scale up was investigated and showed that the devices can be scaled, forming the basis for future work.

Printability of the devices onto low-cost substrates is possible for ease of alignment with current printing and packaging processes. To expand on this, sheet-to-sheet printing of functional inks is investigated in this chapter, enabling multiple devices to be printed simultaneously for larger-scale production. In previous chapters, assembly of components onto the printed devices was performed manually using conductive silver epoxies. This chapter explores alternatives for automated assembly of the devices using pick and place processes and different materials for mounting the components onto the printed devices.

Processes for the scale up of printed electronics have been presented [185, 186], and different epoxies and conductive pastes have been explored for both manual and automated assembly of SMD components onto printed circuitry. These include isotropic and anisotropic conductive adhesives, where the latter only conducts in one direction [187]. Anisotropic adhesive pastes or films can be used for mounting of electronic components onto flexible substrates by applying heat and pressure. For isotropic conductive adhesives, the electrical conductivity is formed by the adhesive itself, as with the silver epoxy used in this work, and is conductive in all directions. Typically, these

adhesives only require heat for the assembly of electronic components, or cure at room temperature.

Internationally, infrastructure for the production of printed electronics is available, and includes sheet-to-sheet and roll-to-roll printing and assembly of hybrid electronics [60, 188]. These dedicated capabilities are not available locally in South Africa. However, existing printing, packaging and pick and place assembly processes that are locally available are explored in this chapter to facilitate the development of a process for the production of printed functionality devices in South Africa. Potential roll-out of the required RFID infrastructure is also briefly explored in this chapter, with inputs from a local RFID company. Initial feasibility and cost analyses are presented to assess the system scalability utilising local production and deployment capabilities, which is desirable from both cost and accessibility perspectives.

The printability of the various SMD components can be explored further towards the long-term goal of a fully integrated printed solution. This has been investigated in-house for printed inductors (Figure 9.6a), as well as printed primary batteries for use with the SL900A printed tags [163]. The in-house development of an inkjet printed RFID tag on photo paper using the die format of the SL900A chip has successfully been demonstrated [189], and has also been initially explored for screen printed tags (Figure 9.6b), showing promise for a more flexible, low-cost and readily disposable solution for this key RFID tag component.

The various aspects investigated in this chapter illustrate the feasibility of large-volume, low-cost production and deployment of the packaged reader solution in resource-limited settings, towards REASSURED POC diagnostics.

9.2 Automation and scale up

9.2.1 Printing

Sheet-to-sheet printing of the functional silver and dielectric inks was carried out using three individual screens: one screen for each layer to be printed. The screens were manufactured by Chemosol, with specifications as described in Chapter 3. Figure 9.1 shows the resulting printed sheets with ten tag devices printed per sheet of vinyl, cut to A4 size (297 mm × 210 mm). Printing was carried out using the manual screen printing process described in Chapter 3. Automated, larger-scale sheet-to-sheet printing of functional inks by local company Electronic Touch Systems (Pty) Ltd. is possible, and initial costing for this has been determined (Table 9.1).

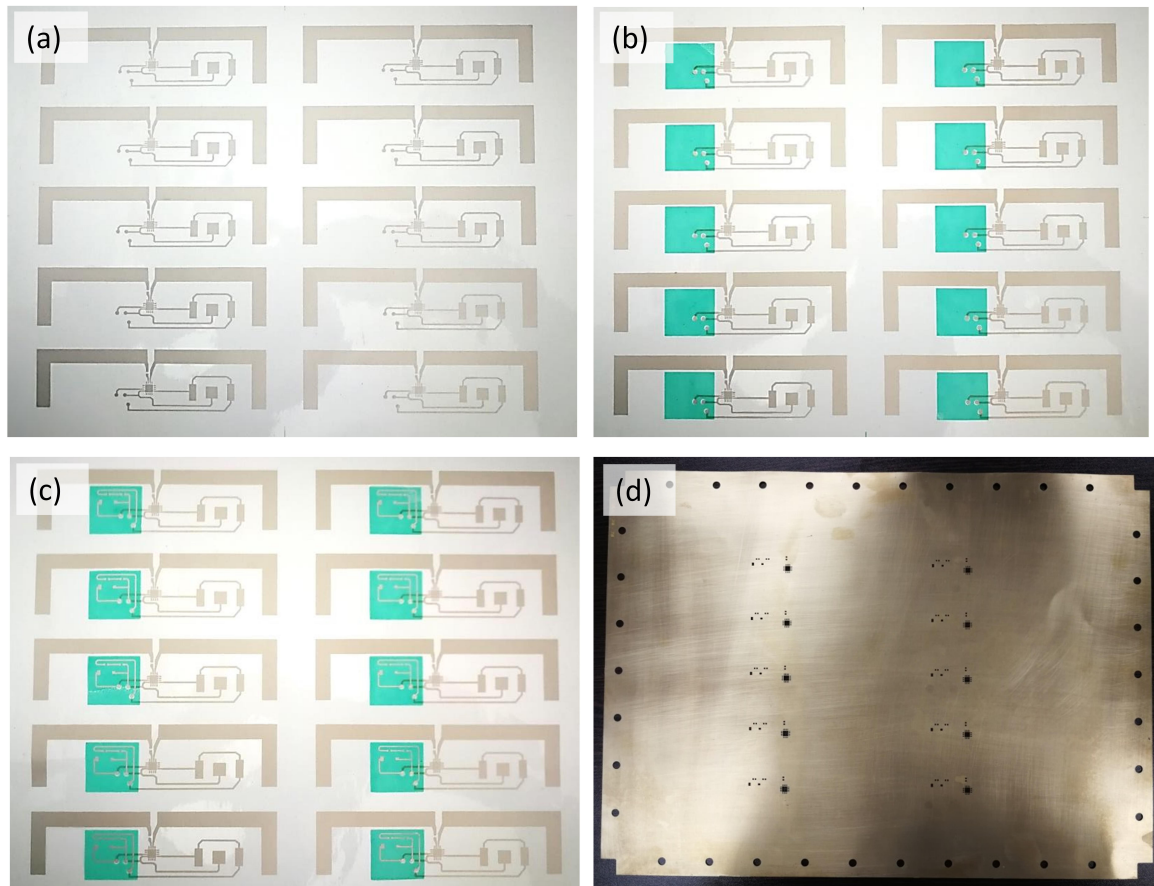


Figure 9.1 Sheet-to-sheet printing of wireless colour detector tag designs, with ten devices per A4 sheet for a) layer 1: printed conductive silver ink, b) layer 2: printed dielectric ink, and c) layer 3: printed conductive silver ink. d) Copper stencil for printing of solder paste and conductive silver epoxy onto printed sheets.

9.2.2 Assembly

Automated assembly of the SMD components onto the printed wireless colour detector tag devices was explored through utilisation of a pick and place process. Electronic Touch Systems is able to perform small production runs using semi-automated pick and place of components, and costing for this has been provided (Table 9.1). For small-scale automated pick and place of SMD components, the Technology Station in Electronics (TSE) facility, which forms part of the Tshwane University of Technology (TUT), South Africa, was utilised.

The manufacturing platform offered by TSE enables prototyping and low-volume manufacturing, capable of handling component dimensions as small as $0.4\text{ mm} \times 0.2\text{ mm}$ and PCB sizes of up to $460\text{ mm} \times 400\text{ mm}$. The equipment housed at the TSE facility includes a component placement line (SM482, Samsung, South Korea), a convection oven system, and a MY600 Jet Printer (Mycronic, Sweden) for dot dispensing of pastes in cases where a stencil is not used.

As a first step in exploring the scalability of the packaged reader devices, a stencil was designed to enable sheet-to-sheet printing of solder paste or conductive epoxy onto the required areas of the tag devices. The copper stencil was manufactured by local company Central Circuits CC (Figure 9.1d). Copper stencils are effective for prototyping using stencil printing and can be used reliably up to 50 or 100 times before they start to warp. For larger-scale production, stainless steel stencils can be used, although these are in the order of 10 times higher in cost than copper stencils, but can be used to produce up to 50000 boards effectively.

For initial testing, the A4 printed sheets were cut in half, resulting in five devices per sheet for ease of handling for the stencil printing process, and set up of the pick and place assembly process. The sheet was mounted onto a PCB using tape or clamps to secure the vinyl to a rigid substrate for the placement process. Future scale up implementations will require a frame to be designed and manufactured to effectively fit on the conveyor of the placement system, and to support and hold the printed sheets.

A low-temperature tin bismuth alloy solder paste (B14:Bi14 Sn43 Pb43, Techmet (Pty) Ltd, South Africa) was first investigated for prototyping purposes. Stencil printing of the solder paste onto the printed sheets was performed using a stainless steel squeegee with the copper stencil (Figure 9.2a). After printing, the stencil was cleaned with isopropanol alcohol and dried with compressed air.

The reflow of the solder paste was tested before setting up the pick and place assembly line. The melting point of the solder paste is specified as 144°C and different temperature profiles were investigated to test the compatibility of the solder paste with the vinyl substrate and printed silver pads. The first and second temperature profiles tested ramped up to 160°C and 170°C , but the solder paste did not melt, likely as a result of the printed silver pads on the vinyl substrate not retaining heat as well as the copper pads on a standard PCB. The third temperature profile tested ramped up to 200°C , causing the solder to melt. However, the solder did not adhere to the printed silver pads and formed small balls of solder (Figure 9.2b) which were weakly attached to the printed circuit. The low-temperature solder paste was thus not a viable option for effective pick and place assembly.

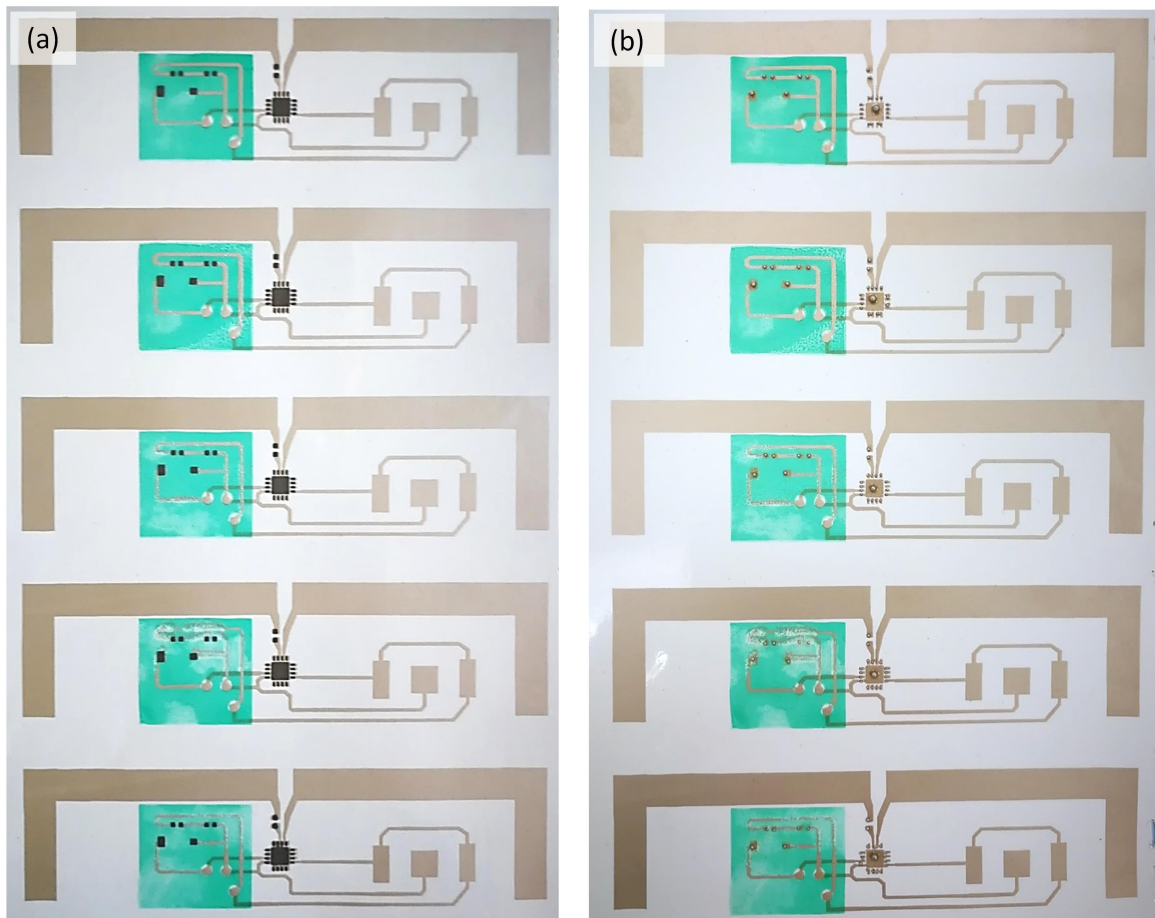


Figure 9.2 a) Stencil printed low-temperature solder paste on printed tags, and b) solder on printed tags after reflow testing in convection oven.

As an alternative, conductive epoxies can be utilised for mounting the SMD components. As a proof of concept for this work, the same two-part conductive epoxy that was used for the manual assembly of the printed tags was tested. The conductive epoxy was mixed and stencil printed onto the printed vinyl sheets using the copper stencil and stainless steel squeegee. This process worked adequately (Figure 9.3a) and was used for testing the automated pick and place of components.

Other screen printable and dot dispensable conductive adhesives could be utilised to provide more cost-effective solutions, and include options such as EP-600 (Applied Ink Solutions, USA), Electrolit 3036 (Panacol Elosol GmbH, Germany) and 112-05 (Creative Materials, USA). These adhesives typically cure at low heat or at room tem-

perature. The MY600 jet printer at TSE could be used for syringe or drop dispensing to pattern the solder pastes or conductive adhesives onto the printed devices without the need for a stencil.

For testing the automated pick and place assembly line process, reel formats of each SMD component were required. Reels with a minimum of 100 components were procured and are reflected in the cost breakdown (Table 9.1). The components were mounted in the reel holders and set up in the automatic feeder of the pick and place machine (Figure 9.4a).

The printed vinyl sheets that were mounted onto rigid PCB supports were placed inside the pick and place machine and dimensions were set through the software interface and a camera positioning system to allow the conveyor to grip and hold the PCB securely. Next, the camera was used to locate the position of each component on the printed circuit (Figures 9.4b and c). For each component, the centre point was located and defined to train the pick and place machine to place each of the components accurately. The inductor, resistor and LED components were standard 0603 formats that were pre-defined in the software, while the photodiode and SL900A required custom definitions to be created. The printed sheet designs did not incorporate fiducial marks for alignment purposes, and for future scale up versions, this will be included. However, defining printed marks on the devices such as the circular via connectors could be used in lieu of fiducials for reference positioning purposes.

The position of each component on the reel was checked and defined via software and the process was tested to ensure that the component placement would be carried out correctly. A small negative vertical distance was set for the pick and place arm ($z = -0.5$ mm) to ensure that the components were pressed firmly onto the conductive epoxy and secure the components to the substrate (Figure 9.4d). The pick and place assembly process was effectively carried out (Figure 9.3b), following which the sheets were stored at room temperature for 24 h for the conductive epoxy to cure before the tags were tested.

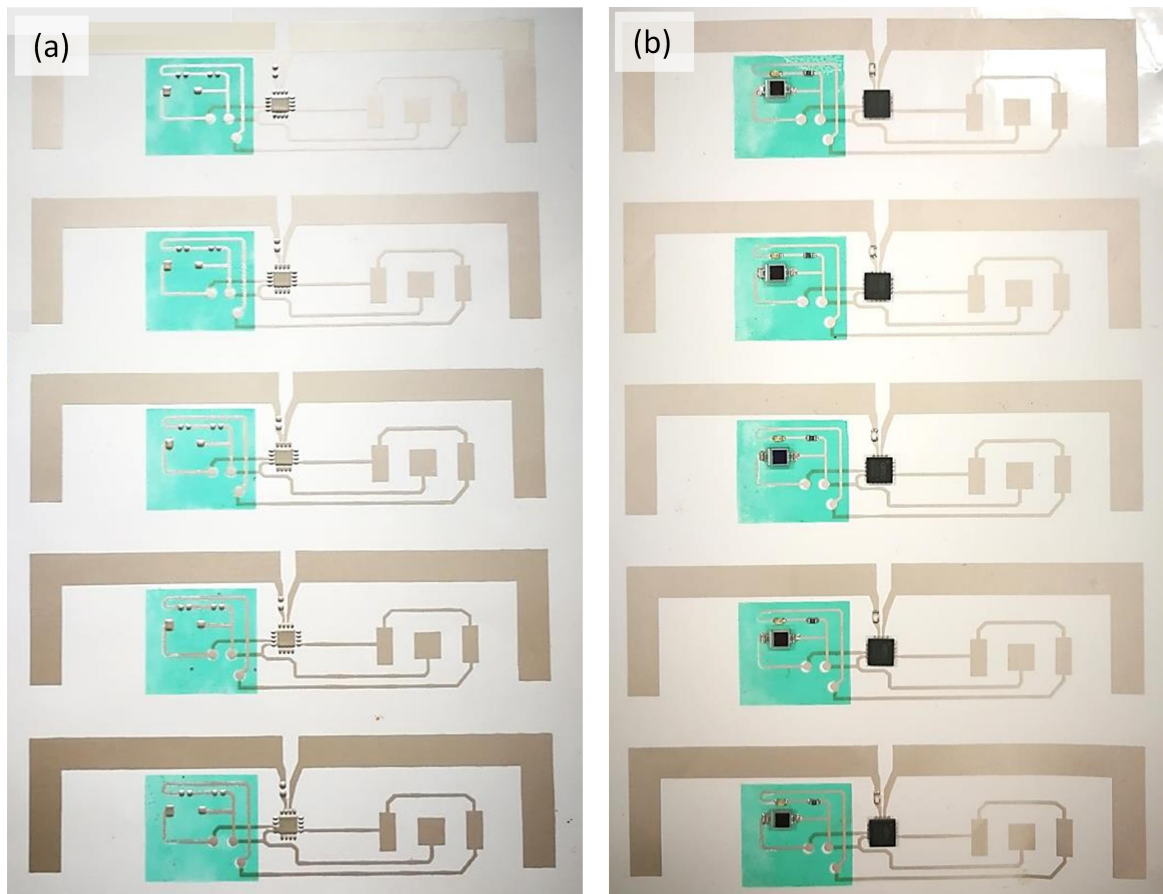


Figure 9.3 a) Stencil printed conductive silver epoxy on printed tags, and b) assembled tag devices using pick and place process.

9.2.3 Device testing

Three vinyl sheets, each containing five printed devices, were assembled using the pick and place assembly line. For one of the sheets, the conductive epoxy used for stencil printing was inadequate to cover the pads, and these devices were not included in the device assessment. However, the sheet was processed using the pick and place assembly line to ensure that the process was executed correctly.

Once cured, the ten automatically assembled devices were tested. The conductivity of the devices was tested, and in addition, microscopy analysis was performed to assess the alignment of the components on the vinyl substrates and printed pads (Figure 9.5). It was found that the print quality of the printed tag designs using

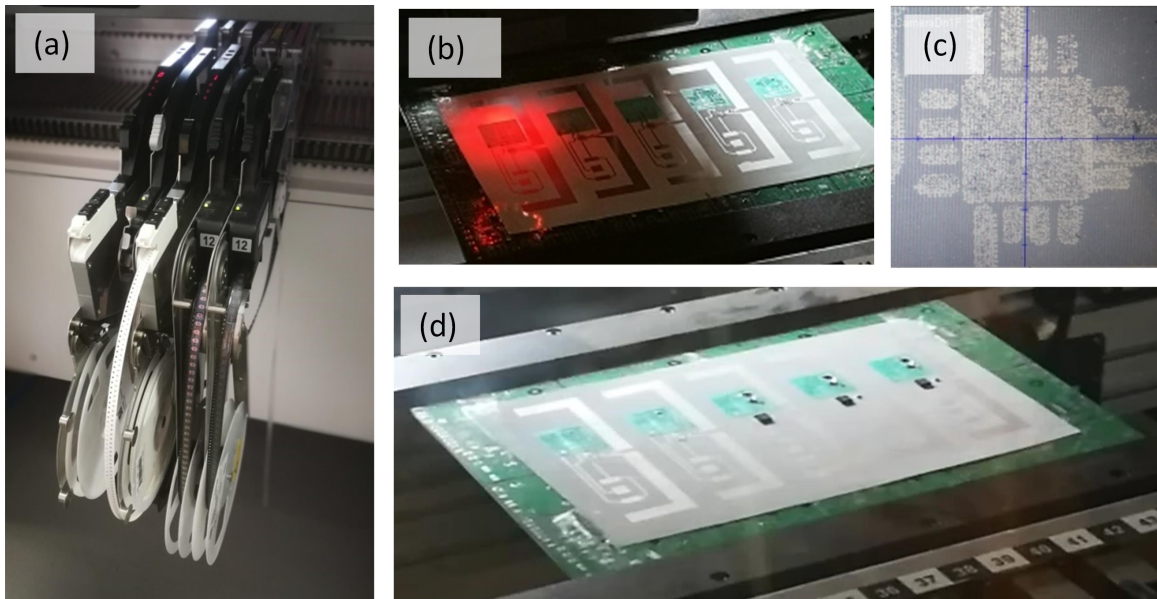


Figure 9.4 Overview of pick and place process performed. a) Set-up of components in reel format on pick and place line, b) and c) identification of positions for pick and place of components using software-based referencing, and d) pick and place assembly in progress.

the manual sheet-to-sheet screen printing process was problematic: on average, two devices per sheet were found to have inadequate conductivity or connections. This is likely as a result of the ink quality degrading over time. This means that, for a sheet of five devices, the print quality of one or two devices would be compromised. When testing the assembled devices, it was found that only seven of the ten devices had adequate print quality and conductivity.

Of the seven devices, four were functional when scanned with the RFID reader. The three devices that did not work were as a result of shorting of the SL900A IC pins. This occurred because of the stencil printed conductive adhesive being too thick on one of the sheets, causing the excess adhesive to spread and short across pins when the components were placed (Figure 9.5d). On the sheet where the conductive epoxy thickness was optimally applied, the assembled devices were all functional.

Individual components on the four functional assembled devices were tested. The LED was found to be correctly connected on all four devices, as was the SL900A IC and inductor, allowing for stable RFID readout from the assembled tags. The average read ranges of the assembled tags tested in passive mode (without connecting a battery to the tag) were 98.75 mm (± 2.5 mm). One tag resulted in a faulty sensor

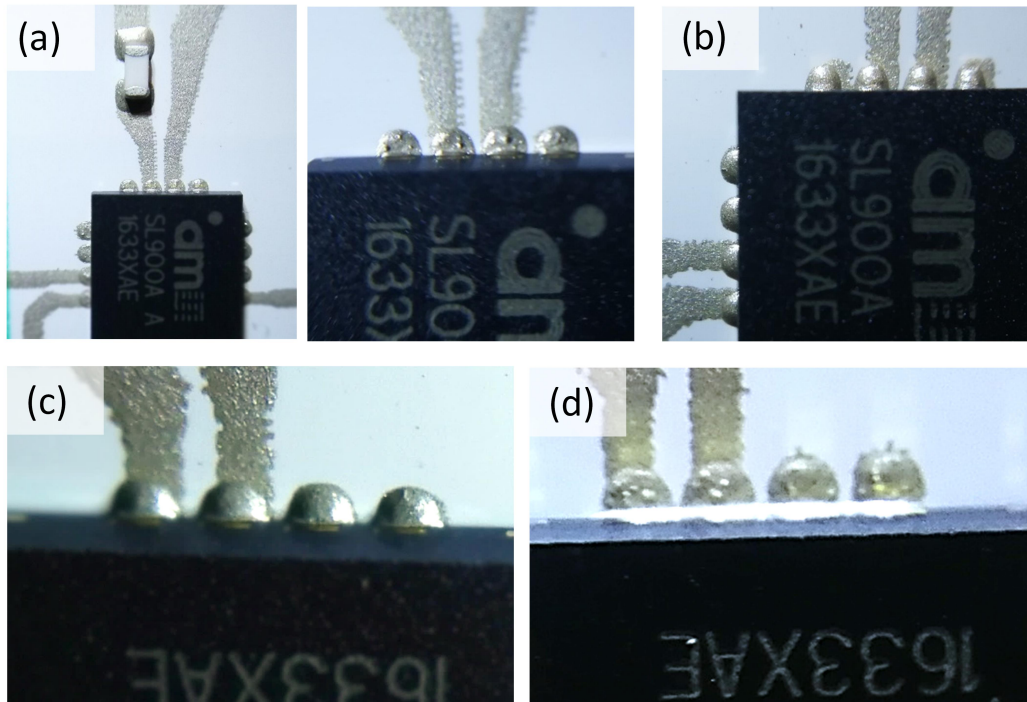


Figure 9.5 Microscope images of assembled tags using pick and place process. a) Effectively assembled components, with close-up showing correct alignment for the SL900A IC, b) example of SL900A IC misaligned in x-direction, c) assembly with optimal amount of conductive epoxy, and d) assembly with too much conductive epoxy, causing shorting of the pads.

readout for temperature, which would indicate that the IC itself was not functioning correctly. The sensor readout from the photodiode on the other three devices provided consistent readouts with a standard deviation of 7% across the devices. The results indicate that although manual aspects of the process such as screen printing and stencil printing can compromise the functionality of the devices, the automated pick and place process does not introduce additional errors, even with slight misalignment of the components (Figure 9.5b).

9.2.4 Packaging

Chapter 7 detailed the matchbox-style packaging design that was conceptualized with assistance from local packaging company Merrypak. Building on this concept design, Merrypak was able to provide inputs as to the processes and costs associated with

scaling up this design, as summarised in Table 9.1. Merrypak provides services for printing of devices onto cardboard, as well as cutting and creasing of devices, where a once-off cost for the design and manufacture of a custom die is required.

9.2.5 Wireless communication and deployment

As discussed in Chapter 6, Synertech assisted with a number of read range measurements for the initial device testing. Building on this collaborative effort, Synertech were able to provide some insights into the roll-out and scale up of the RFID system for this work. A cost estimate was also provided for potential RFID reader options that Synertech have successfully deployed in solutions across South Africa in the past. Options for readers would include a CAEN R1270C Quarkup module and antenna (CAENRFID, Italy), which has a built-in custom command set for the SL900A IC for ease of integration. Lower-cost options include the M6E Nano RFID reader (ThingMagic, Inc., USA) which is more than four times lower in cost than the CAEN reader option. However, custom software would need to be developed for the SL900A command set to enable simple and effective sensor readout, and would contribute to the cost of the system.

Using the lower-cost approach, Synertech projected an initial cost of under R 10000 (EUR \pm 625) per RFID reader system, including software development, reader, antenna, power (either battery or supply), and a small user interface (either a simple display or an LED to provide feedback to the user that the scan was successful). The long-term solution of a black box mounted onto a wall or desk at a clinic is feasible, as Synertech has previously implemented antenna and reader units that are mounted to benchtop surfaces in sophisticated and robust form factors. The option to include further connectivity to each reader unit is a possibility, and Synertech typically implements this with their units to enable remote monitoring and connectivity across systems.

9.3 Cost analysis

Table 9.1 shows a cost comparison between the manual prototyping of devices and automated production for both low and high volumes. The total cost per packaged reader device manufactured using automated, low-volume processes is approximately 40% lower than the cost per device manufactured using manual prototyping methods. With further scale up, this cost point would be expected to reduce by a further 70% depending on the volumes and supplier. In addition to the already evident cost savings

per device in terms of manufacture is the time cost, where automated processes enable complete packaged devices to be produced in a fraction of the time of devices that are manually produced. Although extensive cost analysis for the RFID system and deployment has not yet been performed, the estimated cost of a complete, connected reader solution falls well below the costs of some portable reader solutions without connectivity options. Compared to more affordable readers options, the proposed RFID solution is at least three times lower in cost.

The cost estimate for automated low-volume production of the printed tags is based on semi-manual processes. This cost would be expected to be significantly reduced for fully automated, large-scale manufacture of the printed devices. Ink costs would also be reduced for large-volume production. The estimated time for printed tag manufacture does not take into account the curing times associated with the inks. For high-volume production of the printed tags, costs can be estimated to be similar to UHF RFID tags printed on adhesive labels and supplied in rolls, available through various international companies at a low cost.

The costs of single SMD components and reel formats of components for low volumes are the same, but for larger reel format volumes, the cost would be reduced by more than 40%, and for die on wafer formats (SL900A-ASWB), the cost would be reduced by more than 70%, as shown in Table 9.1. Further scale up for tag device assembly would eliminate the need for a stencil, as dot dispensing processes would be used. Costing for the conductive adhesive used for the stencil printing process was estimated at a third of the cost of the manual assembly process, as substantially less adhesive is used in the stencil printing process. In future, conductive adhesives that are lower in cost and designed for use with automated assembly processes will be utilised, and the costs of these adhesives would be substantially lower. The SM482 assembly line can place up to 28000 components per hour, enabling devices to be assembled in a fraction of the time compared to that achievable with manual assembly. This could be scaled up to larger assembly lines that are available at local electronic manufacturing companies such as Jemstech (Pty) Ltd.

Packaging costs for automated low-volume production were provided by Merrypak and include the cost of the printed graphics, complete box and custom insert. Costs for high-volume production were estimated from international companies supplying matchbox-style white boxes with custom printed graphics in bulk, but it is expected that local production costs could reach similar cost points for large-volume production.

Table 9.1 Cost breakdown in both South African Rand (ZAR) and Euro (EUR) of manual prototyping of devices compared to automated low-volume and high-volume production of devices. Costs are calculated per packaged reader device. Comparisons for manufacture time (min) are also provided. Costs in parentheses indicate once-off tooling costs that are required.

Reader device part	Manual prototyping			Automated low-volume production			Automated high-volume production		
	ZAR	EUR	min	ZAR	EUR	min	ZAR	EUR	min
Printed tag	105	6.6	30	32	2	<10	3.5	0.2	<1
Tooling: screens	(1692)	(106)		(980)	(61)				
Components	120	7.5		120	7.5		35	2.2	
Assembly	90	5.6	30	37	2.3	<0.1	17.5	1.1	<0.1
Tooling: stencil				(500)	(31.3)				
Packaging	25	1.6	30	15	0.9	<0.1	7	0.4	<0.1
Tooling: dieforms				(2000)	(125)				
TOTAL:	340	21.3	90	204	12.7	<10	63	3.9	<1

9.4 Optimisation of printed components and functionality

Based on the costing shown in Table 9.1, it is clear that, although automation and scale up of devices reduces the costs considerably, SMD components contribute to a large part of the cost per device. The packaging of these SMD components in turn makes up a large part of the component costs. For future developments, printing of some or all of the SMD components would reduce costs considerably, and could also assist with the integration of production processes, using an all-printed solution. This approach would also assist with the disposability and long-term biodegradability of all the components that make up a low-cost packaged reader device.

Towards achieving this goal, numerous initial aspects have been explored as part of this work and related work, including using the RF field as a source of power as opposed to a coin cell battery. In addition, printing of individual components and utilizing die formats of components have been investigated.

Initial testing was carried out using the RF field to power the LED in the packaged wireless colour detector devices. Figure 6.2b in Chapter 6 illustrates this concept, where an LED is connected between the V_{POS} and V_{SS} (ground) pins of the SL900A on a paper-based printed tag. When the tag is brought into the range of the AS3993 RFID reader, the LED is powered by the RF field through the RF rectifier output of V_{POS} , which can provide up to 3.4 V.

Individual components investigated in related work have included printed inductors [172], printed batteries [163] and mounting of an unpackaged SL900A die onto inkjet printed circuits on paper [189]. The printability and flexibility of the packaged reader devices were strengthened through the demonstration of printed inductors (Figure 9.6a), and by using the unpackaged SL900A IC die format (Figure 9.6b), as part of the tag devices. The results show successful connection of the printed inductor and the unpackaged die to tag devices, along with successful detection of the tags using the RFID development kit reader.

9.5 Discussion

The printing of functional devices could be a fully automated process in the future. Sheet-to-sheet and roll-to-roll printing of functional inks for printed electronics are currently performed at international facilities. Locally, companies such as Electronic Touch Systems can perform sheet-to-sheet printing of functional inks and printed circuits. Roll-to-roll printing processes are well established on the local scale, and exploratory work for printing of functional inks is underway. Current printing processes will need to be adapted for functional inks in future, or new processes established to achieve this.

After printing, individual devices need to be cut and creased, and this can be achieved using standard packaging production lines that already exist locally. Assembly of all of the required electronic components can then be performed, and these capabilities are available locally for manual, semi-automated and automated assembly. Long term, it may be possible to incorporate large-scale pick and place production lines using roll-to-roll formats, in which case the assembly of components could be completed before the cutting and creasing process.



Figure 9.6 Examples for enhancement of printability and flexibility of packaged wireless colour detector devices through a) printed inductor implementation and b) use of unpackaged SL900A die. In both cases, the printed and assembled tags are successfully scanned by the RFID reader and can be accessed through the user interface.

Low-temperature solder pastes are compatible with certain flexible substrates [190] and could be explored in future work. Further investigations into the different conductive adhesives available, dispensing processes required and associated costs would also need to be carried out to determine the best approach for scale up of the packaged reader devices. Dot dispensing pastes and processes would be favourable for fully automated manufacture of devices and controlled dispensing volumes. As demonstrated for the manual stencil printing process carried out, short circuits of the SL900A IC pads were a limiting factor in the device functionality, which could be addressed by automating the stencilling process or using dot dispensing.

Encapsulation or protective coatings for the printed tracks and components will be an important consideration to ensure protection from environmental factors and to assist with securing SMD components onto the substrate. As an example, Electronic Touch Systems utilizes a low-cost UV curable epoxy resin, which is available from local suppliers, to ensure that components do not dislodge. Conformal coatings have been explored as part of this work. Six different spray and dip coating solutions from

HumiSeal (USA) and Electrolube (UK), available locally, were applied to printed silver tracks on photo paper substrates. In all cases, the coatings prevented oxidation of the printed tracks and maintained the conductivity for up to more than one year after being applied. As a comparison, printed silver tracks on photo paper without any coating were left exposed over the course of one year. The silver tracks became oxidised and were no longer conductive. Conformal coatings are typically low cost and are effective in protecting printed circuits for extended periods. These coatings would be sufficient for use with the packaged reader devices, with a shelf life of months to a year expected.

Packaging for the printed tags has been investigated with a local packaging company for prototyping, and packaging scale up would be feasible and cost-effective in the future. Inserts for the reader devices that could form part of the box design itself have also been initially explored with Merrypak, and could be further developed. This would reduce the number of individual packaging components required for constructing a packaged reader device, and limit errors in the assembly and alignment of the packaging components.

The packaged reader devices can be powered using off-the-shelf coin cell batteries as per the tag design utilised in this work. Automated and effective battery connection would need to be further explored for this to be a viable option. Alternatives would include development of a packaging solution with companies such as Merrypak, where a pouch or holder for the battery could form part of the box design itself, similar to the envisaged insert designs. Initial paper-based battery pouches have been explored as part of work related to this dissertation [163]. As mentioned in the previous section, printed batteries could be an option for future designs, as could the use of the RF field to generate power and drive the LED for colour detection for the brief period for which it is required.

The use of fully printed components and unpackaged dies would reduce the cost of the packaged reader device, and improve the flexibility and disposability of the devices in the long term. Current research and development on printed light sources, such as OLEDs [76] and light-emitting electrochemical cells [74] that have successfully been implemented on paper-based substrates could be utilised in future, as well as printed photodetectors [80]. A recent example showcasing printed photodiode arrays [191] could be applied for multiplexed tests and more complex readouts in future. The printability of components including OLEDs using standard processes such as screen printing have also been explored [73] to facilitate scale up of device manufacture.

RFID reader solutions and deployment have been preliminarily explored, with a number of feasible options available for testing with local RFID company Synertech. Further feasibility and cost analysis studies will be required to assess the scalability of

the system to utilize existing printing and packaging manufacturing capabilities. Local production of these solutions would be desirable from both a cost and accessibility perspective, with the idea being to use existing manufacturing capabilities within local printing and packaging companies. Automated sheet-to-sheet printing of A4-sized designs could initially be implemented, with scaled roll-to-roll processes taking effect at a later stage.

The aspects explored in this chapter assist with providing a platform on which to develop the capabilities to realise printed functionality solutions towards REASSURED diagnostic devices – and various other applications – that are locally produced.

10 Conclusion and outlook

Parts of this chapter are based on previously published work [19] and have been reproduced with permission from the Royal Society of Chemistry.

This work presents a packaged, low-cost, wireless and scalable reader solution for POC diagnostic applications in resource-limited clinics, towards fulfilment of the RE-ASSURED criteria. Specifically, the aim was to develop a solution that aligns with the needs of South African resource-limited clinics, with the ability to be manufactured and distributed locally in South Africa. This dissertation has stepped through the development process to reach these goals, using printed and paper-based functionality as a foundation.

Chapters 2 and 3 introduced the relevant background literature and technical knowledge that was utilised to realise the components and resulting solution presented in this dissertation. Chapters 4 to 7 presented the main technical components required to produce a complete integrated and packaged solution. Expanding on this, Chapter 8 explored real-world testing and usability aspects of the developed packaged readers, to assess the potential for use in real clinic settings. Finally, Chapter 9 provided an outlook on the scalability of the system, focusing on local manufacturing and deployment capabilities and the existing limitations. This chapter also presented a breakdown of the estimated costs for manufacture of the devices and the complete system, which can be significantly reduced by using automated, scaled-up fabrication processes, many of which are already established in South Africa.

Various substrates were explored in Chapter 4 to assess the feasibility of using low-cost, readily available paper and packaging materials for the realisation of printed functionality components, including printed circuits and antennas. Successful printed colour detector RFID tags were showcased in Chapter 5 using model LFTs to assess the colour detection capabilities. Wireless connectivity was successfully demonstrated for the colour detector devices, and sensing RFID tag devices printed and assembled on a variety of substrates (Chapter 6). The technical components developed showed

functional solutions for printed colour detector RFID tags, enabling wireless readout of colour results in practical settings.

Future work could be extended to more detailed assessment of the RFID antennas, where characterisation and modelling could reveal insights into the different substrates and optimal uses thereof. Different detector modules could be explored for optimal result readout from paper-based diagnostic tests. The inclusion of additional printed information could also be explored, such as QR codes and reference colour charts to aid in optimisation of the data collection and colour detection processes, respectively.

Optimisation of the flexible hybrid electronic approach should initially be pursued to harness the advantages of both printed electronics and conventional silicon electronics [64], namely flexibility and low cost compared to high performance, respectively. As printed functionality capabilities advance, all-printed solutions would be the long-term goal for lowering costs, ease of manufacture, and disposability or biodegradability. Chipless RFID solutions are an emerging field and have been demonstrated successfully on standard paper as a low-cost RFID tag solution [192]. This approach could be pursued in future to develop all-printed RFID solutions with additional sensing capabilities. This, along with other individual printed components such as OLEDs, photodetectors and batteries, as discussed in Chapter 9, would be explored to realise a fully printed, integrated solution.

Fully integrated REASSURED systems are crucial as they will remove the subjective and often incorrect human interpretation of results, and allow for robust data collection and data security. From a resource-limited South African clinic perspective, this is vital for easing clinic workflow bottlenecks and ensuring result and data integrity. An integrated, modular system approach, as presented in this work, would enable resource-limited settings to improve diagnoses and healthcare infrastructure in the long term.

Additional integrated functionalities will facilitate modern clinical practices and crisis readiness. Data acquisition and communication are important considerations, which a systems approach can ensure through digitised data and connectivity. Rapid data collection is of increasing importance, especially with contagious diseases and outbreaks, and could be included as an overarching function in augmented REASSURED POC diagnostic solutions. However, data security remains a challenge, where a lack of data certification and confidentiality may result in false diagnosis, stigma, and destruction of lives. This will be a crucial challenge to address as the digitisation of data evolves and information needs to be more tightly managed.

As the need for more data to be collected and processed grows, so will the need for robust, compact and interconnected functionality. From a printed or paper-based perspective, numerous challenges will need to be overcome to achieve this. Many

current solutions make use of hybrid electronics, which have the speed of traditional electronics, but interconnects are not robust and the solution is not fully integrated. In contrast, flexible, paper-based electronics are often limited in terms of speed, and addressing these constraints will need to form part of the roadmap moving forward.

From a South African and resource-limited clinic perspective, and as part of the Ideal Clinics programme, this work can initially assist with patient and result identification and tracking information, thereby alleviating the data management requirements and burden on already constrained resources. Future work may include the RFID labelling of individual tests, so that the tests and packaged reader devices can be linked and tracked to assist with traceability further. The above aspects can be combined to produce a scalable, low-cost printed module for the automated read-out, capture and wireless communication of results from paper-based diagnostic tests, which conforms to the requirements of resource-limited clinics.

Various national benefits would be expected in the long term. Primarily, cost savings would be realised as a result of this technology, as specialised laboratory resources would not be required to operate the automated, user-friendly devices. A nurse or healthcare worker would be able to use the packaged reader devices. The solution presented also offers the potential to be manufactured locally in South Africa, assisting with job creation for the scaled-up printed electronics, printed graphics and packaging processes.

The eventual goal of this work is to address the burden of disease in resource-limited settings in South Africa and on a global scale, by enabling rapid diagnosis times to enable improved quality of life and longevity. The developed technology could be used to test paper-based diagnostic devices with a variety of end applications, ranging from health to environmental to chemical. Initial applications of this technology are designed for medical diagnostic applications at the POC, thus reducing the time and expertise required for diagnosis. Faster diagnosis would reduce the risk of the spread of disease, and ensure that patients receive timely treatment, having a significant health and social impact on communities.

The environmental impact of newly developed technologies is a global concern and should be considered from conceptualization of innovative solutions. Materials and their printability and disposability would form a large part of future developments based on the ideas presented in this work. Printed devices offer the potential to result in less waste being generated, but biodegradability remains an issue to be addressed effectively.

Successful implementation of the packaged reader and similar devices will also depend on the ability to scale the manufacture to produce high volumes of devices, along with the supply chain infrastructure to ensure deployment to remote settings. From

an environmental impact perspective, using paper as a platform may be beneficial as it can be considered CO₂ neutral, i.e. incineration of paper does not unnecessarily produce more of a carbon burden. Incineration of paper also deals with the issue of sterility; in contrast plastic-based medical devices are typically dumped and can pose risks to the public, particularly in resource-limited settings. However, if incineration of paper-based devices begins to occur on a large scale, the logistics and environmental impact of this will need to be evaluated. Self-igniting devices could be explored, as well as biodegradable substrates and materials, where the latter would require further investigations regarding the shelf life and robustness of the devices.

Once the abovesmentioned barriers have been overcome, the real impact of these solutions will be realisable. Ultimately, the success of paper-based diagnostics lies in the development and optimisation of automation, ease of use, and shelf life, while incorporating feedback from users performing field tests in resource-limited settings. Scalability, deployment and disposability will need to form part of the development process from the early stages for large-scale feasible, sustainable solutions to be realised. If this can be achieved, fully REASSURED paper-based diagnostics with augmented functionalities for data, connectivity and environmental sustainability in resource-limited settings are a viable solution for the future.

Bibliography

- [1] Engel, N., M. Davids, N. Blankvoort, N.P. Pai, K. Dheda, and M. Pai: *Compounding diagnostic delays: A qualitative study of point-of-care testing in South Africa*. *Tropical Medicine and International Health*, 20(4):493–500, 2015.
- [2] Cheng, B., B. Cunningham, D.I. Boeras, P. Mafaune, R. Simbi, and R.W. Peeling: *Data connectivity: A critical tool for external quality assessment*. *African Journal of Laboratory Medicine*, 5(2):535, 2016.
- [3] Mashamba-Thompson, T.P., N.A. Jama, B. Sartorius, P.K. Drain, and R.M. Thompson: *Implementation of point-of-care diagnostics in rural primary health-care clinics in South Africa: Perspectives of key stakeholders*. *Diagnostics*, 7(1), 2017.
- [4] Gous, N.M., L.E. Scott, J. Potgieter, L. Ntabeni, I. Sanne, and W.S. Stevens: *Implementation and operational research: implementation of multiple point-of-care testing in 2 HIV antiretroviral treatment clinics in South Africa*. *Journal of Acquired Immune Deficiency Syndromes*, 71(2):e34–e43, 2016.
- [5] Mabey, D., R.W. Peeling, A. Ustianowski, and M.D. Perkins: *Diagnostics for the developing world*. *Nature Reviews Microbiology*, 2(3):231–240, 2004.
- [6] Land, K.J., D.I. Boeras, X.S. Chen, A.R. Ramsay, and R.W. Peeling: *REASSURED diagnostics to inform disease control strategies, strengthen health systems and improve patient outcomes*. *Nature Microbiology*, 4:46–54, 2019.
- [7] Yamada, K., H. Shibata, K. Suzuki, and D. Citterio: *Toward practical application of paper-based microfluidics for medical diagnostics: state-of-the-art and challenges*. *Lab on a Chip*, 17:1206–1249, 2017.
- [8] Nilghaz, A., L. Guan, W. Tan, and W. Shen: *Advances of paper-based microfluidics for diagnostics: The original motivation and current status*. *ACS Sensors*, 1(12):1382–1393, 2016.

- [9] Stevens, W.S., N. Gous, N. Ford, and L.E. Scott: *Feasibility of HIV point-of-care tests for resource-limited settings: challenges and solutions*. BMC Medicine, 12(1):173, 2014.
- [10] Moodley, D., P. Moodley, T. Ndabandaba, and T. Esterhuizen: *Reliability of HIV rapid tests is user dependent*. South African Medical Journal, 98(9):707–711, 2008.
- [11] Morbioli, G.G., T. Mazzu-Nascimento, A.M. Stockton, and E. Carrilho: *Technical aspects and challenges of colorimetric detection with microfluidic paper-based analytical devices (μ PADs) – A review*. Analytica Chimica Acta, 970:1–22, 2017.
- [12] Nayak, S., N. R. Blumenfeld, T. Laksanasopin, and S. K. Sia: *Point-of-care diagnostics: Recent developments in a connected age*. Analytical Chemistry, 89(1):102–123, 2017.
- [13] Chang, J. S., A. F. Facchetti, and R. Reuss: *A circuits and systems perspective of organic/printed electronics: Review, challenges, and contemporary and emerging design approaches*. IEEE Journal on Emerging and Selected Topics in Circuits and Systems, 7(1):7–26, 2017.
- [14] Wang, S., T. Chinnasamy, M.A. Lifson, F. Inci, and U. Demirci: *Flexible substrate-based devices for point-of-care diagnostics*. Trends in Biotechnology, 34(11):909–921, 2016.
- [15] Zhang, X., T. Ge, and J.S. Chang: *Fully-additive printed electronics: Transistor model, process variation and fundamental circuit designs*. Organic Electronics, 26:371–379, 2015.
- [16] Khan, S., L. Lorenzelli, and R. S. Dahiya: *Technologies for printing sensors and electronics over large flexible substrates: A review*. IEEE Sensors Journal, 15(6):3164–3185, 2015.
- [17] Ahmadraji, T., L. Gonzalez-Macia, T. Ritvonen, A. Willert, S. Ylimaula, D. Donaghy, S. Tuurala, M. Suhonen, D. Smart, A. Morrin, V. Efremov, R.R. Baumann, M. Raja, A. Kemppainen, and A.J. Killard: *Biomedical diagnostics enabled by integrated organic and printed electronics*. Analytical Chemistry, 89(14):7447–7454, 2017.

-
- [18] Beni, V., D. Nilsson, P. Arven, P. Norberg, G. Gustafsson, and A.P.F. Turner: *Printed electrochemical instruments for biosensors*. ECS Journal of Solid State Science and Technology, 4(10):S3001–S3005, 2015.
- [19] Smith, S., J.G. Korvink, D. Mager, and K. Land: *The potential of paper-based diagnostics to meet the ASSURED criteria*. RSC Advances, 8:34012–34034, 2018.
- [20] Smith, S., D. Mager, J.G. Korvink, and K.J. Land: *Printed Functionalities on Paper Substrates Towards Fulfilment of the ASSURED Criteria*, pages 123–170. Springer, Cham, Springer Nature Switzerland AG, 2019, ISBN 978-3-319-96870-4.
- [21] Martinez, A.W., S.T. Phillips, M.J. Butte, and G.M. Whitesides: *Patterned paper as a platform for inexpensive, low-volume, portable bioassays*. Angewandte Chemie – International Edition, 46(8):1318–1320, 2007.
- [22] Martinez, A.W., S.T. Phillips, G.M. Whitesides, and E. Carrilho: *Diagnostics for the developing world: Microfluidic paper-based analytical devices*. Analytical Chemistry, 82(1):3–10, 2010.
- [23] Yetisen, A.K., M.S. Akram, and C.R. Lowe: *Paper-based microfluidic point-of-care diagnostic devices*. Lab on a Chip, 13:2210–2251, 2013.
- [24] Cate, D.M., J.A. Adkins, J. Mettakoonpitak, and C.S. Henry: *Recent developments in paper-based microfluidic devices*. Analytical Chemistry, 87(1):19–41, 2015.
- [25] Xia, Y., J. Si, and Z. Li: *Fabrication techniques for microfluidic paper-based analytical devices and their applications for biological testing: A review*. Biosensors and Bioelectronics, 77:774–789, 2016.
- [26] Sher, M., R. Zhuang, U. Demirci, and W. Asghar: *Paper-based analytical devices for clinical diagnosis: recent advances in the fabrication techniques and sensing mechanisms*. Expert Review of Molecular Diagnostics, 17(4):351–366, 2017.
- [27] Bajpai, P.: *Biotechnology for pulp and paper processing*. Springer Science and Business Media, Springer US, 2012.
- [28] Haemokinesis: Group Legible Immunohaematology Format Blood Group (GLIF BG), <https://www.haemokinesis.com/products/bio-active-paper-tests/glif-bg>, 2017.

- [29] Liana, D.D., B. Raguse, J. Gooding, and E. Chow: *Recent advances in paper-based sensors*. *Sensors*, 12(9):11505–11526, 2012.
- [30] Meredith, N.A., C. Quinn, D.M. Cate, T.H. Reilly, J. Volckens, and C.S. Henry: *Paper-based analytical devices for environmental analysis*. *Analyst*, 141:1874–1887, 2016.
- [31] Pires, N.M., T. Dong, U. Hanke, and N. Hoivik: *Recent developments in optical detection technologies in lab-on-a-chip devices for biosensing applications*. *Sensors*, 14(8):15458–15479, 2014.
- [32] Smith, S., P. H. Bezuidenhout, K. Land, J. G. Korvink, and D. Mager: *Development of paper-based wireless communication modules for point-of-care diagnostic applications*. In *Proc SPIE, Fourth Conference on Sensors, MEMS, and Electro-Optic Systems*, volume 10036, 100360J, 2017.
- [33] Bezuidenhout, P., S. Smith, K. Land, and T. H. Joubert: *A low-cost potentiostat for point-of-need diagnostics*. In *2017 IEEE AFRICON conference*, pages 83–87, 2017.
- [34] Singh, A.T., D. Lantigua, A. Meka, S. Taing, M. Pandher, and G. Camci-Unal: *Paper-based sensors: Emerging themes and applications*. *Sensors*, 18(9):2838, 2018.
- [35] Hu, J., S. Wang, L. Wang, F. Li, B. Pingguan-Murphy, T.J. Lu, and F. Xu: *Advances in paper-based point-of-care diagnostics*. *Biosensors and Bioelectronics*, 54:585–597, 2014.
- [36] Martinez, A.W., S.T. Phillips, E. Carrilho, S.W. Thomas III, H. Sindi, and G.M. Whitesides: *Simple telemedicine for developing regions: Camera phones and paper-based microfluidic devices for real-time, off-site diagnosis*. *Analytical Chemistry*, 80(10):3699–3707, 2008.
- [37] Delaney, J.L., E.H. Doeven, A.J. Harsant, and C.F. Hogan: *Use of a mobile phone for potentiostatic control with low cost paper-based microfluidic sensors*. *Analytica Chimica Acta*, 803:123–127, 2013.
- [38] Liu, B., D. Du, X. Hua, X. Y. Yu, and Y. Lin: *Paper-based electrochemical biosensors: From test strips to paper-based microfluidics*. *Electroanalysis*, 26(6):1214–1223, 2014.

- [39] Zhao, C., M.M Thuo, and X. Liu: *A microfluidic paper-based electrochemical biosensor array for multiplexed detection of metabolic biomarkers*. Science and Technology of Advanced Materials, 14(5):054402, 2013.
- [40] Komatsu, T., S. Mohammadi, L. Busa, M. Maeki, A. Ishida, H. Tani, and M. Tokeshi: *Image analysis for a microfluidic paper-based analytical device using the CIE L*a*b* color system*. Analyst, 141:6507–6509, 2016.
- [41] Mobile Assay: Mobile Diagnostic Rapid Test Reader (mReader), <https://mobileassay.com/products>, 2019.
- [42] Ozkan, H. and O.S. Kayhan: *A novel automatic rapid diagnostic test reader platform*. Computational and Mathematical Methods in Medicine, 2016:7498217, 2016.
- [43] Pilavaki, E and A. Demosthenous: *Optimized lateral flow immunoassay reader for the detection of infectious diseases in developing countries*. Sensors, 17(11):2673, 2017.
- [44] Cepheid: GeneXpert Systems, <http://www.cepheid.com/en/cepheid-solutions/systems/software/gx-dx-software>, 2019.
- [45] Drain, P.K. and C. Rousseau: *Point-of-care diagnostics: Extending the laboratory network to reach the last mile*. Current Opinion in HIV and AIDS, 12(5):508, 2017.
- [46] Oldach, L: *Pioneering new diagnostics : Addressing challenges and implications for point-of-care testing in African settings*. Lab Culture – The ASLM Magazine, 13:7–17, February 2015.
- [47] Scott, L.: *A laboratorian’s experience of implementing multiple point-of-care testing in HIV antiretroviral treatment clinics in South Africa*. South African Medical Journal, 103(12):883–884, 2013.
- [48] Watkins, J.O.T. Anstey, J. Goudge, F.X. Gomez-Olive, and F. Griffiths: *Mobile phone use among patients and health workers to enhance primary healthcare: A qualitative study in rural South Africa*. Social Science and Medicine, 198:139–147, 2018.
- [49] Blattner, K., G. Nixon, C. Jaye, and S. Dovey: *Introducing point-of-care testing into a rural hospital setting: Thematic analysis of interviews with providers*. Journal of Primary Health Care, 2(1):54–60, 2010.

- [50] Meyer, W.: *Connectivity in point of care testing*. In *PathCare Pathology Forum – Point of Care Vol. 4 No. 2*, chapter 7, pages 24–25. Dietrich Voight Mia Partners, Goodwood, 1st edition, March 2013.
- [51] Department of Health, Republic of South Africa. Ideal clinic definitions, components and checklists. <https://www.idealclinic.org.za/s>, 2017.
- [52] Hoeng, F., A. Denneulin, and J. Bras: *Use of nanocellulose in printed electronics: a review*. *Nanoscale*, 8:13131–13154, 2016.
- [53] Kim, J., R. Kumar, A.J. Bandodkar, and J. Wang: *Advanced materials for printed wearable electrochemical devices: A review*. *Advanced Electronic Materials*, 3(1):1600260, December 2016.
- [54] Primiceri, E., M.S. Chiriaco, F.M. Notarangelo, A. Crocamo, D. Ardissino, M. Cereda, A. P. Bramanti, M.A. Bianchessi, G. Giannelli, and G. Maruccio: *Key enabling technologies for point-of-care diagnostics*. *Sensors*, 18(11):E3607, 2018.
- [55] Zhang, T., M. Hu, Y. Liu, Q. Guo, X. Wang, W. Zhang, W. Lau, and J. Yang: *A laser printing based approach for printed electronics*. *Applied Physics Letters*, 108(10):103501, 2016.
- [56] Liang, T., X. Zou, and A.D. Mazzeo: *A flexible future for paper-based electronics*. In *Proceedings of SPIE, Micro- and Nanotechnology Sensors, Systems, and Applications VIII*, volume 9836, pages 98361D–1, 2016.
- [57] Ballerini, D.R. and Li, X. and W. Shen: *Patterned paper and alternative materials as substrates for low-cost microfluidic diagnostics*. *Microfluidics and Nanofluidics*, 13(5):769–787, 2012.
- [58] Mace, C.R. and R.N. Deraney: *Manufacturing prototypes for paper-based diagnostic devices*. *Microfluidics and Nanofluidics*, 16(5):801–809, 2014.
- [59] Jiang, X. and Z.H. Fan: *Fabrication and operation of paper-based analytical devices*. *Annual Review of Analytical Chemistry*, 9:203–222, 2016.
- [60] Piila, T., A. Juusti, M. Kylmänen, and K. Ikonen: *Printed electronics and diagnostic products: PrintoCent designer’s handbook*. Neficon Finland Oy, 2015.
- [61] Silveira, C.M., T. Monteiro, and M.G. Almeida: *Biosensing with paper-based miniaturized printed electrodes – a modern trend*. *Biosensors*, 6(4):51, 2016.

-
- [62] IDTechEx Research: Flexible, Printed and Organic Electronics 2019 – 2029: Forecasts, Players & Opportunities, www.idtechex.com, 2018.
- [63] Wu, H., S.W. Chiang, W. Lin, C. Yang, Z. Li, J. Liu, X. Cui, F. Kang, and C.P. Wong: *Towards practical application of paper based printed circuits: capillarity effectively enhances conductivity of the thermoplastic electrically conductive adhesives*. Scientific Reports, 4:6275, 2014.
- [64] Tong, G., Z. Jia, and J. Chang: *Flexible hybrid electronics: Review and challenges*. In *2018 IEEE International Symposium on Circuits and Systems*, pages 1–5, 2018.
- [65] Andersson, H.A., A. Manuilskiy, S. Haller, M. Hummelgård, J. Sidén, C. Hummelgård, H. Olin, and H.E. Nilsson: *Assembling surface mounted components on ink-jet printed double sided paper circuit board*. Nanotechnology, 25(9):094002, 2014.
- [66] Siegel, A.C., S.T. Phillips, M.D. Dickey, N. Lu, Z. Suo, and G.M. Whitesides: *Foldable printed circuit boards on paper substrates*. Advanced Functional Materials, 20(1):28–35, 2010.
- [67] Hamed, M.M., A. Ainla, F. Güder, D.C. Christodouleas, M.T. Fernández-Abedul, and G.M. Whitesides: *Integrating electronics and microfluidics on paper*. Advanced Materials, 28(25):5054–5063, 2016.
- [68] Grau, G., J. Cen, H. Kang, R. Kitsomboonloha, W.J. Scheideler, and V. Subramanian: *Gravure-printed electronics: recent progress in tooling development, understanding of printing physics, and realization of printed devices*. Flexible and Printed Electronics, 1(2):023002, 2016.
- [69] Ostfeld, A.E., I. Deckman, A.M. Gaikwad, C.M. Lochner, and A.C. Arias: *Screen printed passive components for flexible power electronics*. Scientific Reports, 5:15959, 2015.
- [70] Chang, J., X. Zhang, T. Ge, and J. Zhou: *Fully printed electronics on flexible substrates: High gain amplifiers and DAC*. Organic Electronics, 15(3):701–710, 2014.
- [71] Gao, Y., H. Li, and J. Liu: *Directly writing resistor, inductor and capacitor to composite functional circuits: A super-simple way for alternative electronics*. PLOS ONE, 8(8):1–8, 2013.

- [72] Fernández, M.R., E.Z. Casanova, and I.G. Alonso: *Review of display technologies focusing on power consumption*. Sustainability, 7(8):10854, 2015.
- [73] Preinfalk, J.B., T. Eiselt, T. Wehlius, V. Rohnacher, T. Hanemann, G. Gomard, and U. Lemmer: *Large-area screen-printed internal extraction layers for organic light-emitting diodes*. ACS Photonics, 4(4):928–933, 2017.
- [74] Asadpoordarvish, A., A. Sandstrom, C. Larsen, R. Bollstrom, M. Toivakka, R. Osterbacka, and L. Edman: *Light-emitting paper*. Advanced Functional Materials, 25(21):3238–3245, 2015.
- [75] Yoon, D. Y., T. Y. Kim, and D. G. Moon: *Flexible top emission organic light-emitting devices using sputter-deposited Ni films on copy paper substrates*. Current Applied Physics, 10(4):e135–e138, 2010.
- [76] Purandare, S., E. Gomez, and A. Steckl: *High brightness phosphorescent organic light emitting diodes on transparent and flexible cellulose films*. Nanotechnology, 25:094012, 2014.
- [77] Mattana, G. and D. Briand: *Recent advances in printed sensors on foil*. Materials Today, 19(2):88–99, 2015.
- [78] Meiss, T., R. Wertschützky, and B. Stoeber: *Rapid prototyping of resistive mems sensing devices on paper substrates*. In *IEEE 27th International Conference on Micro Electro Mechanical Systems*, pages 536–539, 2014.
- [79] Nassar, J.M., M.D. Cordero, A.T. Kutbee, M.A. Karimi, G.A.T. Sevilla, A.M. Hussain, A. Shamim, and M.M. Hussain: *Paper skin multisensory platform for simultaneous environmental monitoring*. Advanced Materials Technologies, 1(1):1600004, 2016.
- [80] Pace, G., A. Grimoldi, M. Sampietro, D. Natali, and M. Caironi: *Printed photodetectors*. Semiconductor Science and Technology, 30(10):104006, 2015.
- [81] Xie, C. and F. Yan: *Flexible photodetectors based on novel functional materials*. Small, 13(43):1701822, 2017.
- [82] Aga, R.S., J.P. Lombardi, C.M. Bartsch, and E.M. Heckman: *Performance of a printed photodetector on a paper substrate*. IEEE Photonics Technology Letters, 26(3):305–308, 2014.

- [83] Lilliu, S., M. Boberl, M. Sramek, S.F. Tedde, J.E. Macdonald, and O. Hayden: *Inkjet-printed organic photodiodes*. *Thin Solid Films*, 520(1):610–615, 2011.
- [84] Pierre, A., I. Deckman, P.B. Lechene, and A.C. Arias: *High detectivity all-printed organic photodiodes*. *Advanced Materials*, 27(41):6411–6417, 2015.
- [85] Gomathi, P. T., P. Sahatiya, and S. Badhulika: *Large-area, flexible broadband photodetector based on ZnS-MoS₂ hybrid on paper substrate*. *Advanced Functional Materials*, 27(31):1701611, 2017.
- [86] intelliPaper: <https://www.intellipaper.info/>, 2017.
- [87] Madakam, S., R. Ramaswamy, and S. Tripathi: *Internet of Things (IoT): A literature review*. *Journal of Computer and Communications*, 3:164–173, 2015.
- [88] NXP Semiconductors: *Wireless Connectivity*, <https://www.nxp.com/products/>, 2017.
- [89] Ghafar-Zadeh, E.: *Wireless integrated biosensors for point-of-care diagnostic applications*. *Sensors*, 15(2):3236–3261, 2015.
- [90] Chia, S., A. Zalzal, L. Zalzal, and A. Karim: *Intelligent technologies for self-sustaining, RFID-based, rural e-Health systems*. *IEEE Technology and Society Magazine*, 32(1):36–43, 2013.
- [91] Chowdhury, B. and R. Khosla: *RFID-based hospital real-time patient management system*. In *Proc. 6th IEEE/ACIS International Conference on Computer and Information Science*, pages 363–368, 2007.
- [92] Yao, W., C. Chu, and Z. Li: *The use of RFID in healthcare: Benefits and barriers*. In *2010 IEEE International Conference on RFID-Technology and Applications*, pages 128–134, 2010.
- [93] Lopez, Y., J. Franssen, G. Narciandi, J. Pagnozzi, I. Gonzalez-Pinto Arrillaga, and F. Las-Heras Andres: *RFID technology for management and tracking: e-Health applications*. *Sensors*, 18(8):2663, 2018.
- [94] Gaynor, M. and J. Waterman: *Design framework for sensors and RFID tags with healthcare applications*. *Health Policy and Technology*, 5(4):357–369, 2016.

- [95] Rahman, F., M.Z. Alam Bhuiyan, and S.I. Ahamed: *A privacy preserving framework for RFID based healthcare systems*. *Future Generation Computer Systems*, 72:339–352, 2016.
- [96] Atlas RFID Solutions: The Basics of an RFID system, www.atlasRFIDstore.com, 2018.
- [97] Rao, K.V.S., P.V. Nikitin, and S.F. Lam: *Antenna design for UHF RFID tags: a review and a practical application*. *IEEE Transactions on Antennas and Propagation*, 53(12):3870–3876, 2005.
- [98] Amin, Y.: *Printable green RFID antennas for embedded sensors*. PhD thesis, KTH Royal Institute of Technology, 2013.
- [99] Smiley, S.: *RFID tag antennas*, RFIDinsider, atlasRFIDstore, <https://blog.atlasrfidstore.com/rfid-tag-antennas>, February 2017.
- [100] Yang, L. and M.M. Tentzeris: *Design and characterization of novel paper-based inkjet-printed RFID and microwave structures for telecommunication and sensing applications*. In *IEEE MTT-S International Microwave Symposium Digest*, pages 1633–1636, 2007.
- [101] Ullah, M. A., M.T. Islam, T. Alam, and F.B. Ashraf: *Paper-based flexible antenna for wearable telemedicine applications at 2.4 GHz ISM band*. *Sensors*, 18:4214, 2018.
- [102] Lo Hine Tong, D., P. Minard, C. Person, P. Borel, and D. Izoard: *Dipole antenna printed on paper substrate for WLAN applications*. In *2018 15th European Radar Conference*, pages 457–460, 2018.
- [103] Kisic, M., B. Dakic, M. Damnjanovic, A. Menicanin, N. Blaz, and L. Zivanov: *Design and simulation of 13.56 MHz RFID tag in ink-jet printing technology*. In *36th International Spring Seminar on Electronics Technology*, pages 263–267, 2013.
- [104] Abutarboush, H.F. and A. Shamim: *Paper-based inkjet-printed tri-band U-slot monopole antenna for wireless applications*. *IEEE Antennas and Wireless Propagation Letters*, 11:1234–1237, 2012.
- [105] Shaker, G., A. Rida, S. Safavi-Naeini, M.M. Tentzeris, and S. Nikolaou: *Inkjet printing of UWB antennas on paper based substrates*. In *Proc. of the 5th European Conference on Antennas and Propagation*, pages 3001–3004, 2011.

- [106] Yang, L., A. Rida, R. Vyas, and M.M. Tentzeris: *RFID tag and RF structures on a paper substrate using inkjet-printing technology*. IEEE Transactions on Microwave Theory and Techniques, 55(12):2894–2901, 2007.
- [107] Sipilä, E., J. Virkki, J. Wang, L. Sydänheimo, and L. Ukkonen: *Brush-painting and photonic sintering of copper oxide and silver inks on wood and cardboard substrates to form antennas for UHF RFID tags*. International Journal of Antennas and Propagation, 2016:3694198, 2016.
- [108] He, H., L. Sydänheimo, J. Virkki, and L. Ukkonen: *Experimental study on inkjet-printed passive UHF RFID tags on versatile paper-based substrates*. International Journal of Antennas and Propagation, 2016:9265159, 2016.
- [109] Çiftçi, T., B. Karaosmanoğlu, and O. Ergül: *Low-cost inkjet antennas for RFID applications*. IOP Conference Series: Materials Science and Engineering, 120(1):012005, 2016.
- [110] Kavcic, U., M. Maek, and T. Muck: *Ultra-high frequency radio frequency identification tag antennas printed directly onto cardboard used for the manufacture of pharmaceutical packaging*. Journal of Imaging Science and Technology, 59(5):50504, 2015.
- [111] Kavcic, U., M. Pivar, M. Dokic, D. Gregor-Svetec, L. Pavlovic, and T. Muck: *UHF RFID tags with printed antennas on recycled papers and cardboards*. Materials and Technology, 48(2):261–267, 2014.
- [112] Smith, S., P. Bezuidenhout, K. Land, J.G. Korvink, and D. Mager: *Printed wireless devices for low-cost, connected sensors for point-of-care applications*. In *RAPDASA 2017 conference*, pages 243–249, 2017.
- [113] Salmerón, J.F., F. Molina-Lopez, D. Briand, J.J. Ruan, A. Rivadeneyra, M. Carvajal, L. F. Capitan-Vallvey, N. Derooij, and A. J. Palma: *Properties and printability of inkjet and screen-printed silver patterns for RFID antennas*. Journal of Electronic Materials, 43(2):604–617, 2014.
- [114] Cook, B.S., J.R. Cooper, and M.M. Tentzeris: *An inkjet-printed microfluidic RFID-enabled platform for wireless lab-on-chip applications*. IEEE Transactions on Microwave Theory and Techniques, 61(12):4714–4723, 2013.
- [115] Su, W., B.S. Cook, Y. Fang, and M. Tentzeris: *Fully inkjet-printed microfluidics: A solution to low-cost rapid three-dimensional microfluidics fabrication*

- with numerous electrical and sensing applications.* Scientific Reports, 6:35111, 2016.
- [116] Zhang, J., G. Y. Tian, A.M.J. Marindra, A.I. Sunny, and A.B. Zhao: *A review of passive RFID tag antenna-based sensors and systems for structural health monitoring applications.* Sensors, 17(2):265, 2017.
- [117] Singh, R., E. Singh, and H.S. Nalwa: *Inkjet printed nanomaterial based flexible radio frequency identification (RFID) tag sensors for the internet of nano things.* RSC Advances, 7:48597–48630, 2017.
- [118] Bibi, F., C. Guillaume, N. Gontard, and B. Sorli: *A review: RFID technology having sensing aptitudes for food industry and their contribution to tracking and monitoring of food products.* Trends in Food Science and Technology, 62:91–103, 2017.
- [119] Vyas, R., V. Lakafosis, A. Rida, N. Chaisilwattana, S. Travis, J. Pan, and M.M. Tentzeris: *Paper-based RFID-enabled wireless platforms for sensing applications.* IEEE Transactions on Microwave Theory and Techniques, 57(5):1370–1382, 2009.
- [120] IDTechEx Research: RFID Forecasts, Players & Opportunities 2018 – 2028, www.idtechex.com, 2018.
- [121] Alimenti, F., C. Mariotti, V. Palazzi, M. Virili, G. Orecchini, P. Mezzanotte, and L. Roselli: *Communication and sensing circuits on cellulose.* Journal of Low Power Electronics and Applications, 5(3):151–164, 2015.
- [122] Yuan, M., E. C. Alocilja, and S. Chakrabartty: *Self-powered wireless affinity-based biosensor based on integration of paper-based microfluidics and self-assembled RFID antennas.* IEEE Transactions on Biomedical Circuits and Systems, 10(4):799–806, 2016.
- [123] Colella, R., D. De Donno, L. Tarricone, and Catarinucci: *Unconventional UHF RFID tags with sensing and computing capabilities.* Journal of Communications Software and Systems, 10(2):83–89, 2014.
- [124] Arjowiggins Creative Papers: PowerCoat ALIVE, <http://powercoatpaper.com/products/powercoat-alive/>, 2017.

- [125] Gaikwad, A.M., A.C. Arias, and D.A. Steingart: *Recent progress on printed flexible batteries: Mechanical challenges, printing technologies, and future prospects*. Energy Technology, 3(4):305–328, 2015.
- [126] Berggren, M., D.T. Simon, D. Nilsson, P. Dyreklev, P. Norberg, S. Nordlinder, P.A. Ersman, G. Gustafsson, J.J. Wikner, J. Hederen, and H. Hentzell: *Browsing the real world using organic electronics, Si-chips, and a human touch*. Advanced Materials, 28(10):1911–1916, 2016.
- [127] Sani, N., M. Robertsson, P. Cooper, X. Wang, M. Svensson, P. Andersson Ersman, P. Norberg, M. Nilsson, D. Nilsson, X. Liu, H. Hesselbom, L. Akesso, M. Fahlman, X. Crispin, I. Engquist, M. Berggren, and G. Gustafsson: *All-printed diode operating at 1.6 GHz*. Proceedings of the National Academy of Sciences, 111(33):11943–11948, 2014.
- [128] Turner, A.P.F.: *Biosensors: Sense and sensibility*. Chemical Society Reviews, 42(8):3184–3196, 2013.
- [129] Lee, B. H., D. Lee, H. Bae, H. Seong, S. B. Jeon, M. L. Seol, J. W. Han, M. Meyyappan, S. G. Im, and Y. K. Choi: *Foldable and disposable memory on paper*. Scientific Reports, 6:38389, 2016.
- [130] Liu, H. and R.M. Crooks: *Paper-based electrochemical sensing platform with integral battery and electrochromic read-out*. Analytical Chemistry, 84(5):2528–2532, 2012.
- [131] Yang, L., R. Zhang, D. Staiculescu, C.P. Wong, and M.M. Tentzeris: *A novel conformal RFID-enabled module utilizing inkjet-printed antennas and carbon nanotubes for gas-detection applications*. IEEE Antennas and Wireless Propagation Letters, 8:653–656, 2009.
- [132] Liana, D.D., B. Raguse, J.J. Gooding, and E. Chow: *An integrated paper-based readout system and piezoresistive pressure sensor for measuring bandage compression*. Advanced Materials Technologies, 1(9):1600143, 2016.
- [133] Liana, D.D., B. Raguse, J.J. Gooding, and E. Chow: *A balance-in-a-box: an integrated paper-based weighing balance for infant birth weight determination*. Analytical Methods, 9:66–75, 2017.
- [134] Diagnostics for All (DFA): Low-cost, easy-to-use, point-of-care diagnostics for the developing world, <http://dfa.org/>, 2018.

- [135] INSiGHT: Institute for Nutritional Sciences, Global Health, and Technology, <http://insight.cornell.edu>, 2018.
- [136] Deloitte Development LLC: *Capturing value from the smart packaging revolution*, Deloitte Insights, 2018.
- [137] Kumar, A.A., J.W. Hennek, B.S. Smith, S. Kumar, P. Beattie, S. Jain, J.P. Rolland, T.P. Stossel, C. Chunda-Liyoka, and G.M. Whitesides: *From the bench to the field in low-cost diagnostics: Two case studies*. *Angewandte Chemie International Edition*, 54(20):5836–5853, 2015.
- [138] Smith, S., A. Oberholzer, K. Land, J.G. Korvink, and D. Mager: *Functional screen printed radio frequency identification tags on flexible substrates, facilitating low-cost and integrated point-of-care diagnostics*. *Flexible and Printed Electronics*, 3(2):025002, 2018.
- [139] Pathmanathan, I., A. Date, W. L. Coggin, J. Nkengasong, A. S. Piatek, and H. Alexander: *Rolling out Xpert® MTB/RIF for TB detection in HIV-infected populations: An opportunity for systems strengthening*. *African Journal of Laboratory Medicine*, 6(2):a460, 2017.
- [140] Creswell, J., A.J. Codlin, E. Andre, M.A. Micek, A. Bedru, E.J. Carter, R. P. Yadav, A. Mosneaga, B. Rai, S. Banu, M. Brouwer, L. Blok, S. Sahu, and L. Ditiu: *Results from early programmatic implementation of Xpert MTB/RIF testing in nine countries*. *BMC Infectious Diseases*, 14:2, 2014.
- [141] Zhou, S., W. Ling, and Z. Peng: *An RFID-based remote monitoring system for enterprise internal production management*. *The International Journal of Advanced Manufacturing Technology*, 33(7):837–844, 2007.
- [142] Occhiuzzi, C., C. Vallese, S. Amendola, S. Manzari, and G. Marrocco: *NIGHT-Care: A passive RFID system for remote monitoring and control of overnight living environment*. *Procedia Computer Science*, 32:190–197, 2014.
- [143] Bahadir, E.B. and M.K. Sezginurk: *Lateral flow assays: Principles, designs and labels*. *TrAC Trends in Analytical Chemistry*, 82:286–306, 2016.
- [144] Smith, T. and J. Guild: *The C.I.E. colorimetric standards and their use*. *Transactions of the Optical Society*, 33(3):73, 1931.
- [145] X-Rite, Inc.: *A Guide to Understanding Colour*, www.xrite.com, 2016.

- [146] Drevinskas, T., A. Maruska, E. Gladkauskas, L. Telksnys, V. Girdauskas, J. Gorbatsova, M. Kaljurand, and O. Ragazinskiene: *Design and applications of miniaturized, portable LED based colorimeter*. Chemija, 29(4):209–218, 2018.
- [147] Schweber, B.: How to Use Photodiodes and Phototransistors Most Effectively, <https://www.digikey.com/en/articles/techzone/2018/sep/how-to-use-photodiodes-and-phototransistors-most-effectively>. Digikey, 2018.
- [148] Tam, J.O., H. de Puig, C.W. Yen, I. Bosch, J. Gomez-Marquez, C. Clavet, K. Hamad-Schifferli, and L. Gehrke: *A comparison of nanoparticle-antibody conjugation strategies in sandwich immunoassays*. Journal of Immunoassay and Immunochemistry, 38(4):355–377, 2016.
- [149] Stutzman, W.L. and G.A. Thiele: *Antenna Theory and Design*. Wiley USA, 3rd Edition, 2012.
- [150] Singh, P., A. Sharma, N. Uniyal, and R. Kala: *Half-wave dipole antenna for GSM applications*. International Journal of Advanced Computer Research, 2(4):354–357, 2012.
- [151] Tareq, M., D. Ashraful Alam, M. Islam, and R. Ahmed: *Simple half-wave dipole antenna analysis for wireless applications by CST microwave studio*. International Journal of Computer Applications, 94(7):21–23, 2014.
- [152] AMS: *Application Note: 5-SL900A - RF Characteristics*. Technical report, AMS, Austria, 2013.
- [153] Salmerón, J.F., F. Molina-Lopez, A. Rivadeneyra, A.V. Quintero, L.F. Capitán-Vallvey, N.F. de Rooij, J.B. Ozáez, D. Briand, and A.J. Palma: *Design and development of sensing RFID tags on flexible foil compatible with EPC Gen 2*. IEEE Sensors Journal, 14(12):4361–4371, 2014.
- [154] HL7 International: <http://www.hl7.org/>, 2018.
- [155] Iggesund Paperboard: Reference Manual, <https://www.iggesund.com/en/knowledge/knowledge-publications/>, 2019.
- [156] Tomaszewski, G., P. Jankowski-Miśkiewicz, M. Węglarski, and W. Lichoń: *Inkjet-printed flexible RFID antenna for UHF RFID transponders*. Materials Science-Poland, 34(4):760–769, 2016.

- [157] Fernández-Salmerón, J., A. Rivadeneyra, F. Martínez-Martí, L.F. Capitán-Vallvey, A.J. Palma, and M.A. Carvajal: *Passive UHF RFID tag with multiple sensing capabilities*. *Sensors*, 15(10):26769–26782, 2015.
- [158] Liakos, D., S. Smith, and T. H. Joubert: *Colorimetric system for paper-based assays*. In *Proc. SPIE, Fifth Conference on Sensors, MEMS, and Electro-Optic Systems*, volume 110430, 110430J, 2019.
- [159] Salmeron, J.F., A. Rivadeneyra, M. Agudo-Acemel, L.F. Capitán-Vallvey, J. Banqueri, M.A. Carvajal, and A.J. Palma: *Printed single-chip UHF passive radio frequency identification tags with sensing capability*. *Sensors and Actuators A: Physical*, 220:281–289, 2014.
- [160] Pichorim, S.F., N.J. Gomes, and J.C. Batchelor: *Two solutions of soil moisture sensing with RFID for landslide monitoring*. *Sensors*, 18(2):452, 2018.
- [161] Escobedo, P., M.A. Carvajal, L.F. Capitán-Vallvey, J. Fernández-Salmerón, A. Martínez-Olmos, and A.J. Palma: *Passive UHF RFID tag for multispectral assessment*. *Sensors*, 16(7):1085, 2016.
- [162] Falco, A., J.F. Salmerón, F.C. Loghin, P. Lugli, and A. Rivadeneyra: *Fully printed flexible single-chip RFID tag with light detection capabilities*. *Sensors*, 17(3):534, 2017.
- [163] Smith, S., A. Oberholzer, P. Madzivhandila, K. Land, J.G. Korvink, and D. Mager: *Printed, flexible wireless temperature logging system*. In *Proc. SPIE, Fifth Conference on Sensors, MEMS, and Electro-Optic Systems*, volume 11043, 110430I, 2019.
- [164] DesignCAD 3D Max: www.turbocad.com/designcad/.
- [165] Shen, L., J.A. Hagen, and I. Papautsky: *Point-of-care colorimetric detection with a smartphone*. *Lab on a Chip*, 12:4240–4243, 2012.
- [166] AMS: *Application Note: External Sensor Interface for SL900A*. Technical report, AMS, Austria, 2013.
- [167] Kuntzleman, T.S. and E.C. Jacobson: *Teaching Beer’s Law and absorption spectrophotometry with a smart phone: A substantially simplified protocol*. *Journal of Chemical Education*, 93(7):1249–1252, 2016.

- [168] Pridmore, R.W.: *Complementary colors: The structure of wavelength discrimination, uniform hue, spectral sensitivity, saturation, chromatic adaptation, and chromatic induction*. *Color Research and Application*, 34(3):233–252, 2009.
- [169] Nguyen, H. D., J. Coupez, V. Castel, C. Person, A. Delattre, L. Crowther-Alwyn, and P. Borel: *RF characterization of flexible substrates for new conformable antenna systems*. In *2016 10th European Conference on Antennas and Propagation*, pages 1–5, 2016.
- [170] Taklo, M.M.V., B. Belle, D.N. Wright, A.S.B. Vardøy, A. Garcia, T. Eriksson, O. Hagel, and M. Danestig: *Smart tags that are exactly reliable enough*. In *2017 Pan Pacific Microelectronics Symposium*, page 8, 2017.
- [171] Molina-Farrugia, B., A. Rivadeneyra, J. Fernández-Salmerón, F. Martínez-Martí, J. Banqueri, and M.A. Carvajal: *Read range enhancement of a sensing RFID tag by photovoltaic panel*. *Journal of Sensors*, 2017:7264703, 2017.
- [172] Le Grange, P., S. Smith, and T. H. Joubert: *Inductor design for inkjet-printed electronics*. In *Proc. SPIE, Fifth Conference on Sensors, MEMS, and Electro-Optic Systems*, volume 11043, 110430L, 2019.
- [173] Grosinger, J., L.W. Mayer, C. Mecklenbrauker, and A. Scholtz: *Input impedance measurement of a dipole antenna mounted on a car tire*. In *The 2009 International Symposium on Antennas and Propagation*, pages 1175–1178, 2009.
- [174] Gao, Y., Z. Zhang, H. Lu, and H. Wang: *Calculation of read distance in passive backscatter RFID systems and application*. *Journal of System and Management Sciences*, 2(1):40–49, 2012.
- [175] Srikant, S.S. and R.P. Mahapatra: *Read range of UHF passive RFID*. *International Journal of Computer Theory and Engineering*, 2(3):323–325, 2010.
- [176] Luh, Y. P. and Y. C. Liu: *Measurement of effective reading distance of UHF RFID passive tags*. *Modern Mechanical Engineering*, 3:115–120, 2013.
- [177] Griffin, J.D. and G.D. Durgin: *Complete link budgets for backscatter-radio and RFID systems*. *IEEE Antennas and Propagation Magazine*, 51(2):11–25, 2009.
- [178] Björninen, T., S. Merilampi, L. Ukkonen, L. Sydänheimo, and P. Ruuskanen: *The effect of fabrication method on passive UHF RFID tag performance*. *International Journal of Antennas and Propagation*, 2009:920947, 2009.

- [179] Bangor, A., P.T. Kortum, and J.T. Miller: *An empirical evaluation of the system usability scale*. International Journal of Human-Computer Interaction, 24(6):574–594, 2008.
- [180] Lewis, J.R.: *Psychometric evaluation of an after-scenario questionnaire for computer usability studies: The ASQ*. SIGCHI Bull, 23(1):78–81, 1991.
- [181] Schiettecatte, J., E. Anckaert, and J. Smits: *Interferences in Immunoassays*, *Advances in Immunoassay Technology*, chapter 3, pages 45–62. InTech, Available from: <http://www.intechopen.com/books/advances-in-immunoassay-technology/interference-in-immunoassays>, 2012.
- [182] Gao, M. and P. Kortum: *Measuring the usability of home healthcare devices using retrospective measures*. Proceedings of the Human Factors and Ergonomics Society Annual Meeting, 61(1):1281–1285, 2017.
- [183] Georgsson, M. and N. Staggers: *Quantifying usability: an evaluation of a diabetes mHealth system on effectiveness, efficiency, and satisfaction metrics with associated user characteristics*. Journal of the American Medical Informatics Association, 23(1):5–11, 2016.
- [184] UNICEF/UNDP/World Bank/WHO Special Programme for Research and Training in Tropical Diseases. Laboratory-based evaluation of 19 commercially available rapid diagnostic tests for tuberculosis. Geneva: World Health Organization. <http://www.who.int/iris/handle/10665/43967>, 2008.
- [185] Avuthu, S.G.R., M. Gill, N. Ghalib, M. Sussman, G. Wable, and J. Richstein: *An introduction to the process of printed electronics*. In *Proc. of SMTA International*, pages 246–252, 2016.
- [186] Wasley, T., J. Li, R. Kay, D. Ta, J. Shephard, J. Stringer, P. Smith, E. Esenturk, and C. Connaughton: *Enabling rapid production and mass customisation of electronics using digitally driven hybrid additive manufacturing techniques*. In *2016 IEEE 66th Electronic Components and Technology Conference*, pages 849–856, 2016.
- [187] Xie, Li: *Heterogeneous integration of silicon and printed electronics for intelligent sensing devices*. PhD thesis, KTH Royal Institute of Technology, 2014.

- [188] VTT Technical Research Centre of Finland Ltd., <https://www.vttresearch.com/services/smart-industry/printed-and-hybrid-manufacturing-services/pilot-manufacturing-services-and-infrastructure>, 2019.
- [189] Bezuidenhout, P., S. Smith, K. Land, and T. H. Joubert: *Inkjet-printed interconnects for unpackaged dies in printed electronics*. *Electronics Letters*, 55(5):252–254, 2019.
- [190] Juric, D., S. Hämmerle, K. Gläser, W. Eberhardt, and A. Zimmermann: *Assembly of components on inkjet-printed silver structures by soldering*. *IEEE Transactions on Components, Packaging and Manufacturing Technology*, 9(1):156–162, 2019.
- [191] Deckman, I., P.B. Lechene, A. Pierre, and A.C. Arias: *All-printed full-color pixel organic photodiode array with a single active layer*. *Organic Electronics*, 56:139–145, 2018.
- [192] Herrojo, C., M. Moras, F. Paredes, A. Nunez, E. Ramon, J. Mata-Contreras, and F. Martín: *Very low-cost 80-bit chipless-RFID tags inkjet printed on ordinary paper*. *Technologies*, 6:52, 2018.

A Own publications

Publications related to the work presented in this dissertation are listed below.

Journal articles

1. **Smith, S.**, Madzivhandila, P., Ntuli, L., Bezuidenhout, P., Zheng, H. and Land, K. (2019). “Printed Paper-Based Electrochemical Sensors for Low-Cost Point-of-Need Applications”, *Electrocatalysis*, 2019, 1–10. <https://doi.org/10.1007/s12678-019-0512-8>.
2. Bezuidenhout, P., **Smith, S.**, Land, K. and Joubert, T.-H. (2019). “Inkjet-Printed interconnection of unpackaged die in paper-based electronics”, *IET Electronics Letters*, 55, 5, 252–254. <https://doi.org/10.1049/el.2018.6839>.
3. **Smith, S.**, Korvink, J.G., Mager, D. and Land, K. (2018). “The potential of paper-based diagnostics to meet the ASSURED criteria.” *RSC Advances*, 8, 34012–34034. <https://doi.org/10.1039/C8RA06132G>.
4. Bezuidenhout, P., **Smith, S.**, Joubert, T.-H. (2018). “A Low-Cost Inkjet-Printed Paper-Based Potentiostat”, *Applied Sciences*, 8(6), 968. <https://doi.org/10.3390/app8060968>.
5. **Smith, S.**, Oberholzer, A., Land, K., Korvink, J.G. and Mager, D. (2018). “Functional screen printed RFID tags on flexible substrates, facilitating low-cost and integrated point-of care diagnostics”, *IOP Flexible and Printed Electronics*, 3(2), 025002. <https://doi.org/10.1088/2058-8585/aabc8c>.
6. Wiederoder, M.S., **Smith, S.**, Madzivhandila, P., Mager, D. and Moodley, K. (2017). “Novel functionalities of hybrid paper-polymer centrifugal devices for assay performance enhancement”, *Biomicrofluidics*, 11(5), 054101. <https://doi.org/10.1063/1.5002644>.

7. **Smith, S.**, Mager, D., Perebikovskiy, A., Shamloo, E., Kinahan, D., Mishra, R., Torres Delgado, S.M., Kido, H., Saha, S., Ducreé, J., Madou, M., Land, K. and Korvink, J.G. (2016). “CD-based Microfluidics for Primary Care in Extreme Point-of-Care Settings”, *Micromachines*, 7(2), 22. <https://doi.org/10.3390/mi7020022>.
8. **Smith, S.**, Moodley, K., Govender, U., Chen, H., Fourie, L., Ngwenya, S., Kumar, S., Mjwana, P., Cele, H., Mbanjwa, M.B., Potgieter, S., Joubert, T., Land, K. (2015). “Paper-based smart microfluidics for education and low cost diagnostics”, *South African Journal of Science*, 111 (11/12). <https://doi.org/10.17159/sajs.2015/20140358>.
9. Joubert, T.-H., Bezuidenhout, P.H., Chen, H., **Smith, S.** and Land, K.J. (2015). “Inkjet-printed Silver Tracks on Different Paper Substrates”. *Materials Today: Proceedings*, 2(7), 3891–3900. <http://doi.org/10.1016/j.matpr.2015.08.018>.

Revised submission

1. **Smith, S.**, Oberholzer, A., Korvink, J.G., Mager, D. and Land, K. “Wireless colorimetric readout to enable resource-limited point-of-care”, Resubmitted with revisions to *Scientific Reports*.

Book chapters

1. **Smith, S.**, Mager, D., Korvink, J.G. and Land, K.J. (2019). “Printed Functionalities on Paper Substrates Towards Fulfilment of the ASSURED Criteria”. In: Land K. (eds) Paper-based Diagnostics. Springer, Cham, Springer Nature Switzerland AG. https://doi.org/10.1007/978-3-319-96870-4_5
2. Land, K.J., **Smith, S.** and Peeling, R.W. (2019). “Unmet Diagnostics Needs for the Developing World”. In: Land K. (eds) Paper-based Diagnostics. Springer, Cham, Springer Nature Switzerland AG. https://doi.org/10.1007/978-3-319-96870-4_1

Patents

1. **Smith, S.** and Land, K. (2018). Medical testing device and manufacturing method therefor. Patent number: 2018/06947. UK provisional patent number: 1717113.3. Filed 18 October 2018.
2. Bezuidenhout, P., **Smith, S.**, Land, K. and Joubert, T.-H. (2018). Potentiostat and method for manufacturing a potentiostat. UK provisional patent number: 1717259.4. Filed 18 October 2018.

Conference contributions

1. **Smith, S.**, Bezuidenhout, P., David, S. and Land, K. (accepted). “Advanced printing technologies for future manufacturing of paper-based devices”, *COMA 19 International Conference on Competitive Manufacturing*.
2. **Smith, S.**, Oberholzer, A., Madzivhandila, P., Land, K., Korvink, J.G. and Mager, D. (2019). “Printed, flexible wireless temperature logging system”, *Proc. SPIE 11043, Fifth Conference on Sensors, MEMS, and Electro-Optic Systems*, 110430I. <https://doi.org/10.1117/12.2500747>.
3. Liakos, D., **Smith, S.** and Joubert, T.-H. (2019). “Colorimetric system for paper-based assays”, *Proc. SPIE 11043, Fifth Conference on Sensors, MEMS, and Electro-Optic Systems*, 110430J. <https://doi.org/10.1117/12.2502538>.
4. Le Grange, P., **Smith, S.** and Joubert, T.-H. (2019). “Inductor design for inkjet-printed electronics”, *Proc. SPIE 11043, Fifth Conference on Sensors, MEMS, and Electro-Optic Systems*, 110430L. <https://doi.org/10.1117/12.2502526>.
5. Madzivhandila, P., **Smith, S.**, Ntuli, L. and Land, K. (2019). “Development of a printed paper-based origami electrochemical sensor for the detection of heavy metals in water”, *Proc. SPIE 11043, Fifth Conference on Sensors, MEMS, and Electro-Optic Systems*, 110430H. <https://doi.org/10.1117/12.2322333>.
6. **Smith, S.**, Oberholzer, A., Land, K., Korvink, J.G. and Mager, D. (2018). “Printed RFID tags on paper and flexible substrates towards low-cost connected sensor systems”, *Proceedings of RAPDASA 2018 conference*, ISBN: 978-0-620-80987-0.

7. **Smith, S.**, Land, K., Korvink, J.G. and Mager, D. (2017). “Connected, low-cost point-of-care diagnostics for rural South African clinics”, *MicroTAS 2017 conference*.
8. Bezuidenhout, P., **Smith, S.**, Land, K., Joubert, T.-H. (2017). “Hybrid paper-based potentiostat for low-cost point-of-need diagnostics”, *MicroTAS 2017 conference*.
9. **Smith, S.**, Bezuidenhout, P., Land, K., Korvink, J.G. and Mager, D. (2017), “Printed wireless devices for low-cost connected sensors for point-of-care applications”, *Proceedings of RAPDASA 2017 conference*.
10. **Smith, S.**, Bezuidenhout, P., Land, K., Korvink, J.G. and Mager, D. (2017). “Development of paper-based wireless communication modules for point-of-care diagnostic applications”, *Proc SPIE, Vol.10036, Fourth Conference on Sensors, MEMS, and Electro-Optic Systems, 100360J*. <http://dx.doi.org/10.1117/12.2244296>.
11. Bezuidenhout, P., **Smith, S.**, Land, K. and Joubert, T.-H. (2017). “A low-cost potentiostat for point-of-need diagnostics”, *2017 IEEE AFRICON conference*, 83–87. <https://doi.org/10.1109/AFRCON.2017.8095460>.
12. **Smith, S.**, Bezuidenhout, P., Mbanjwa, M., Zheng, H., Conning, M., Palaniyandy, N., Ozoemena, K. and Land, K. (2017). “Development of paper-based electrochemical sensors for water quality monitoring”, *Proc. SPIE 10036, Fourth Conference on Sensors, MEMS, and Electro-Optic Systems, 100360C*. <http://dx.doi.org/10.1117/12.2244290>.
13. Wiederoder, M.S., **Smith, S.**, Madzivhandila, P., Mager, D., Moodley, K., DeVoe, D.L. and Land, K.J. (2016). “A paper-polymer centrifugal device for low-cost sample pre-concentration and colorimetric lateral flow assay enhancement”, *MicroTAS 2016 conference*, 842–843.
14. **Smith, S.**, Moodley, K. and Land, K. (2015). “Plug-and-play paper-based toolkit for rapid prototyping of microfluidics and electronics towards point-of-care diagnostic solutions”, *Proceedings of RAPDASA 2015 conference*.
15. Bezuidenhout, P.H., **Smith, S.**, Mbanjwa, M., Land, K. and Joubert, T.-H. (2015). “A comparison of different silver inks for printing of conductive tracks on paper substrates for rapid prototyping of electronic circuits”, *Proceedings of RAPDASA 2015 conference*.

-
16. **Smith, S.**, Chen, H., Moodley, K., Joubert, T.-H. and Land, K. (2014). “Rapid development of paper-based fluidic diagnostic devices”, *Proceedings of RAP-DASA 2014 Conference*.

Other

1. Feature article, March 2019: “Worth the paper it’s printed on”, *Electronics Letters*, 55(5), 231. <https://doi.org/10.1049/el.2019.0508>.
2. Online article by Synertech, October 2018: “Point-of-care diagnostics”, *ITWeb*, <https://www.itweb.co.za/content/DZQ58vVJ5bavzXy2>.

B Usability questionnaire

The questions and information that were included in the questionnaire for the usability study are provided below.

Information recorded at the start of the session:

General information:

- Date and time:
- Location:
- Lighting conditions/environment:

Participant information:

- Name:
- Gender:
- Age:
- Qualifications/background:
- Experience with medical devices:
- Consent form signed? Yes No

Questions on understanding of study:

Participants are provided with a brief verbal overview of the study when signing the consent form and asked to answer the following questions:

1. Please provide a brief description of your understanding about what this device does?
2. Please provide a brief description of your understanding of where this device will be used?
3. Please provide a brief description of your understanding of who would typically use this device?

Device testing:

With the above understanding, participants are asked to assess the device according to the following tests and questions. User instructions (Figure 8.4) are provided, and the participant is asked to carry out the test.

- Time taken to carry out manual readout successfully:
- Time taken to carry out automated readout successfully:
- Number of attempts required to perform successful manual readout:
- Number of attempts required to perform successful automated readout:

Device form factor:

While the participant looks at / handles the device, make notes of the handling / most interesting / most challenging aspects for the participant (mark with X):

- Pulling of tab on tray:
- Sliding tray in and out:
- Positioning/alignment of tray in outer sleeve:
- Inside of box – inspection, handling:
- Outside of box – inspection, handling:
- Text – inspection:
- Insert/holder for test strip – positioning, handling:
- pH test strip handling:

Questions on device form factor:

Please rate the following questions on a scale of 1 to 5, with 1 being the worst and 5 being the best. For each question, please provide additional comments.

1. What is your overall opinion or impression of the device?
1 2 3 4 5
2. How would you rate the overall appearance of the device?
1 2 3 4 5
3. How would you rate the feel/handling of the device?
1 2 3 4 5

Please answer the following:

1. How many times do you think the device could be used?
< 10 10 – 20 times 20 – 50 times 50 – 100 times 100 + times
2. What do you think would happen to the device when it is not used anymore?
.....
3. Do you think people would use the device?
Yes No Don't know
4. What do you like about the device?
5. What don't you like about the device?
6. What would you change about the device?

Device usability (SUS)

Based on the test instructions and the test procedure carried out, please rate the following questions on a scale of 1 to 5, with 1 being the worst (strongly disagree) and 5 being the best (strongly agree). Please provide an explanation/reason for each answer.

1. I think that I would like to use this device frequently:
1 2 3 4 5
2. I found the device unnecessarily complex:
1 2 3 4 5
3. I thought the device was easy to use:
1 2 3 4 5
4. I think that I would need the support of a technical person to be able to use this device:
1 2 3 4 5
5. I found that the various functions in this device were well integrated:
1 2 3 4 5
6. I thought that there was too much inconsistency in this device:
1 2 3 4 5
7. I would imagine that most people would learn to use this device very quickly:
1 2 3 4 5

8. I found the device very awkward to use:

1 2 3 4 5

9. I felt very confident using the device:

1 2 3 4 5

10. I needed to learn a lot of things before I could get going with this device:

1 2 3 4 5

Device usability (ASQ)

Based on the test instructions and the test procedure carried out, please rate the following questions on a scale of 1 to 7 with 1 being the worst (strongly disagree) and 7 being the best (strongly agree). Please provide an explanation/reason for each answer.

1. Overall, I am satisfied with the ease of completing the tasks in this scenario:

1 2 3 4 5 6 7

2. Overall, I am satisfied with the amount of time it took to complete the tasks in this scenario:

1 2 3 4 5 6 7

3. Overall, I am satisfied with the support information (on-line help, messages, documentation) when completing the tasks:

1 2 3 4 5 6 7

Operational characteristics:

Based on the test instructions and the test procedure carried out, please rate the following questions and provide an explanation/reason for each answer:

1. Clarity of the instructions/user guide and training:

Difficult to follow Fairly clear Very clear Excellent
0 1 2 3

2. Technical complexity (overall):

Complex Fairly easy Very easy
0 1 2

3. What contributed to the complexity (1 = not complex, 4 = very complex):

Multiple steps:	1	2	3	4
Adding of sample:	1	2	3	4
Handling of test strips:	1	2	3	4
Handling of box:	1	2	3	4
Other issues:	1	2	3	4

4. Ease of result interpretation:

Difficult	Fairly easy	Very easy
0	1	2

5. Equipment/extras required but not provided:

Yes, extras needed	No, nothing needed
0	1

If Yes, what is required?

6. How could the whole system best be improved? What would you change?

.....

Acknowledgements

The completion of this dissertation was made possible by contributions from a number of people, to whom I am sincerely grateful. Specifically, I would like to thank ...

- ... my PhD supervisor, *Prof. Dr. Jan G. Korvink*, to whom I am grateful for the opportunity to be registered as a PhD student within *the Institute of Microstructure Technology (IMT) at the Karlsruhe Institute of Technology (KIT)*, Germany, and for his invaluable knowledge and insights.
- ... *Prof. Dr. Uli Lemmer* for being the second reviewer for this dissertation.
- ... my co-supervisor at KIT, *Dr. Dario Mager*. I am grateful for the supervisory role provided, assistance with securing funding for travel, and technical guidance and support.
- ... my co-supervisor at *the Council for Scientific and Industrial Research (CSIR)*, South Africa, *Dr. Kevin Land*, who I would like to thank for the day-to-day mentorship and for helping to shape and guide my PhD. I am truly grateful for the constant support and the collaborative networks established.
- ... *KIT* and *CSIR* for financial support during the course of my PhD, as well as *the Deutsche Forschungsgemeinschaft*, Germany, through grant number MA5859/1-1 and *the National Research Foundation (NRF)*, South Africa, for funding parts of this PhD work and related travel funding. Without these various channels of financial support, this PhD would not have been possible.
- ... my colleagues at the CSIR, who each made valuable contributions to my PhD: *Adelaide Oberholzer* for technical assistance and performing various experiments. *Phophi Madzivhandila* for laboratory assistance, printing and testing of devices. *Petrone Bezuidenhout* for technical inputs and assistance with inkjet printing and device assembly. *Thabang Noge* and *Alma Truyts* for assistance with real-world experiments as well as providing insights – additionally by *Shavon David* – regarding LFT assays and results. *Louis Fourie*, for conducting LSM experiments and providing practical laboratory support.

Acknowledgements

- ... *Oelof Kruger* at the National Metrology Institute of South Africa (NMISA), South Africa, for conducting profilometry measurements.
- ... *Dr Trudi Joubert* at the University of Pretoria, South Africa, for support through research collaborations and for providing funding to attend a workshop that enabled face-to-face interactions with experts and my supervisors.
- ... researchers and students at IMT, KIT, for their hospitality during my international visits. In particular, I would like to thank *Omar Nassar* for assistance with antenna characterization experiments.
- ... *Synertech (Pty) Ltd.*, South Africa, for the use of their equipment, resources and expertise in RFID systems.
- ... *the Technology Station in Electronics (TSE)*, South Africa, for assistance with pick and place set-up and execution.
- ... *Electronic Touch Systems (ETS)* for printed electronic prototyping, costing and insights, *MerryPak* for support in development of printing and packaging designs and practical insights, and *Techsolutions (Pty) Ltd.* for initial RFID investigations and experiments.
- ... the nurses and healthcare workers at clinics visited in Gauteng for taking the time to participate in interviews, as well as the participants that took part in the usability study for giving their time and providing constructive feedback.
- ... my co-authors for their contributions to the publications related to and based on the work in this PhD.
- ... *Hildegard Prigge* for providing various illustrations, and my sister *Danielle Hugo* for proof reading my dissertation and related publications.
- ... *Friederike Dominick*, *Laura Weber* and *Dario Mager* for translation of the abstract.
- ... my family; my incredible support system, during my PhD and always. I love you all.
- ... my husband *Stu*, my best friend, biggest supporter and inspiration; this is for you. I love you.